NUREG/CR-2077
UCRL-53026

Uncertainty in Soil-Structure Interaction Analysis Arising from Differences in Analytical Techniques

O. R. Maslenikov, J. C. Chen, and J. J. Johnson

Prepared for
U.S. Nuclear Regulatory Commission

Lawrence
Livermore
National
Laboratory

DISCLAIMER

DISCLAIMER

This work was supported by the United States Nuclear Regulatory Commission under a Memorandum of Understanding with the United States Department of Energy.

Available from
GPO Sales Program
Division of Technical Information and Document Control
U.S. Nuclear Regulatory Commission
Washington, D.C. 20555

and

National Technical Information Service
Springfield, Virginia 22161

NUREG/CR-2077
UCRL-53026
RD, RM

NUREG/CR--2077

DE82 021087

Uncertainty in Soil-Structure Interaction Analysis Arising from Differences in Analytical Techniques

Manuscript Completed: July 1982
Date Published:

Prepared by
O. R. Maslenikov and J. C. Chen, LLNL
J. J. Johnson, Structural Mechanics Associates, San Ramon, CA

Lawrence Livermore National Laboratory
7000 East Avenue
Livermore, CA 94550

Prepared for
Office of Nuclear Regulatory Research
U.S. Nuclear Regulatory Commission
Washington, D.C. 20555
NRC FIN No. A-0130

THIS PAGE

WAS INTENTIONALLY

LEFT BLANK

UNCERTAINTY IN SOIL-STRUCTURE INTERACTION ANALYSIS ARISING FROM DIFFERENCES IN ANALYTICAL TECHNIQUES

ABSTRACT

This study addresses uncertainties arising from variations in different modeling approaches to soil-structure interaction of massive structures at a nuclear power plant. As part of the Nuclear Regulatory Commission's Seismic Safety Margins Research Program, its findings will be incorporated in a comprehensive systems analysis methodology for assessing nuclear safety requirements more realistically than current processes allow.

To perform a comprehensive systems analysis, it is necessary to quantify, for each phase of the traditional analysis procedure, both the realistic seismic response and the uncertainties associated with them. In this study two linear soil-structure interaction techniques were used to analyze the Zion, Illinois nuclear power plant: a direct method using the FLUSH computer program and a substructure approach using the CLASSI family of computer programs. In-structure response from two earthquakes, one real and one synthetic, was compared. Structure configurations from relatively simple to complicated multi-structure cases were analyzed. The resulting variations help quantify uncertainty in structure response due to analysis procedures.

THIS PAGE

WAS INTENTIONALLY

LEFT BLANK

CONTENTS

LIST OF ILLUSTRATIONS

LIST OF TABLES

EXECUTIVE SUMMARY

Under the Nuclear Regulatory Commission's Seismic Safety Margins Research Program (SSMRP), Lawrence Livermore National Laboratory (LLNL) is developing probabilistic methods to realistically estimate the behavior of nuclear power plants during earthquakes. Two requirements govern the analysis methodology: (1) the analysis should be realistic, and (2) probabilistic methods should be used to model uncertainties. This study investigates potential uncertainties in soil-structure interaction (SSI) arising from two alternative analysis techniques.

The process of predicting the seismic response of stiff, massive structures, such as those found at a nuclear power plant, while taking into account the effects of SSI, introduces a number of uncertainties. A principal source of uncertainty is the differences in SSI analysis techniques. Two procedures are available to treat SSI: (1) the direct method, which analyzes the soil-structure system in a single step, and (2) the substructure approach, which treats the problem in a series of steps (determining the foundation input motion, determining foundation impedances, and analyzing the coupled soil-structure system). Both methods can be discussed in terms of two basic procedures: specifying the local free-field ground motion and idealizing the soil-structure system. In the second of these, it is necessary to model the configuration and properties of the soil, the geometry and stiffness of the foundation, and the complexities of the soil itself. This study addresses the uncertainties that arise from both of these procedures with regard to the soil-structure system.

A demonstration of the SSMRP methodology is currently being applied to the Zion Nuclear Power Plant in Zion, Illinois. This plant is the subject of the present study. It consists of two nuclear steam supply system (NSSS) units with power ratings of 1100 MW(e) each. The plant has three basic foundation structures to which SSI applies: the two reactor containment buildings, each with its own foundation; and the auxiliary, fuel-handling, and turbine generator (AFT) complex of buildings, which is supported on a foundation of various elevations and thicknesses. The complex is also connected by continuous slabs and walls in its upper stories.

We applied two alternative analytical techniques to the Zion plant. The first was a linear finite element approach using the FLUSH computer program. To allow for the two-dimensional character of FLUSH, we took several cross sections throughout the plant to estimate three-dimensional response. The significant dynamic characteristics of the structures were represented by simple sets of models with a single degree of freedom and with appropriate mass, stiffness, and damping characteristics. We obtained quasi-three-dimensional response at the basemat level at intersections of analytical cross sections. A second-stage structural analysis then enabled us to compute detailed structural response.

Our second method was a substructure approach employing the CLASSI computer program. CLASSI is in general three-dimensional. Its formulation allows us to incorporate detailed structural models into the analysis. The structures' dynamic characteristics are represented by their modal properties. In our analysis, the reactor building (containment shell, internal structure, and simplified NSSS model) was modeled by 72 modes and the AFT complex by 113. In the CLASSI analysis, embedment effects for the reactor building were obtained by generating the foundation input motion and impedances for assumed axisymmetric embedded foundations. The AFT foundation impedances were calculated using a flat foundation of appropriate shape with corrections applied to account for embedment. Embedment also has a significant effect on the AFT foundation input motions, and therefore they were calculated assuming an equivalent embedded cylindrical foundation. Structure-to-structure interaction effects were computed assuming flat foundations.

We compared in-structure response, in the form of peak values and response spectra, at selected points throughout the structures. The results demonstrate the variability in response due to alternative analysis techniques. In a systems analysis context, variations in in-structure response spectra are interpreted as variations in subsystem or component response. Subsystems are components supported within the structure, identified as important to accident mitigation, and whose seismic response may be related to spectral acceleration at its fundamental frequency and estimated damping.

To evaluate the effects of structure-to-structure interaction, we analyzed the reactor buildings and AFT complex first as isolated structures and then together as a coupled soil-structure system. Our analysis of the reactor building as an isolated structure represented a benchmark comparison between FLUSH and CLASSI. The physical situation was relatively simple but representative of a real structure and foundation. Results of this comparison showed excellent agreement between FLUSH and CLASSI for horizontal response--there was less than 10% difference over the entire response spectra, except at narrow frequency ranges near the resonant frequencies of the coupled soil-structure system, where differences approached 35%. Vertical response did not compare as well as horizontal. Variations in peak acceleration ranged up to about 25%, and in the amplified frequency range (<33 Hz) went as high as 50%, depending on structure location and the control motion. Subsequent investigations of the elements of each analysis revealed basic differences that require further study.

Whereas the reactor building was straightforward to model, the AFT complex required significant simplification. In the CLASSI analysis, the structure model was very detailed, but the foundation embedment and rigidity were idealized. In the FLUSH analysis, two-dimensional models of the structure and foundation were required, and modal equivalent models of the structure were used. Results from the analyses of the AFT complex as an isolated structure showed that peak horizontal accelerations varied by less than 25% (about 10% on the average). Spectral accelerations in the amplified frequency range varied somewhat more.

Variations in the vertical direction were less than for the horizontal, typically less than 20%. The agreement between the FLUSH and CLASSI results for the isolated AFT complex was surprisingly good, considering the differences in the assumptions for the two methods. This may be explained by the fact that, because of the large horizontal area of the foundation, there was relatively little rocking. If foundation rocking had been more important, we would expect to see greater differences in the structural response.

Two aspects of the multi-structure analyses were considered: the effect of structure-to-structure interaction on structure response and the variability in structure response as predicted by CLASSI and FLUSH, including structure-to-structure interaction. The effect of structure-to-structure

interaction on the response of the Zion reactor buildings and the AFT complex was assessed by comparing the results of the CLASSI analyses with and without interaction between the structures. The results show that the reactor buildings have a very small effect on the AFT complex. However, the effect of structure-to-structure interaction on the reactor buildings is substantial.

A comparison of the reactor building's response as predicted by CLASSI and FLUSH, including structure-to-structure interaction, showed substantial differences--200% or more in some cases. Poor correlation between the two was due to the FLUSH modeling assumptions for the AFT complex. The FLUSH model properly represented the state of stress in the soil under the AFT complex but underestimated the structure's total mass. Consequently, the reactor building mass in the FLUSH model was twice that of the AFT complex. Modeling three-dimensional configurations with equivalent two-dimensional models is an issue that requires careful consideration.

Several conclusions concerning the application of SSI analysis techniques were drawn.

- Variability in structural response due to SSI analysis procedures increases with increased complexity in the physical situation to be modeled.
- Variability of in-structure response is greatest near the resonant frequencies of the coupled soil-structure system and least at the zero period amplitude (ZPA).
- Equipment and components with frequency characteristics in the amplified frequency range (< 33 Hz) have greater uncertainty in response than those subjected to the ZPA.
- Reduced models, in terms of two dimensions vs three dimensions or fewer degrees of freedom must be developed carefully, reproducing three-dimensional detailed model characteristics.
- When performing a second-stage analysis, it is essential to recognize that both translations and rotations must be used in exciting the system. In addition, horizontal translation and rocking have a unique phase relationship, which should be maintained.
- The effect of structure-to-structure interaction was found to have a significant effect on the amplitude and frequency content of the response of the least massive of the two structures.

1.0 INTRODUCTION

1.1 BACKGROUND

For some time it has been evident that traditional seismic analysis and design of nuclear power plants does not fully address the issue of uncertainties. At each stage of this complex, multidisciplinary process, conservatism is introduced to account for uncertainties, and it accumulates from one stage to the next. Because the uncertainties are unquantified, however, the effect of compounding this conservatism has not been established. The result may be a design that is too conservative for the estimated seismic hazard in relation to, and perhaps at the expense of, other accident conditions, as well as for normal operating conditions.

To address this problem, Lawrence Livermore National Laboratory (LLNL) is currently developing a methodology for examining the seismic analysis and design of nuclear power plants in a comprehensive systems context.[1] Phase I of our Seismic Safety Margins Research Program (SSMRP) concentrates on developing a probabilistic procedure that more realistically estimates the behavior of nuclear power plant structures and systems during a hypothetical earthquake. This methodology will be used to perform sensitivity studies which can yield new, more fundamental insights into seismic safety requirements.

To perform a comprehensive systems analysis, it is necessary to obtain quantitative values for both the realistic or best-estimate seismic response and for the uncertainties associated with these values. This entails examining traditional seismic analysis and design methodology, which comprises four phases: seismic input characteristics, soil-structure interaction (SSI), major structural response, and subsystem response.

The seismic input consists of the earthquake hazard near a nuclear power plant and a description of the free-field motion. (The earthquake hazard is defined by an estimate of the seismic hazard function, i.e., the relationship between the probability of occurrence and a measure of an earthquake's size.) SSI analysis has the broad objective of transforming the free-field ground motion into basemat or in-structure response, taking into account the interaction of the soil with the massive stiff structures usually

present at a nuclear power plant. In the major structure response phase, major structures commonly denote buildings but may also include very large components. The final step, predicting subsystem structural response, uses the response of the major structures as input. This report concentrates on uncertainties in the SSI phase of the process.

1.2 OBJECTIVE AND SCOPE

Predicting the effects of SSI on the seismic response of stiff, massive structures, such as those at a nuclear power plant can be discussed in terms of two basic elements: specifying the local free-field ground motion and idealizing the soil-structure system. Describing the free-field ground motion includes specifying the control point, the amplitude and frequency characteristics of the motion, and the spatial variation of the motion. Idealizing the soil-structure system entails modeling the configuration and properties of the soil, the geometry and stiffness of the structural foundations, and the complexities of the structures themselves. In addition, structure-to-structure interaction and localized nonlinear behavior (primarily, separation of soil and structure during the earthquake) require consideration. To perform SSI analysis, modeling decisions concerning each of these aspects of SSI must be made. In addition, uncertainties are introduced due to our inability to represent all facets of SSI precisely.

Several side studies were performed to guide us in our modeling decisions and provide a perspective on the approximations we elected to use in the SSMRP Phase I systems analysis. Each side study emphasizes the best estimate modeling of the phenomenon and quantifying uncertainty associated with it. Initially, Wong and Luco[2] investigated: the effect of assuming nonvertically incident plane waves as the wave propagation mechanism at the Zion site; embedment of the Zion reactor building foundation; and the effect of soil layering on SSI parameters. The present study uses the results of Ref. 2 while expanding the side studies to investigate the effects of structure-to-structure interaction at the Zion site and uncertainties in structure response introduced by different SSI analysis techniques.

We applied two alternative linear analysis techniques to the SSI analysis of the Zion Nuclear Power Plant. The first was a direct method using the FLUSH computer program.[3] The second was a substructure approach using the CLASSI computer program.[4] In each case, significant simplifications were necessary due to the complexity of the physical situation. These simplifications, and the differences inherent in the two approaches, led to nonunique predictions of response. We studied each of the major Category 1 structures at Zion first as isolated structures, unaffected by motions from adjacent structures, and then as a multistructure system with foundations coupled through the underlying soil. In-structure response in the form of peak values and response spectra were then computed and compared to quantify variability due to analysis procedures.

Section 2.0 describes the structural and geotechnical configuration of the Zion Nuclear Power Plant, comprising soil conditions and structures. Section 3.0 contains a brief description of the two categories of SSI analysis techniques: substructure methods and direct methods. Section 4.0 itemizes the elements of the analyses, such as defining the free-field ground motion and modeling soil and structural characteristics. Section 5.0 presents the results of the analyses for a hypothetical isolated reactor building and AFT complex and for the multi-structure Zion Nuclear Power Plant. Conclusions are given in Section 6.0.

2.0 ZION NUCLEAR POWER PLANT

The Zion Nuclear Power Plant is situated on the southwestern shore of Lake Michigan, approximately 40 miles north of Chicago, Illinois. The plant consists of two nuclear steam supply system (NSSS) units which were licensed to operate in 1973. Each has a power rating of 1100 MW(e). The facility's design was completed in the late 1960s and early 1970s. Figure 2.1 shows a plan view of the plant. For SSI analysis, three structures are of interest: the two reactor buildings and the auxiliary/fuel-handling/turbine building complex (AFT complex). Each reactor building houses an NSSS unit, and the AFT complex contains the power generation and safety equipment for both.

The Zion site is characterized by approximately 110 ft of soil overlying a bedrock of Niagara dolomite. The soil is stratified in three major layers, as shown in Fig. 2.2. The top layer, 30 to 35 ft in thickness, consists of granular lake deposits of dense, fine-to-medium sands with variable amounts of coarse sand and gravel and occasional pockets of peat and organic material. In general, the foundations of the major plant structures were excavated through this material into the second layer. This second layer is about 30 ft thick and is a cohesive, firm-to-hard glacial till and glacial Lacustrine

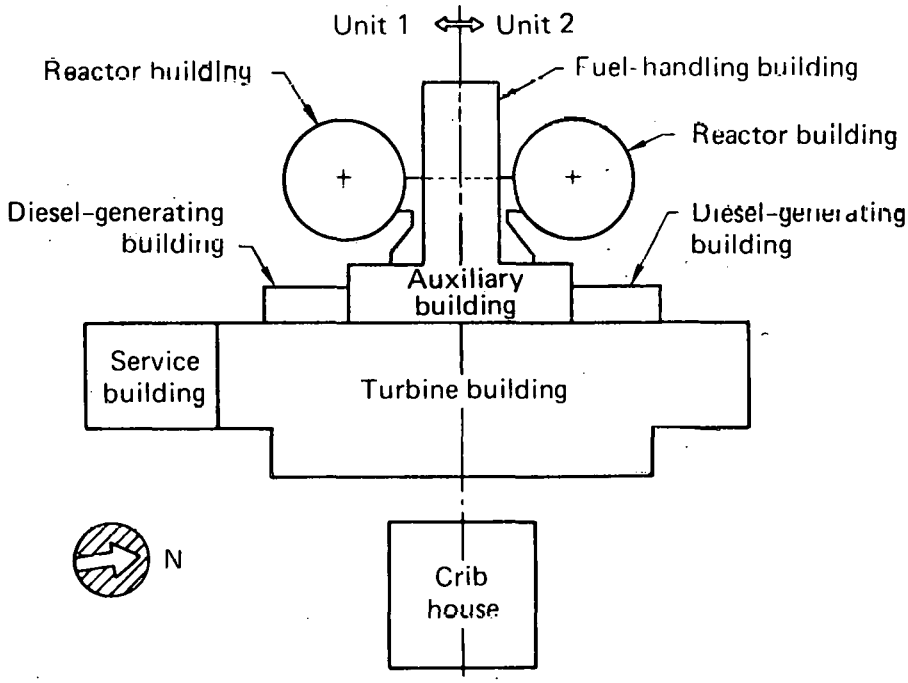

FIG. 2.1. Plan view of the Zion Nuclear Power Plant.

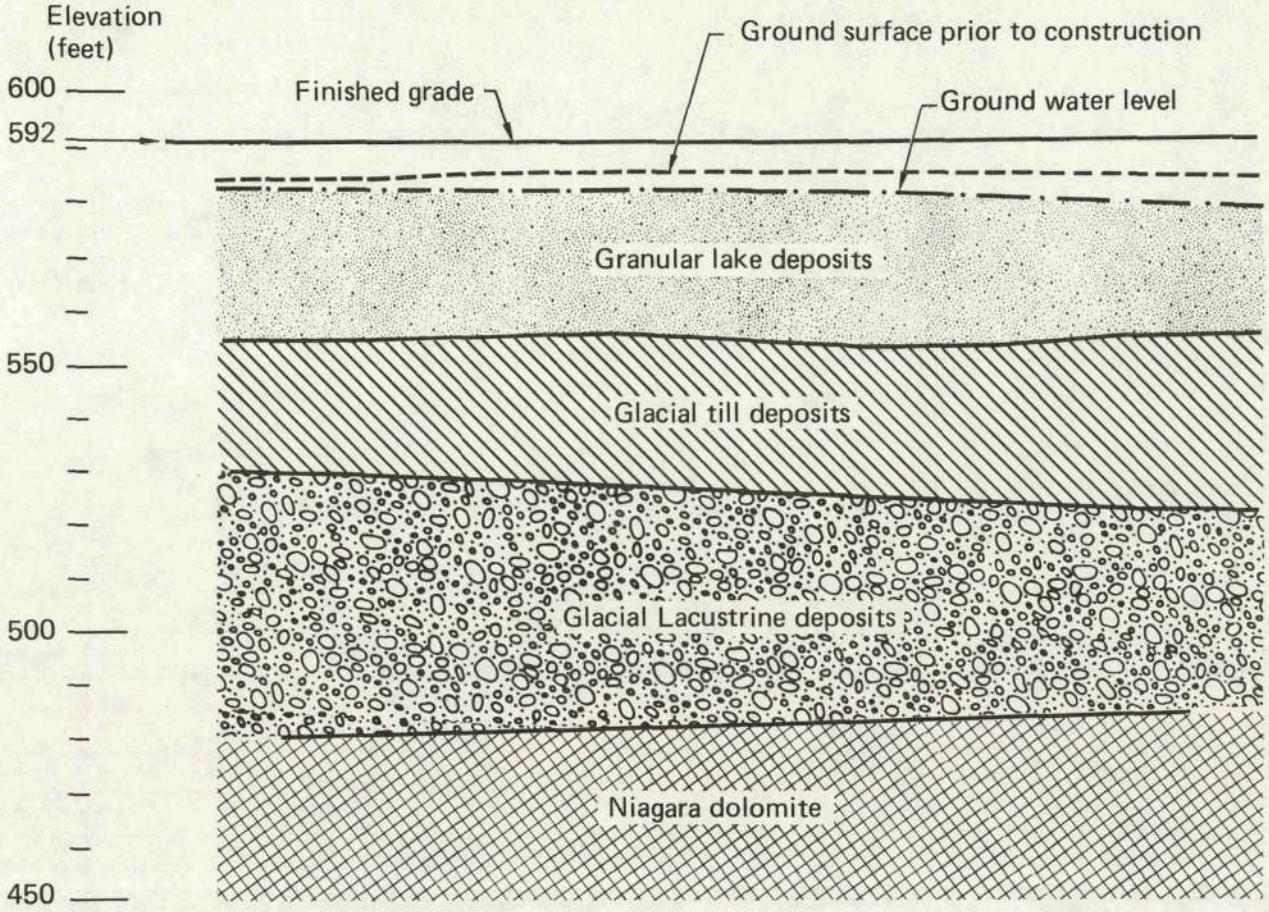

FIG. 2.2. Elevation view of the Zion site, showing geological stratification. View is taken through the reactor building centerline.

deposit with variable amounts of sand and gravel. The bottom layer, about 45 ft thick, is primarily a cohesionless glacial deposit of dense sands and gravels. The average low-strain, shear-wave velocity in the upper layer, as determined from in-situ tests made prior to construction of the plant, is about 920 ft/sec. The average shear-wave velocity in the two lower layers is about 1650 ft/sec. The water table is about 5 ft below finished grade.

The Zion reactor building is composed of two essentially independent structures--the containment shell and the internal structure. Figure 2.3 shows a simplified elevation view of the building. The containment shell is a prestressed-concrete right circular cylinder topped by an elliptical dome. It is 147 ft in diameter and rises 211 ft above the foundation mat. (Note the point on the containment shell at which the structural response was computed.) For this study, the term "internal structure" denotes both the NSSS's reinforced concrete support structure and the NSSS itself (including the reactor pressure vessel, steam generators, piping, and coolant pumps).

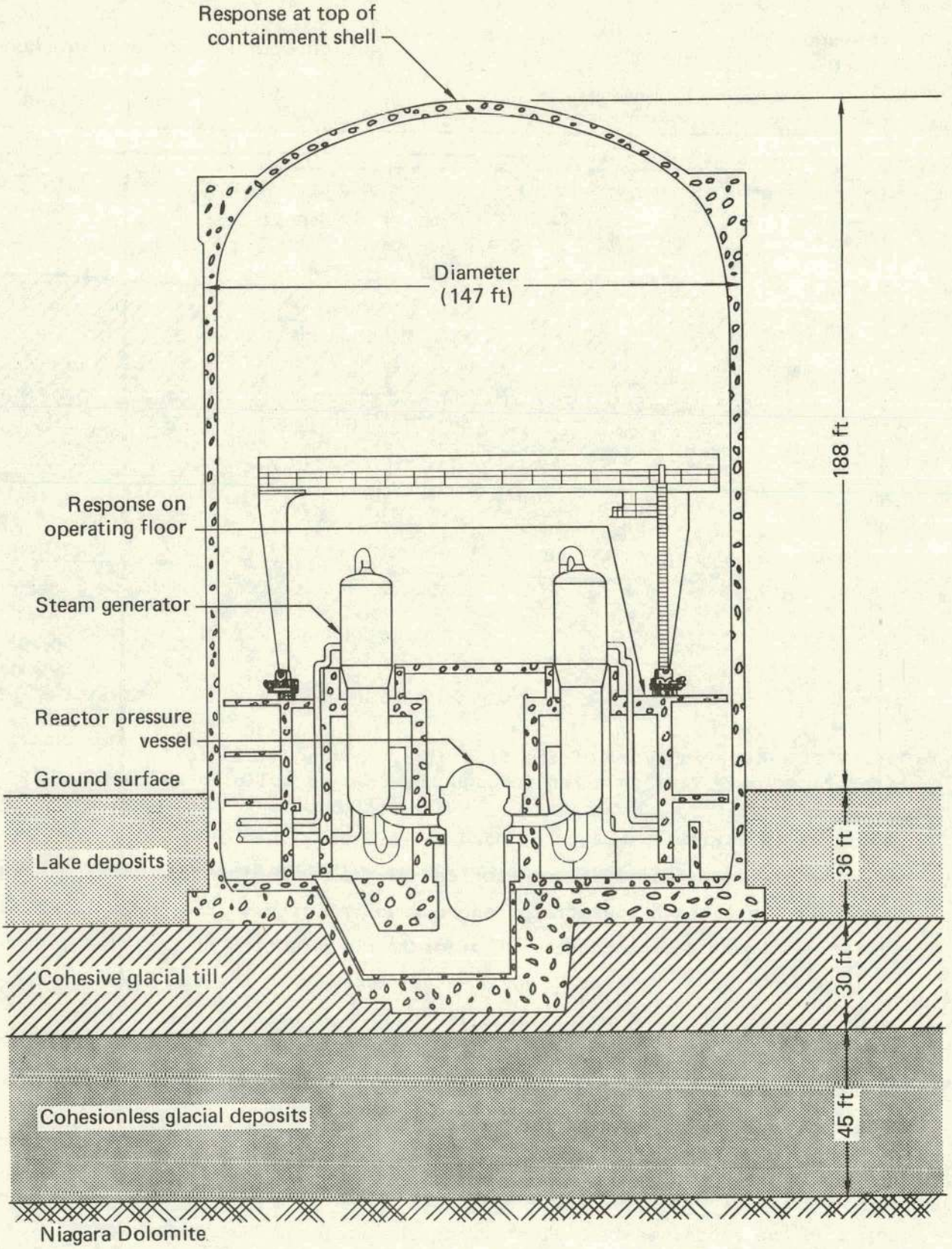

FIG. 2.3. Simplified elevation view of Unit 1 reactor building, facing west.

The internal structure extends about 50 ft above the foundation mat to the operating floor, at which an additional response was computed. The containment shell and the internal structure interact only through the foundation, which is 157 ft in diameter and about 13 ft thick, with an embedment depth of 36 ft. A sump, located at the center of the slab, extends about 30 ft below the bottom of the foundation. Only the mass properties of the sump were included in the SSI analyses. The foundation was assumed flat, with no additional lateral or vertical resistance due to the sump.

The AFT complex consists of a T-shaped auxiliary building, two turbine buildings, a fuel-handling building, and two diesel generator buildings. The denotation of the different buildings is functional rather than structural; physically, the AFT complex is a single structure supported on a common foundation and interconnected throughout by continuous walls and floor slabs. An isometric view of the foundation configuration is shown in Fig. 2.4. The auxiliary, fuel-handling, and diesel generator buildings are constructed of reinforced concrete, with the turbine building made of braced steel frames. The complex is essentially symmetric with respect to an east-west plane that divides the two generating units. The foundation consists of adjoining,

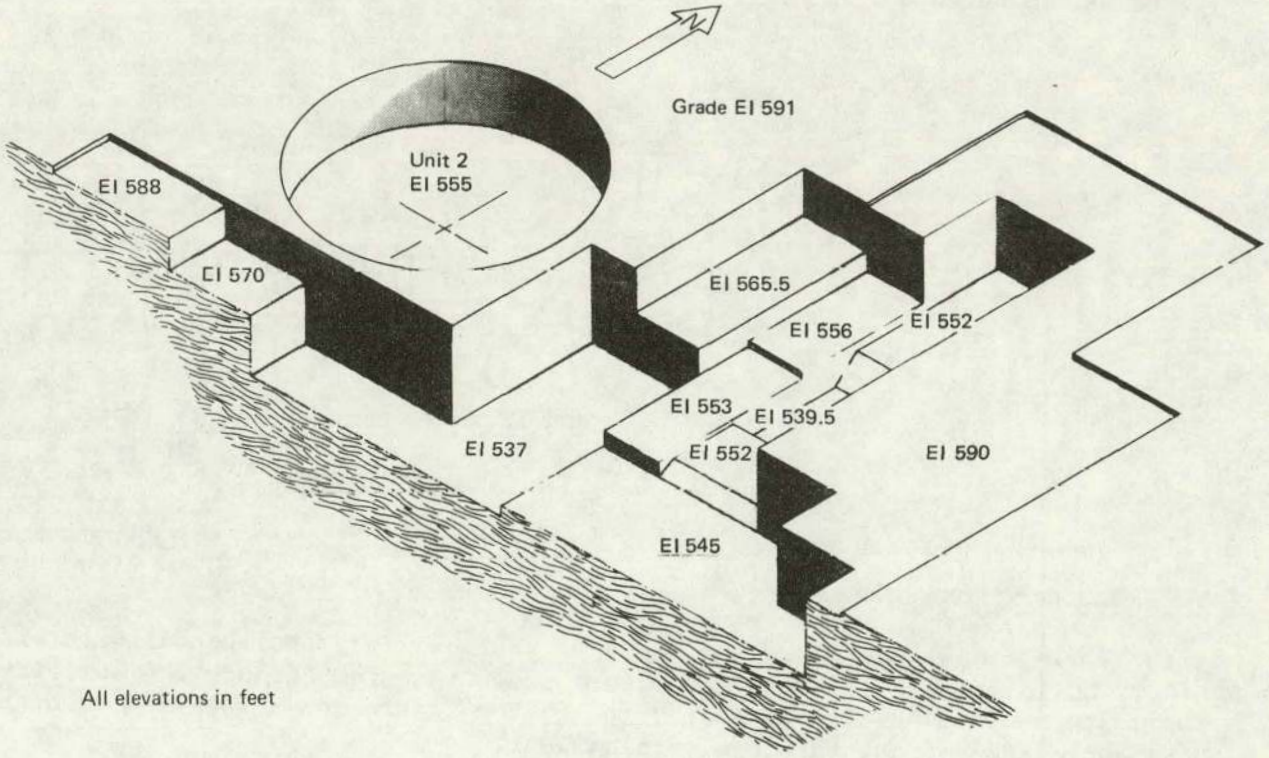

FIG. 2.4. Isometric view of the Zion foundation excavation configuration.

deeply embedded basemats having light peripheral foundations at the ground surface. The deeper portions vary in depth from 20 to 54 ft and in thickness from 4 to about 15 ft, except for the turbine pedestals, which are about 20 ft thick. Figure 2.5 shows simplified elevations taken through two cross sections of the AFT complex.

The mass distributions of the structures are shown in Table 2.1. About 60% of the structural mass of the AFT complex is concentrated in the auxiliary and fuel-handling buildings, even though their foundation areas are much less

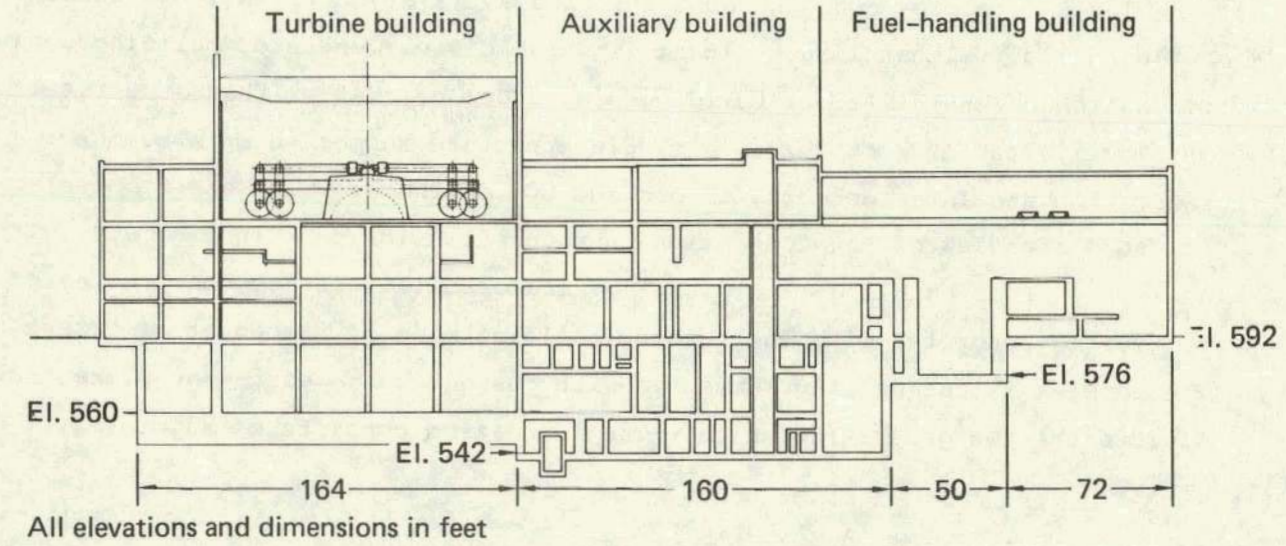

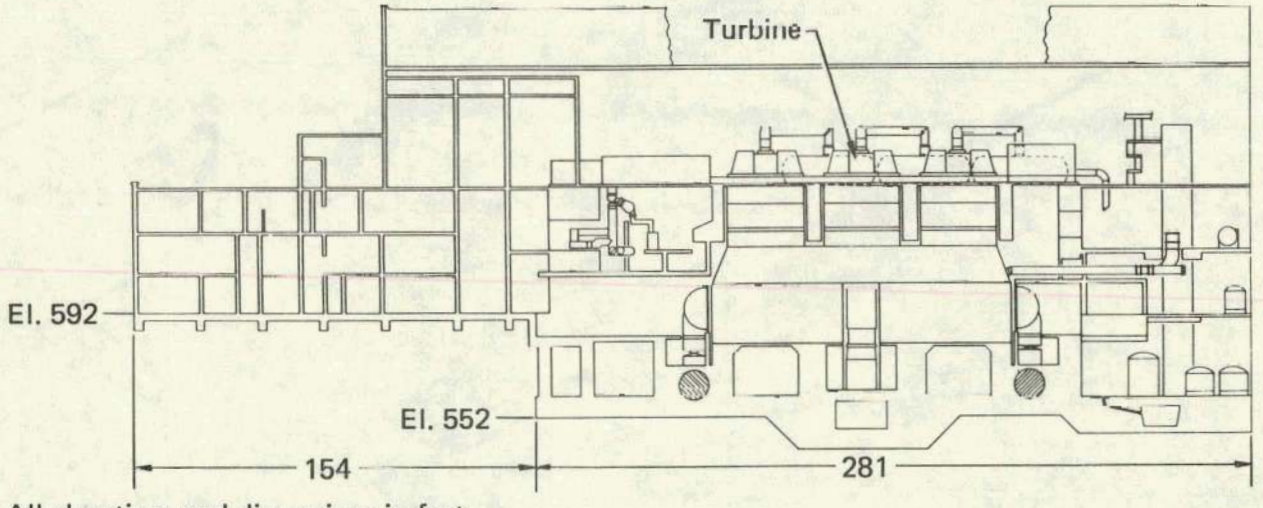

FIG. 2.5. Simplified elevation views of the auxiliary/fuel-handling/turbine (AFT) building complex. The top figure shows the view through the auxiliary building centerline, facing south; the bottom figure shows the view through the centerline of the turbines, facing west.

TABLE 2.1. Distribution of mass among major structures of the Zion Nuclear Power Plant (kip-sec^2/ft).

Reactor buildings	
Containment shell	1,850
Internal structure (including NSSS)	940
Foundation	1,270
Total	4,060
AFT complex	
Auxiliary and fuel-handling building	7,000
Turbine buildings (both)	5,000
Foundation	9,000
Total	21,000

than 60% of the total. Table 2.1 shows the total mass of the AFT complex to be about five times the total for each reactor building, which suggests that the effect of structure-to-structure interaction should be more significant on the reactor buildings.

The reactor buildings and the AFT complex are quite close together at the foundation level and in the superstructure. The distance between foundations varies around the circumference of the reactor building, averaging 15 to 20 ft at the deeper foundation levels and having a minimum separation of 1 in. at locations where piping tunnels from the AFT complex abut the containment shell.

3.0 METHODS OF ANALYSIS

There are two broad categories of SSI analytical techniques: the direct method and the substructure approach. The direct method analyzes the idealized soil-structure system in a single step, whereas the substructure approach treats the problem in a series of steps, typically three, that culminate in a prediction of the response of the coupled soil-structure system.

3.1 DIRECT METHOD

In general, a direct analysis proceeds by applying a consistent free-field ground motion to the boundaries of a discrete model and then computing the response of the combined soil-structure system. Hence a direct method determines the response of the soil and structure simultaneously. In practice, the structural model used in a direct method of analysis represents only the overall dynamic behavior of the structure. A second-stage structural analysis, using the results of the SSI analysis as input, must then be performed to obtain detailed structural response. This was the procedure we used.

Direct methods have several unique features:

- The soil and structure are idealized by discrete finite-element or finite-difference models.
- The free-field motion of the boundaries of the model must be known, assumed, or computed as a precondition of the analysis.
- During SSI, the vibration of the structure introduces motions in the soil not present in the free field. To simulate free-field conditions at large distances from the structure, the boundaries of the model must receive special treatment.
- The state of stress in the soil can be computed easily.
- Three-dimensional nonlinear analysis is theoretically possible.

Implementation of a direct method requires (1) solution of the free-field ground-motion problem (sometimes called the site response problem), (2) analysis of the coupled soil-structure system, and (3) a detailed second-stage analysis to determine structural response. To carry out our analysis, we used the FLUSH computer program, which is characterized by several key features:

- FLUSH employs the complex response method, which uses a complex modulus to describe the stiffness and damping of the soil. The solution is implemented in the frequency domain.
- An iterative linear procedure is used to approximate nonlinear material behavior. Although a nonlinear process cannot be broken into component parts, analyzed, and the results superposed, a conceptual separation is helpful for understanding the aspects of nonlinear behavior treated by an analysis technique. "Primary nonlinearity" is attributed to the seismic excitation alone. It is the nonlinear soil behavior associated with the state of deformation induced by the free-field ground motion. "Secondary nonlinearity" is due to the SSI process. It is associated with the soil deformations caused by structural vibration, and can, in a sense, be thought of as a perturbation of the primary nonlinearity. Our analysis of the soil and structure was, strictly speaking, linear. However, linear material properties were determined by an iterative process that estimates material constants as functions of an average strain level over the duration of the excitation. In general, a direct method accounts for both primary and secondary elements of nonlinear behavior.
- The basic formulation of FLUSH is two-dimensional. Hence the analysis of a single structure or a multiple set of structures requires consideration of several slices through the layout. In these cases structural response is assumed to be uncoupled in two orthogonal horizontal directions. To simulate three-dimensional radiation damping effects, additional viscous dampers are applied to soil elements.
- Transmitting boundaries are located on the lateral boundaries of the models to simulate radiation of energy away from the structure in the free field.
- A second-stage fixed-base structural analysis was performed to obtain detailed three-dimensional structural response for comparison with the substructure approach. Because the fixed-base analysis is three-dimensional, the effect of coupled horizontal and torsional motion in the structure is obtained. The excitation for this second-state analysis consists of translations and rotations of the foundation.

3.2 SUBSTRUCTURE APPROACH

The substructure approach divides the SSI problem into a series of simpler problems, solves each independently, and superposes the results. The following steps comprise the substructure approach we applied:

- As a preliminary step, the free-field ground motion is specified and free-field soil properties are obtained from a one-dimensional solution of the site response problem.
- The foundation input motion is determined. In this step, kinematic boundary conditions are applied along the soil-foundation interface to model the expected deformation of the foundation. This step is sometimes called the kinematic interaction problem or determination of the response of a massless foundation.
- The foundation stiffnesses or impedance functions are determined.
- The coupled soil-structure system is analyzed by solving the appropriate equations of motion.

In this study we used the substructure approach implemented in the CLASSI family of computer programs. These programs are characterized by the following key elements:

- The problem is solved in the frequency domain, which permits the behavior of the soil to be modeled by frequency-dependent impedances. Fourier transform techniques are applied to find the time-history response.
- Our analysis assumed rigid foundations, the most common assumption in the substructure approach. The reactor building foundations were assumed embedded and cylindrical in shape. This assumption is appropriate because it accurately describes the actual configuration of the reactor buildings. But significant simplification was required for the AFT complex because of its extremely complicated foundation geometry. Thus, for the purposes of computing impedances, the AFT foundation was modeled as a flat T-shaped surface foundation, appropriately shaped and situated on a soil layer equal in thickness to the average soil thickness beneath the actual foundation. The impedances thus calculated were corrected for embedment effects using an embedded cylinder equal in area and

excavated volume to that of the foundation, (i.e., the soil depth beneath the cylinder was equal to that beneath the T-shaped model). The foundation input motions for the AFT complex were computed using the equivalent embedded cylinder. A further discussion is found in paragraph 4.4.

- The final step in the substructure approach is the actual SSI analysis. The foundation input motions and impedance functions are combined with a dynamic model of the structure to solve the equations of motion for the coupled soil-structure system. The technique used in CLASSI to complete this final step is extremely powerful. As the structure is modeled by its eigensystem and modal damping factors, a great degree of complexity may be included; the effect of the structure is then projected onto the foundation. The computation for a single foundation requires the solution of six simultaneous equations.
- Structure-to-structure interaction is included in the multiple structure case. The coupling characteristics of the soil are modeled in an approximate fashion. In our case we used the same assumption of flat surface foundations as for the AFT complex.

4.0 SSI ANALYSIS

There are two basic elements of any SSI analysis--specifying the free-field ground motion and idealizing the soil-structure system. The latter involves modeling the configuration and properties of the soil, the geometry and stiffness of the structural foundation, and the complexities of the structure itself. Specification of the SSI problem and aspects of the solution procedures that apply to our study are discussed in this section. Elements unique to a solution procedure--CLASSI or FLUSH--follow more general discussions.

4.1 FREE-FIELD GROUND MOTION

Specification of the free-field ground motion is one of the most important factors in SSI analysis. Hence it is essential, in comparing analysis techniques, to maintain a consistent definition of the free-field ground motion. Three aspects of the free-field motion are important: location of the control point, the spatial variation of the motion, and the frequency characteristics of the control motion. In all analyses reported here, (1) the control point was located on the surface of the soil, (2) the spatial variation of motion was defined by vertically propagating shear and dilatational waves, and (3) the frequency characteristics of the motion were represented by two earthquakes, one real and one synthetic.

These earthquakes each consisted of three components of motion: two horizontal, aligned in the north-south (N-S) and east-west (E-W) directions, and one vertical. The real earthquake was recorded in the Imperial Valley of California, at El Centro, on May 19, 1940. It is identified in the California Institute of Technology data set[5] as accelerogram IIA001 and is denoted here as El Centro. The first 36 sec, digitized at 0.02 sec, were used in the analysis. CLASSI and FLUSH solve the SSI problem in the frequency domain using the Fast Fourier Transform (FFT) technique; hence a quiet zone was added to create excitations totalling 40.96 sec in duration, corresponding to 1024 frequency points. The major component, N-S, was scaled to a peak acceleration of 0.2 g, which approximately corresponds to the Zion SSE level of 0.17 g. The remaining two components were scaled by the same factor. The resulting

peak accelerations of the N-S, E-W, and vertical components are 0.2 g, 0.12 g, and 0.12 g, respectively. The accelerograms are shown in Fig. 4.1, and the corresponding response spectra are plotted in Fig. 4.2.

The comparative analyses were also performed for a synthetic earthquake generated to loosely match target pseudo-velocity spectra considered typical of 0.20 g free-field motion at the Zion site. Each acceleration time history was from a random seed. The horizontal components were scaled to 0.2 g; the

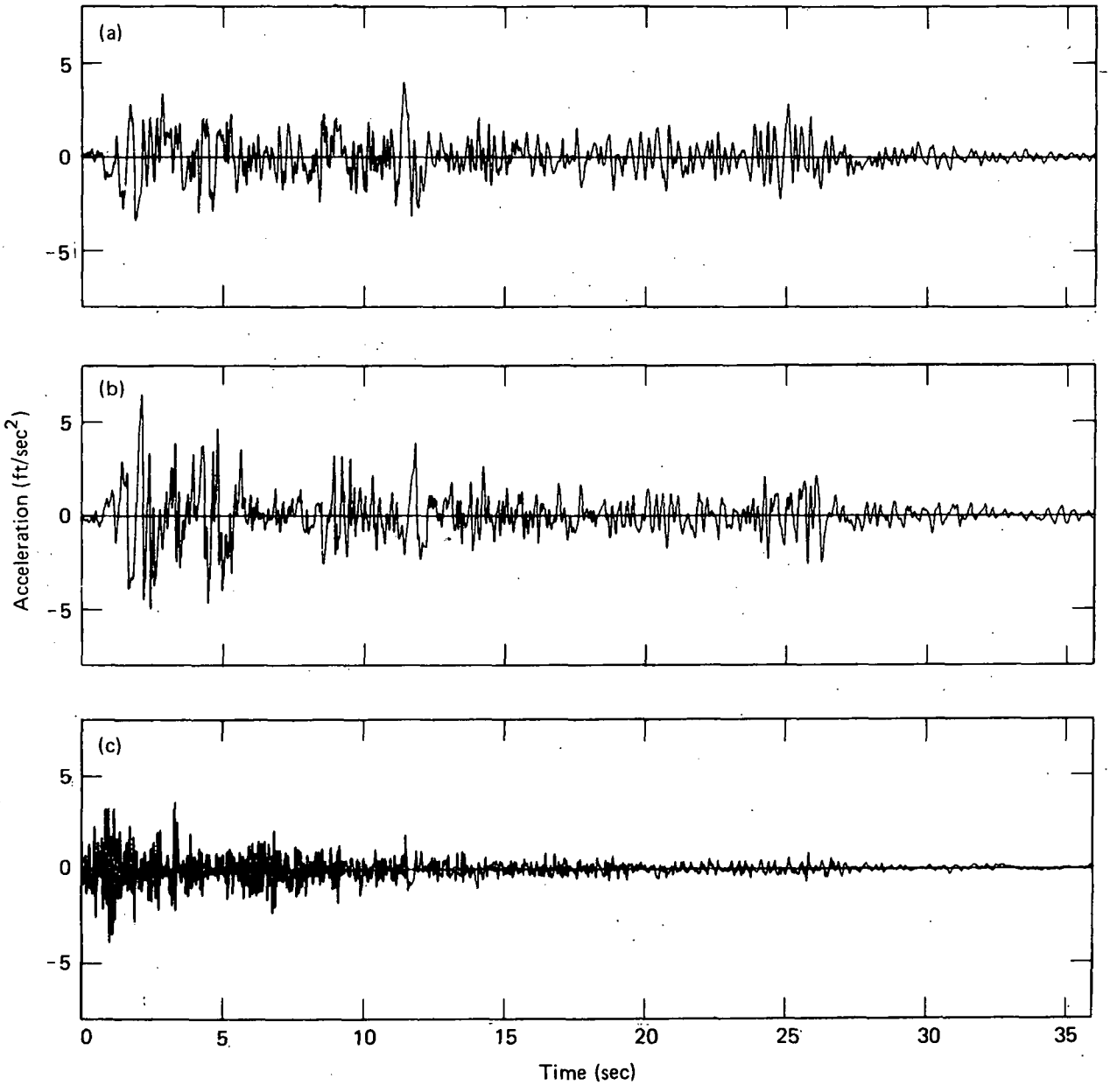

FIG. 4.1. Accelerograms recorded at El Centro, California in the Imperial Valley earthquake of May 14, 1940. Shown are (a) E-W translation, (b) N-S translation, and (c) vertical translation.

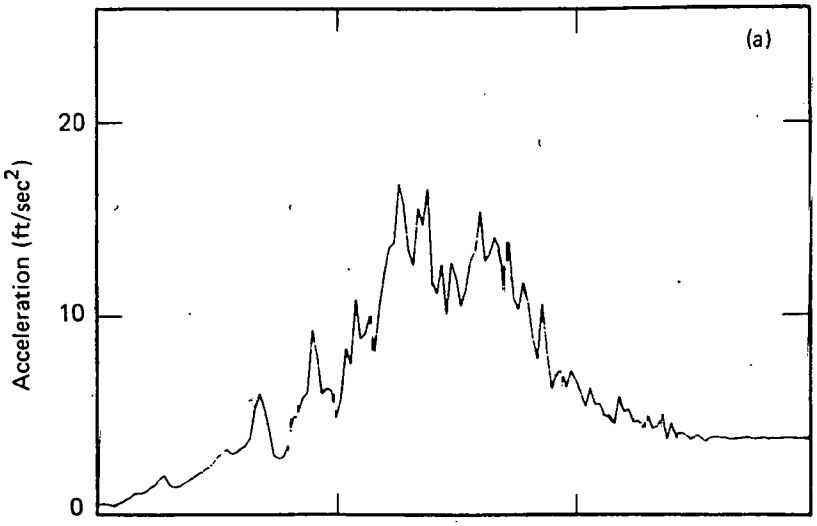

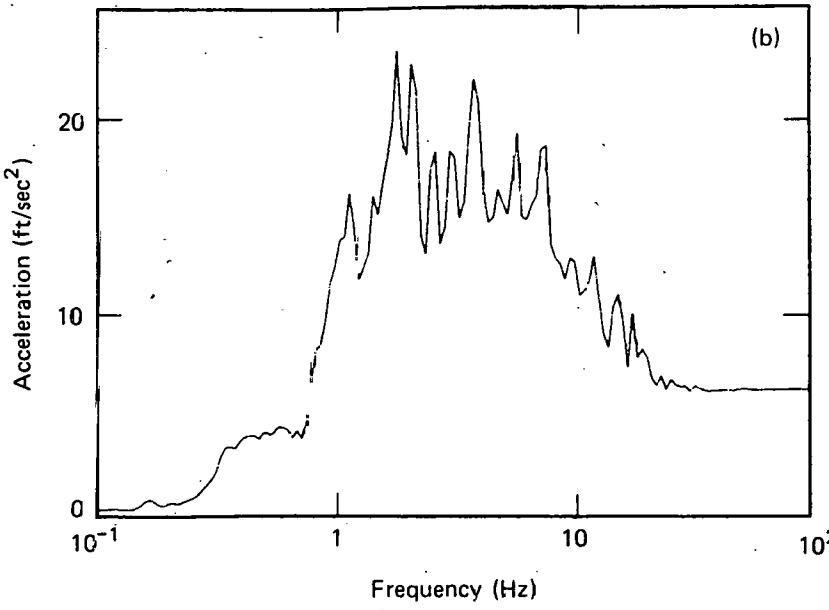

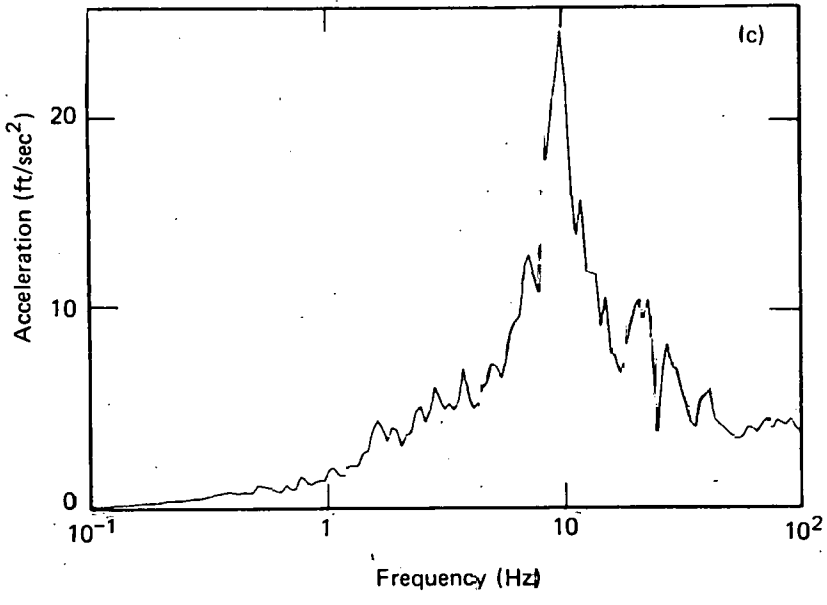

Fig. 4.2. El Centro earthquake response spcetra at 2% damping. Shown are (a) E-W translation, (b) N-S translation, and (c) vertical translation.

vertical to 0.13 g. The duration of motion was 15 sec, discretized at time intervals of 0.01 sec. A quiet zone was added to produce excitations totalling 20.48 sec, which corresponds to 1024 frequency points as above. The acceleration time histories are plotted in Fig. 4.3 and the corresponding spectra in Fig. 4.4.

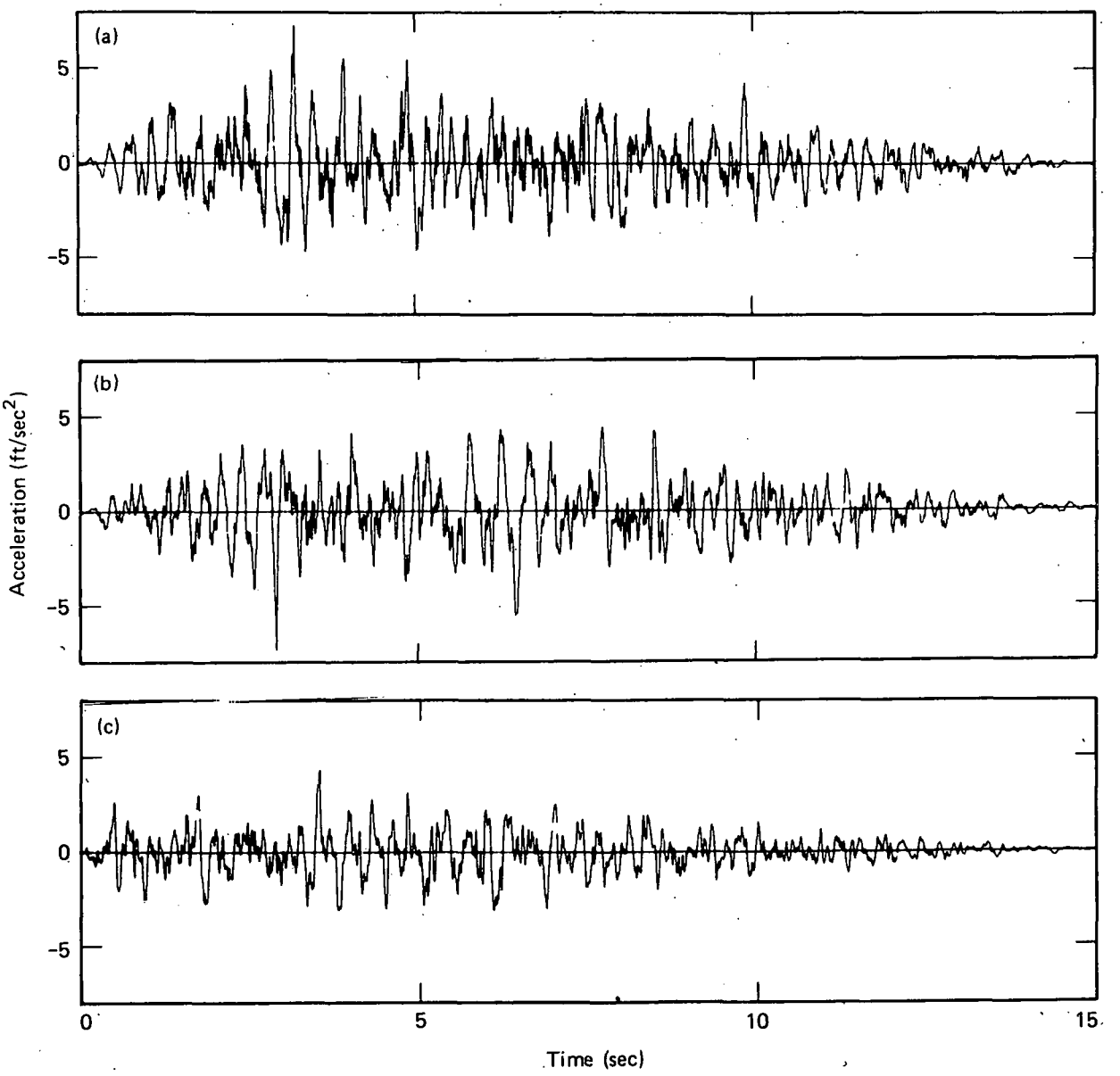

FIG. 4.3. Synthetic earthquake accelerograms. Shown are (a) E-W translation, (b) N-S translation, and (c) vertical translation.

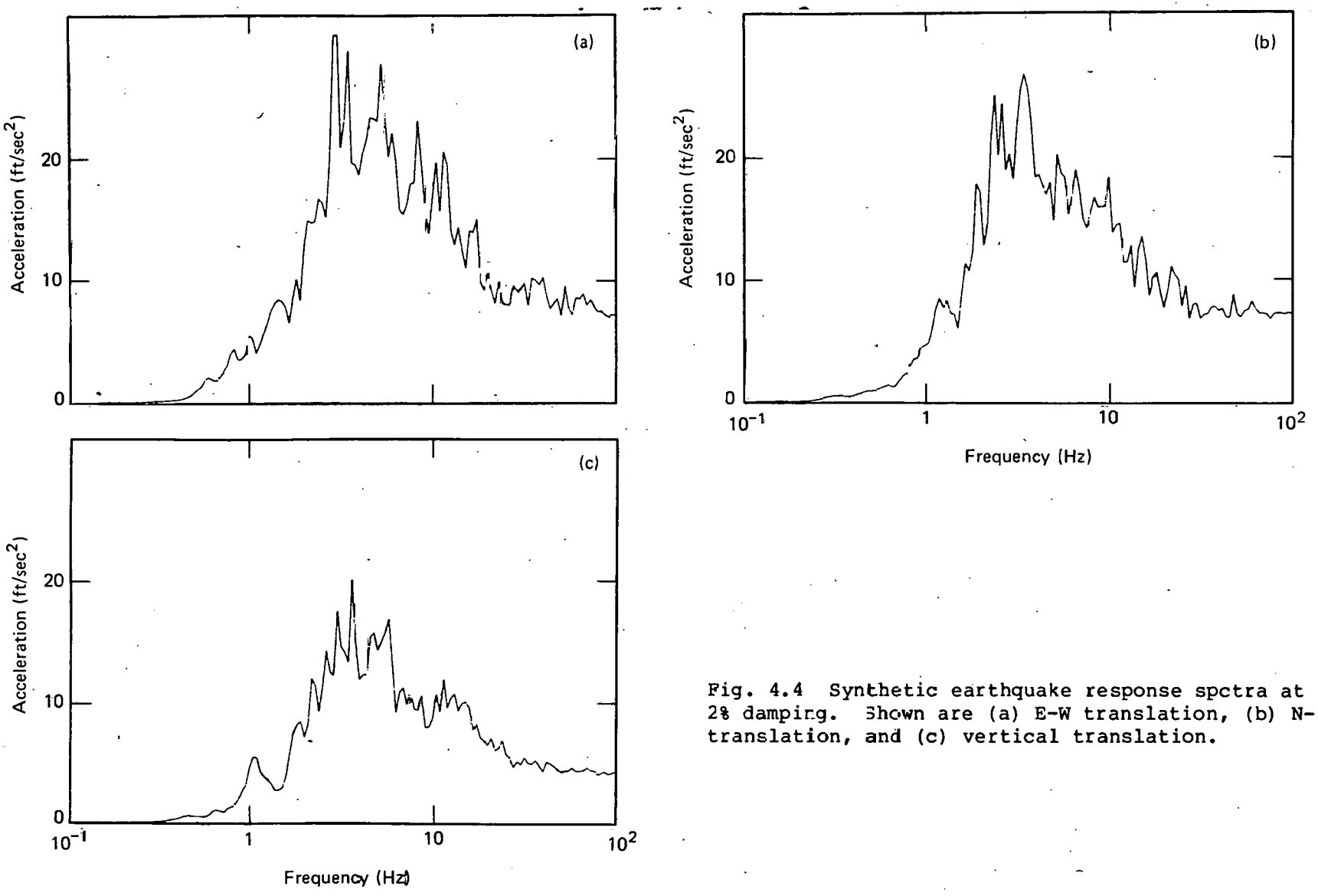

Fig. 4.4 Synthetic earthquake response spctra at 2% damping. Shown are (a) E-W translation, (b) N-S translation, and (c) vertical translation.

4.2 MODELING STRESS-STRAIN BEHAVIOR OF SOIL

The mathematical model selected to represent the stress-strain behavior of soil for the CLASSI and FLUSH analyses is based on a linear visco-elastic theory. The parameters defining the model produce constant hysteretic (i.e., frequency-independent) damping. They consist of two elastic constants, in our case shear modulus and Poisson's ratio, and a damping factor.

In general, the stress-strain behavior of soil is nonlinear. For the Zion site, estimates of shear modulus and damping as functions of depth and strain level are shown in Figs. 4.5 and 4.6. The figures also show variations in the parameters for a constant strain level, emphasizing our inability to

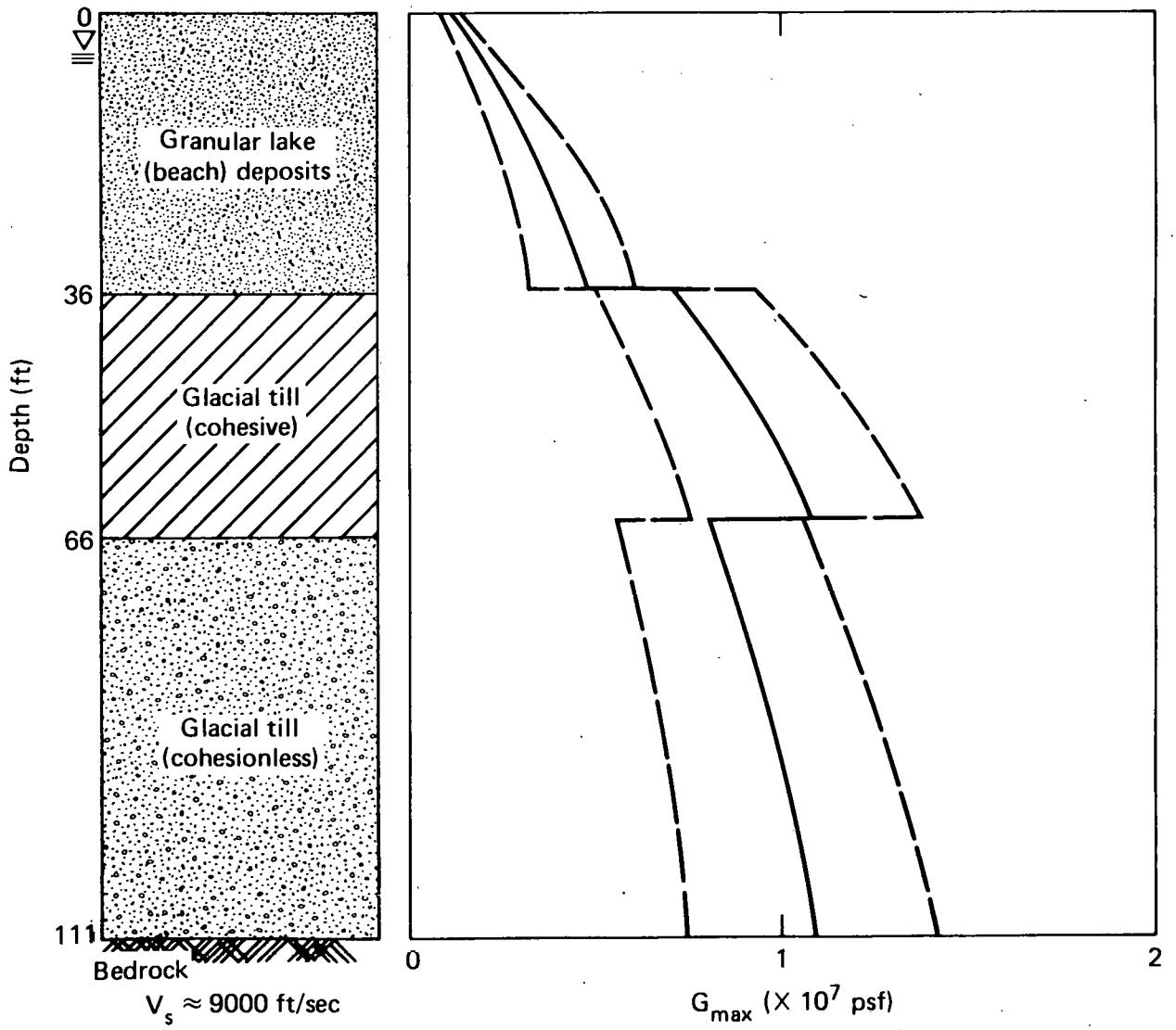

FIG. 4.5. Variation of soil low-strain shear modulus with depth.

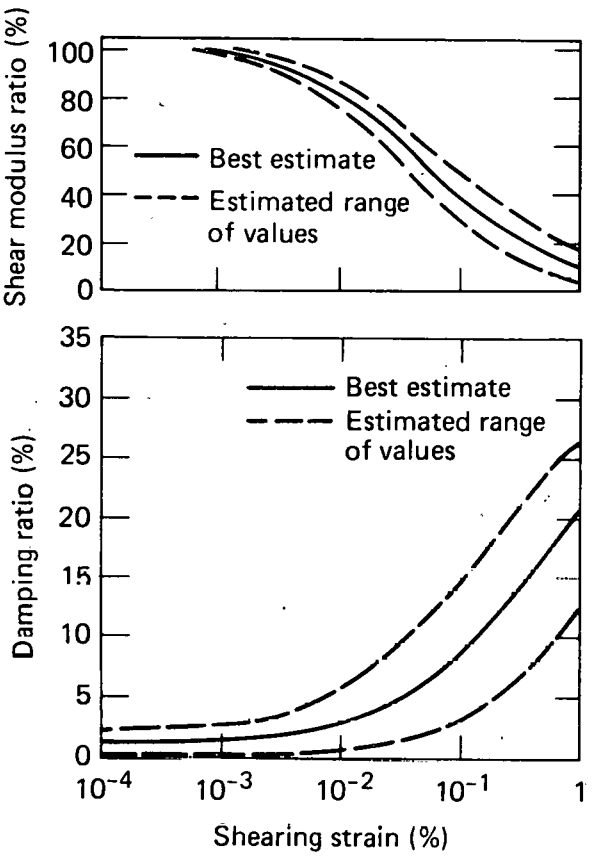

Fig. 4.6. Variation of soil shear modulus ratio and damping ratio with strain level.

define their values precisely. Although we fully recognize the need to consider parameter variations, especially in a design context, our present comparison was based on the "best estimate" curve.

The nonlinear behavior of soil was taken into account in both analyses by using equivalent linear techniques. The basic procedure was iterative; maximum strains were computed at representative points for each soil sublayer or finite element. Values of shear modulus and damping corresponding to a characteristic strain (65% of maximum in our analysis) were obtained from the curves shown in Figs. 4.5 and 4.6. A new analysis was then performed using the soil properties so determined. The process was continued until soil properties obtained in two consecutive analyses differed by less than the specified tolerance.

Because only the "primary nonlinearity" is treated in the CLASSI analysis (paragraph 3.2), this iterative process was applied to the free-field ground-motion problem. The soil profile was discretized into a series of uniform layers, and a one-dimensional wave propagation analysis was performed. The excitations were vertically propagating shear and dilatational

waves, normalized to a peak acceleration of 0.2 g on the soil surface. The resulting equivalent linear material properties are shown in Fig. 4.7, discretized for the FLUSH analyses. Figure 4.7 also depicts the discrete soil-layer model input to CLASSI. The mass density and Poisson's ratio assumed for the analyses are summarized in Table 4.1.

Two cases were considered in the FLUSH analysis. The first, referred to as "free-field properties," corresponds to the representation of material properties discussed above. The second case is a result of applying the iterative process to the coupled soil-structure system, which accounts for both "primary" and "secondary" nonlinearities. We refer to this case as "iterated properties."

Finally, in both cases we assumed a constant Poisson's ratio, which implies that bulk behavior of soil is functionally the same as deviatoric behavior. It is doubtful, however, that the degradation of stiffness observed in shear behavior also occurs in bulk behavior, especially for saturated soils. This assumption requires further evaluation beyond the scope of this study.

4.3 THREE-DIMENSIONAL STRUCTURAL MODELS

Three structures were included in our SSI analysis--the two reactor buildings, which we assumed were identical, and the AFT complex. Detailed

TABLE 4.1. Summary of soil properties.

Soil depth (ft)	Mass density ($lb\text{-}sec^2/ft^4$)	Poisson's ratio	Description
0-6	3.6	0.39	Lake deposits above water table
6-36	4.1	0.39	Lake deposits below water table
36-111	4.4	0.46	Glacial till
111-	5.0	0.27	Niagara dolomite

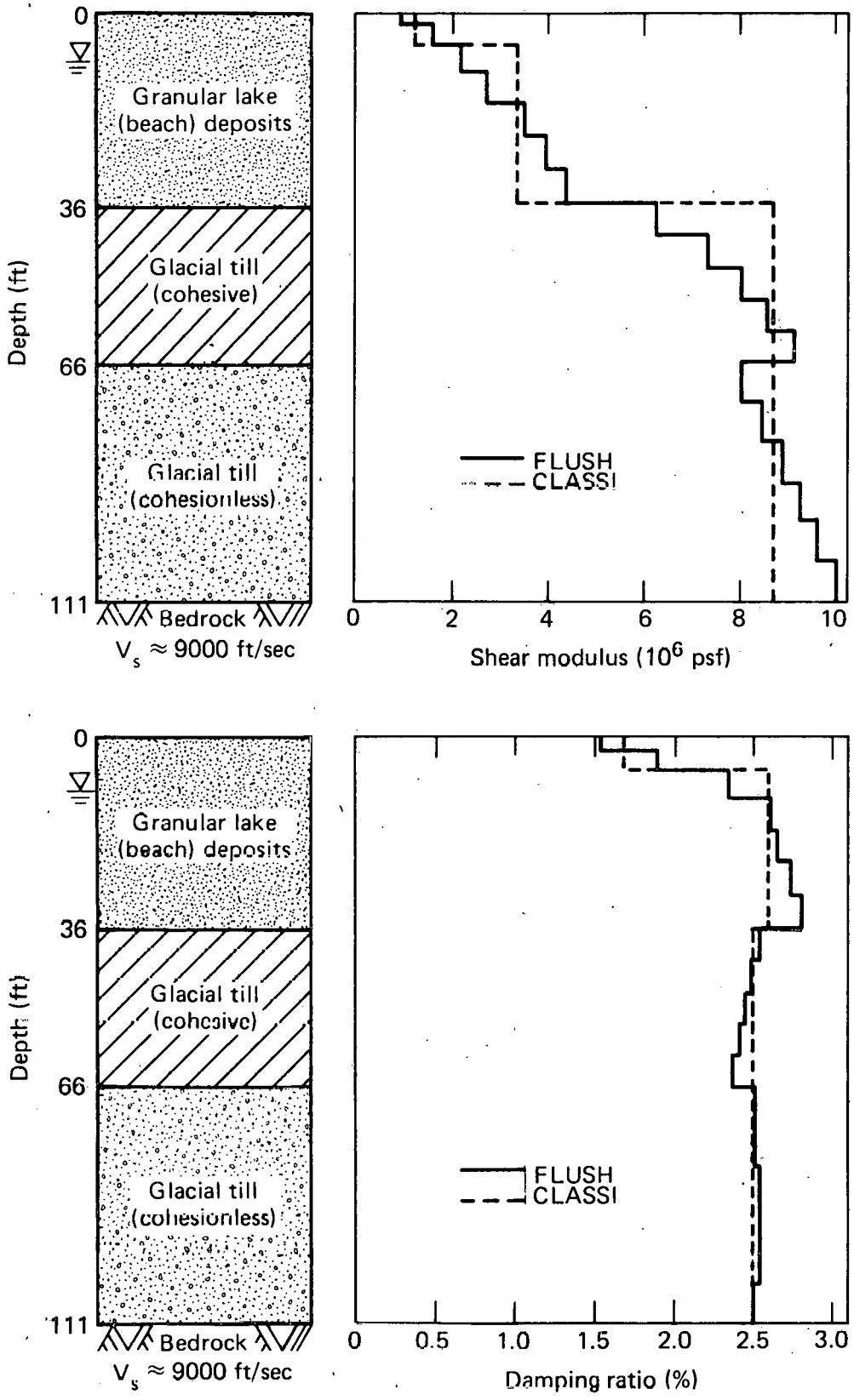

FIG. 4.7. Equivalent linear free-field soil properties used for CLASSI and FLUSH analyses.

three-dimensional structural models developed for the SSMRP response calculations[6] were used in our CLASSI and FLUSH analyses. These models are capable of defining in-structure response at a large number of points, and their sophistication reflects current state-of-the-art "best estimate" modeling. The solution procedure in the final step of the substructure approach, as implemented by CLASSI, permits the incorporation of extremely detailed structural models (paragraph 3.2). In fact, the structural models discussed here were used directly in the CLASSI analysis. A two-stage analysis was performed with FLUSH. In the first stage we used simplified structural models based on their detailed counterparts as described in paragraph 4.5. In the second-stage analysis we used the detailed structural models.

The fixed-base dynamic characteristics of the structural models were obtained and serve as the basis of the following discussion. Table 4.2 contains a summary of the important vibrational modes of these models. A detailed description of the structures and the way in which they were modeled may be found in Ref. 6.

4.3.1 Reactor Building Models

The two reactor buildings (Units 1 and 2) were constructed as mirror images. For the purposes of this study, the structures were assumed to be identical and were represented by the same models. As the containment shell and the internal structure composing the reactor building are connected only through the basemat (Section 2.0), we modeled each structure separately.

The containment shell was modeled using a series of vertical beam elements, with shear and bending characteristics appropriate for a circular cylindrical shell. Masses and rotational inertias were lumped at nodal points. Inertias affecting both bending and torsional response of the shell were included. The top element was assigned special stiffness properties to simulate the response of the elliptical dome. We investigated two fixed-base conditions--one in which the shell was fixed at its basemat and one in which it was fixed everywhere along the soil-structure interface. We found that the difference in coupled SSI response was minimal in the two cases, and we used the latter in the analysis. This is consistent with the basic assumption in the CLASSI analysis that there is a rigid embedded cylindrical boundary at the soil-structure interface. The model of the containment shell included 12

TABLE 4.2. Summary of significant structural modes. Table includes all modes having at least 5% mass participation.

Mode number	Frequency (Hz)	Participating mass (%)	Mode description
Reactor containment shell			
1	4.8	77.6	First N-S shear mode
2	4.8	77.6	First E-W shear mode
3	8.5	84.6	First torsional mode
4	12.0	92.3	First vertical mode
5	14.8	16.0	Second N-S shear mode
6	14.8	16.0	Second E-W shear mode
Reactor building internal structure			
1	6.5	10.8	E-W lateral, steam generators
17	12.9	6.8	E-W lateral, pressurizer compartment
20	14.0	11.5	Vertical, NSSS
22	14.3	6.9	E-W lateral, reactor coolant loop
		15.6	N-S lateral reactor coolant loop
23	14.5	17.7	E-W lateral, reactor coolant loop
24	15.4	8.5	N-S lateral, steam generators
25	16.2	17.9	E-W lateral, steam generators
26	17.2	15.6	N-S lateral, steam generators
29	19.4	13.8	Torsion mode
39	22.6	12.5	N-S shear mode
44	25.8	10.1	Torsion mode
46	26.7	11.2	Torsion mode
54	31.7	11.1	Vertical mode

TABLE 4.2 (cont'd)

Mode number	Frequency (Hz)	Participating mass (%)	Mode description
AFT complex			
6	3.7	18.4	Torsion mode, turbine pedestal
7	3.7	17.4	E-W lateral, turbine building
8	3.8	25.8	Torsion mode, turbine building
11	4.8	17.4	N-S lateral, turbine building
12	4.9	6.9	E-W lateral, turbine and diesel generator buildings
21	8.5	21.3	E-W lateral, auxiliary building
22	8.8	6.6	N-S lateral, fuel-handling and auxiliary buildings
22	8.8	7.1	Torsion mode, fuel-handling and auxiliary buildings
24	9.9	6.5	N-S shear, turbine building
30	11.3	5.1	Vertical, auxiliary building
34	13.2	6.7	Vertical, auxiliary building
38	14.4	5.5	Vertical, fuel-handling and auxiliary buildings
65	21.2	9.2	E-W shear, auxiliary building

modes below 33 Hz, and it was used for both the FLUSH and CLASSI analyses so that in-structure response could be directly compared. Two-percent damping was used for all modes.

The reinforced concrete internal structure was represented by a three-dimensional finite element model consisting of plate and beam elements and included a simplified model of the NSSS. Important modes are itemized in Table 4.2. The internal structure model contained about 3800 structural degrees of freedom; 60 modes, with 2% damping, were used to represent its dynamic characteristics up to 33 Hz.

4.3.2 Model of the AFT Complex

The finite element model of the AFT complex employed thin plate and shell elements to represent the concrete shear walls, and beam and truss elements to model the braced frames. To reduce the number of dynamic degrees of freedom in the modal representation of this extremely complicated structure, mass was lumped at selected node points, leaving other node points massless. This method reduces the number of dynamic degrees of freedom, yet retains the more detailed stiffness definition of the model for computing modal characteristics. The location and number of lumped-mass points were chosen to minimize the errors this procedure introduces on the response in the auxiliary building area and to suppress "local modes" in the turbine building.

The size of the model was further reduced by taking advantage of the structure's planar symmetry around the centerline of the auxiliary and fuel-handling buildings. Applying symmetrical and antisymmetrical boundary conditions at the centerline, we used a half-model to obtain the symmetrical and antisymmetrical modes of the full structure. In total, 113 modes were used to represent the dynamic characteristics of the AFT complex. Two-percent damping was used for all modes.

4.4 CLASSI SSI ANALYSIS

As discussed in paragraph 3.2, the substructure approach divides the SSI problem into a series of simpler problems, solves each independently, and superposes the results. There are three steps to the final solution: determination of the foundation input motion, determination of the foundation

impedances, and analysis of the coupled soil-structure system. All calculations are performed in the frequency domain.

The first two steps depend on the characteristics of the soil and the geometry and stiffness of the foundations. For our CLASSI analyses, we modeled the vertical distribution of free-field soil properties (Fig. 4.7) with three soil layers and an underlying halfspace, using the average soil properties (modulus and damping) within each layer. Preliminary calculations indicated that this model of the soil adequately represented its behavior in the CLASSI analyses.

We computed the soil impedances and foundation input motions for the reactor building foundations assuming that they were rigid cylinders with radii of 78.5 ft, embedded 36 ft in soil. A previous study by Wong and Luco[2] concluded that embedment of the reactor building foundation has a significant effect on reactor building response to earthquake excitations and warrants the additional computational effort necessary for embedded foundations. The above assumptions are realistic for the reactor building foundations, as they give an accurate representation of the actual geometric conditions.

We modeled the foundation of the AFT complex as a flat, T-shaped surface foundation having the same plan configuration as the deeply embedded portions of the actual structure. We corrected the impedances for embedment based on studies which indicated that embedment has a significant effect on horizontal translations, due largely to radiation damping effects. Foundation input motion was generated for an equivalent embedded cylinder discussed below.

We modeled foundation-to-foundation interaction effects using the same methods as described above. The reactor building foundation impedances were computed for an embedded cylinder. The AFT foundation impedances were for a flat T-shaped surface foundation corrected for embedment. Impedance terms for interaction between foundations were computed for the multiple flat surface foundations. The terms of the scattering matrix were the same as those for the individual isolated foundations, with no coupling terms between foundations.

The final step in the substructure approach is to perform the actual SSI analysis. The results of the first two steps are combined with dynamic models of the structures to solve the equations of the coupled soil-structure system. The structure's dynamic characteristics are projected as modal participation factors to a reference point on the foundation where SSI

response of the foundation is determined. For a single rigid foundation, the SSI response computation requires simultaneous solution of, at most, six complex-valued equations for each frequency. The models used for the CLASSI analyses are the detailed three-dimensional structural models described in Section 4.3.

Each step of the substructure approach is discussed in the following paragraphs.

4.4.1 Foundation Impedance Studies

Foundation impedances are complex-valued, frequency-dependent functions relating the dynamic forces the foundation exerts on the soil to the resulting soil displacements. Impedance functions depend on the geometry and flexibility of the foundation and on the dynamic characteristics of the soil deposit. For a single rigid foundation, the impedance functions are defined for each frequency by a 6 x 6, complex-valued matrix. Each complex term in the impedance matrix can be regarded as a pair of normalized coefficients representing the soil's stiffness and damping effects.[7]

Reactor Building. Figure 4.8 shows representative impedances for a rigid embedded cylinder with a radius of 78.5 ft and an embedment depth of 36 ft. We used this idealization for the foundations of the reactor buildings. The left half of each figure shows the real part of the impedance, which represents the stiffness of the foundation-soil system. The right half shows the imaginary part divided by frequency, which represents energy dissipation in the soil medium, including both radiation and material damping. These impedances are the same as those used by Wong and Luco[2] for their sensitivity studies.

AFT Complex. Significant effort was devoted to modeling the foundation of the AFT complex. Our final model (for impedances) idealized it as a flat, T-shaped surface foundation corrected for embedment effects. In arriving at this idealization, several cases were investigated and are itemized below. (In all cases, the bottom of the foundation was assumed to lie 42 ft from

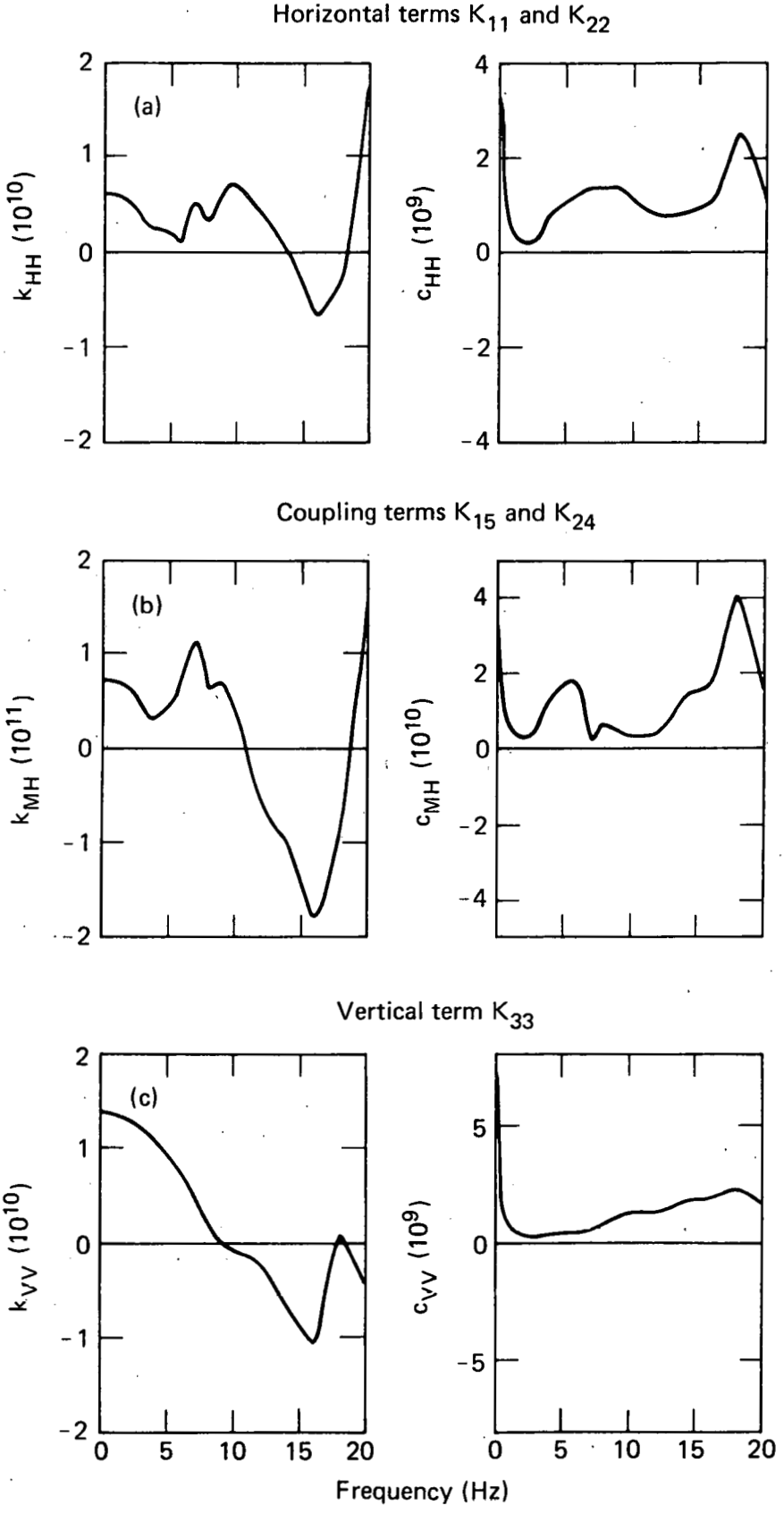

FIG. 4.8. Reactor building impedance functions. The following terms are shown: (a) horizontal terms K_{11} and K_{22}, (b) coupling terms K_{15} and K_{24}.

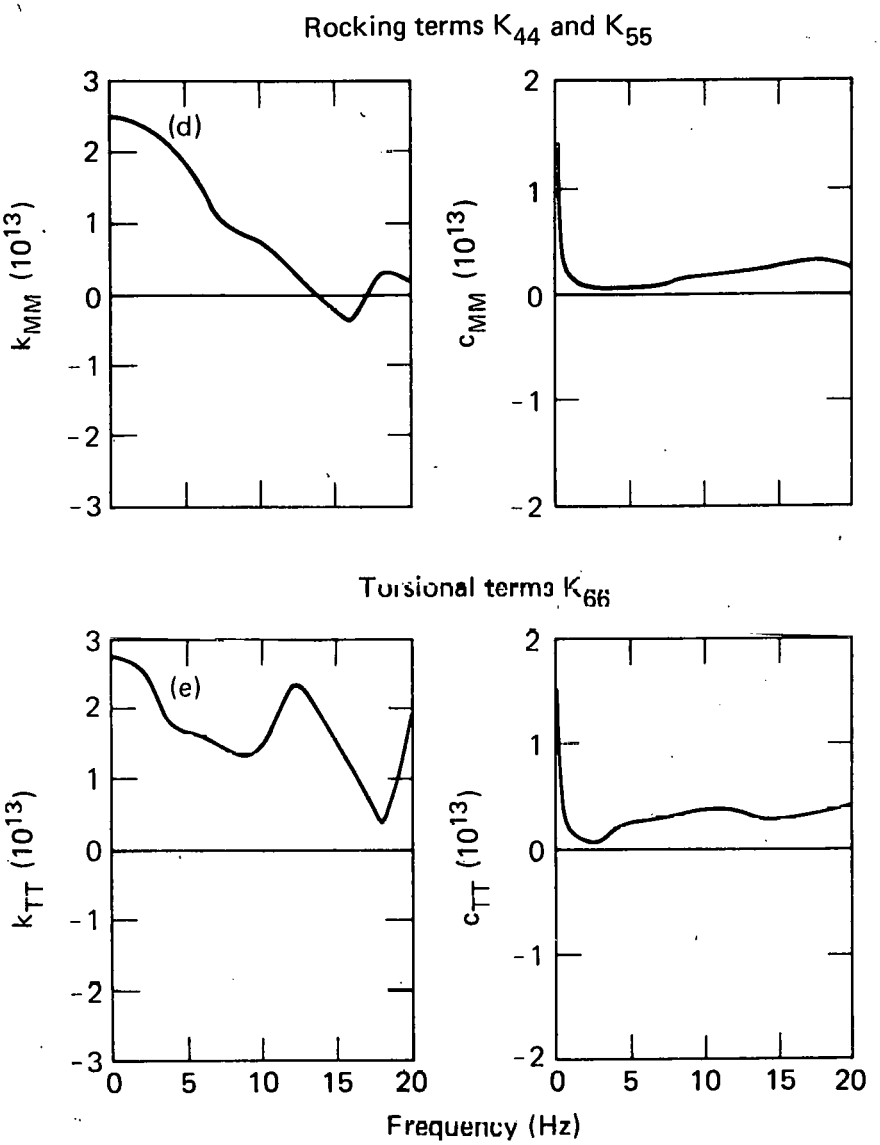

Fig. 4.8. (Continued). (c) vertical term K_{33}, (d) rocking terms K_{44} and K_{55}, (e) torsional terms K_{66}.

the soil surface, which corresponds to the average soil depth of the actual foundation.) The cases examined in significant detail were:

- Flat, T-shaped surface foundation. The flat, T-shaped foundation has the same configuration in the plan view as the deeply embedded positions of the actual structure. Figure 4.9 shows a plan view of the model's geometry, including the discretization used in computing the impedances. One advantage of this idealization is the retention of basic characteristics of the impedances, such as different horizontal and rocking impedances for the two horizontal

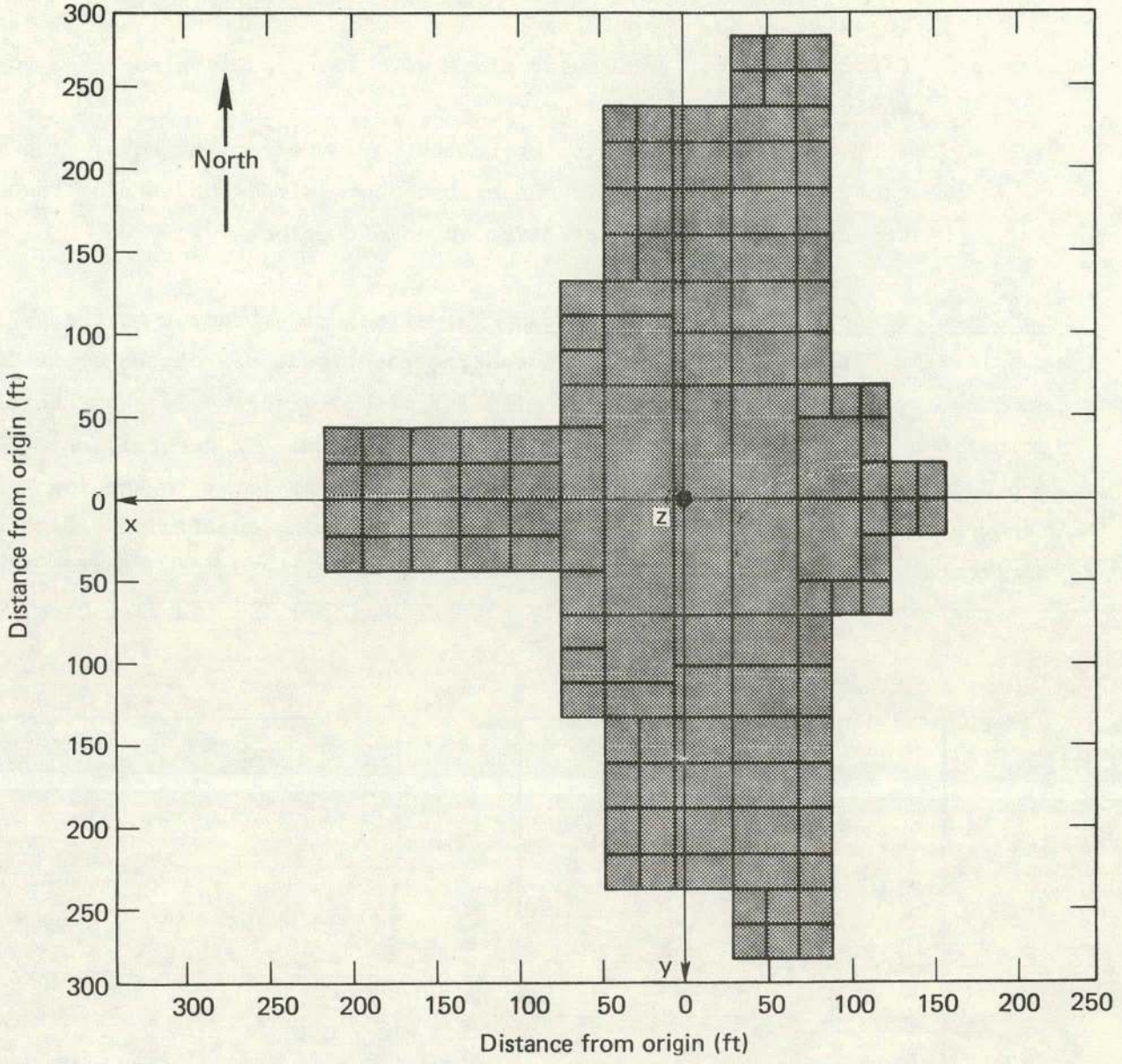

FIG. 4.9. Plan view of the AFT foundation model used for calculating impedances for CLASSI analyses.

directions. Note that the reference point (origin of coordinate system) is located approximately at the center of gravity of the foundation shape and was selected to minimize the coupling impedances between N-S horizontal and torsional motion, and vertical and E-W rocking motion, as discussed below.

- Equivalent embedded cylinder. A circular cylinder with dimensions selected to yield equal surface area and excavated volume to that of the actual foundation was considered. This resulted in an equivalent cylinder with a radius of 175 ft and embedment depth of

42 ft. Its impedance and scattering characteristics are discussed below.

- Circular plate. A circular plate with identical surface area to the equivalent embedded cylinder.
- Flat, T-shaped foundation corrected for embedment effects. The flat, T-shaped foundation described above with each term of the impedance matrix corrected for embedment effects.

Embedment effects for the AFT complex. The effect of embedment on the AFT complex impedances was assessed by comparing the impedances of the equivalent embedded cylinder with those of the circular disk. Figure 4.10 shows this comparison for horizontal, vertical and rocking terms. In general, the embedded and flat foundation impedances agree well, at least in the low frequencies. One exception worth noting is the damping coefficient for the horizontal term (Fig. 4.10a). From about 3 to 20 Hz the damping coefficient for the embedded case is consistently higher than that for the flat case, due

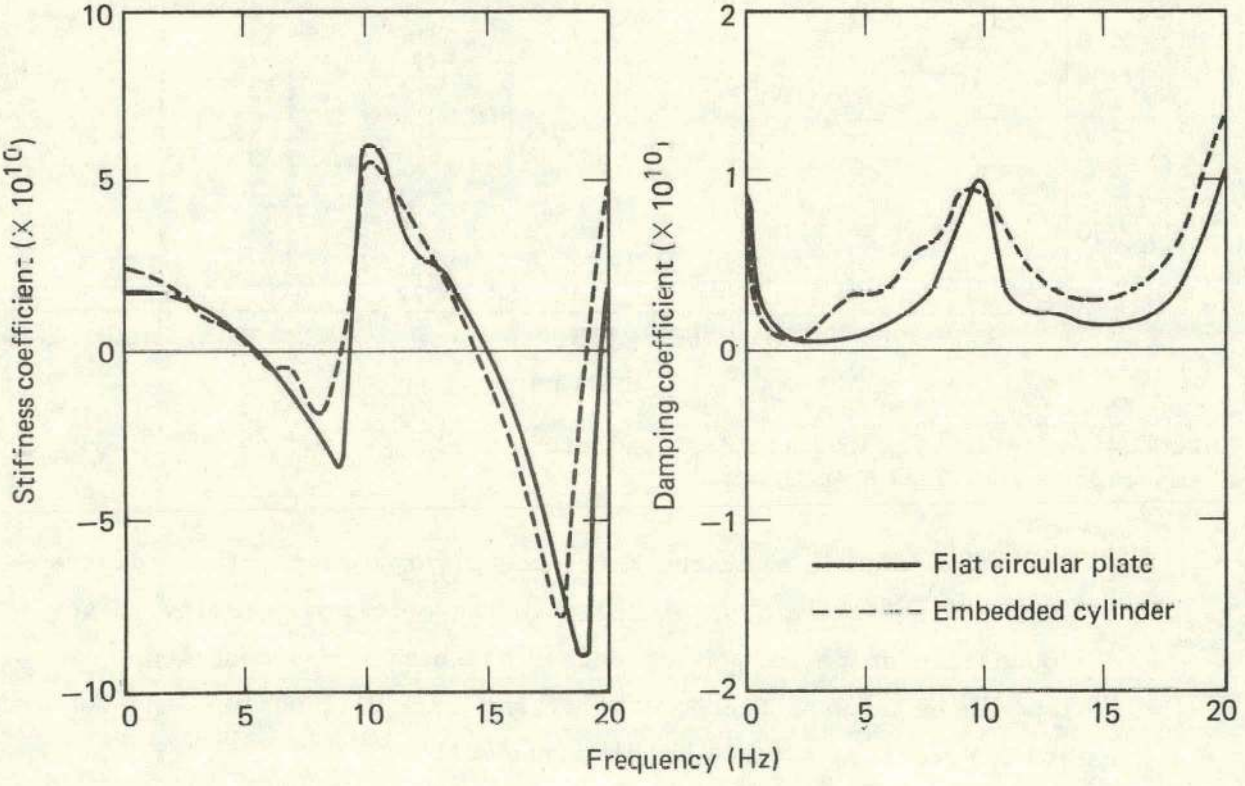

Fig. 4.10. Comparison of impedances for the flat circular plate and embedded circular cylinder of the AFT complex. Shown are (a) horizontal translation terms K_{11} and K_{22}.

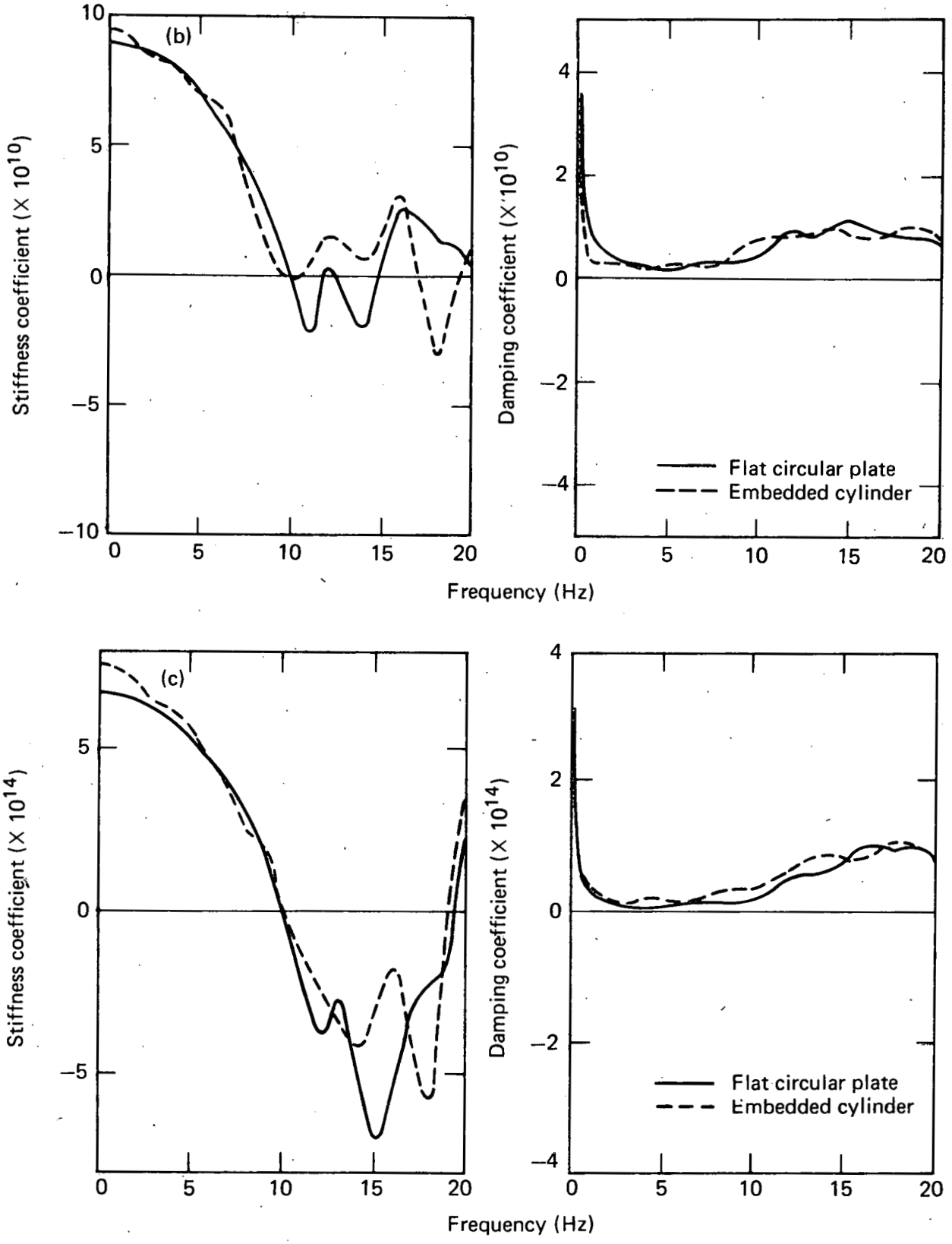

Fig. 4.10. (Continued). (b) vertical term K_{33}, and (c) AFT complex flat circular foundation, rocking term K_{44} and embedded circular cylinder, rocking term K_{55}.

to the effects of radiation damping. We found that this difference was significant; we performed SSI analyses of the AFT complex using impedances for both flat and embedded cases and found that the flat case gave us horizontal foundation response that showed spectral amplification greater than free-field values in the range from 3 to 5 Hz. This amplification was not present in the results from the embedded case. Hence, we concluded that embedment effects are significant for the AFT complex.

AFT complex foundation shape. The effects of foundation shape on the impedances were assessed by comparing the impedances for the flat circular plate described above with those of our flat, T-shaped foundation model. One effect is the coupling of translational and rotational motions caused by the foundation's lack of symmetry in the east-west direction. In the case of a circular plate, coupling impedances between horizontal translation and torsion, and between vertical translation and rocking, are zero at all frequencies due to symmetry of the foundation shape. For the AFT foundation, the location where these terms decouple varies with frequency and, in general, will not be the same for horizontal/torsional coupling as for vertical/rocking coupling. At low frequencies, however, where the impedances are dominated by soil stiffness, these locations remain fairly constant and close to that for the static solution. To decouple these impedance terms for our T-shaped foundation model (Fig. 4.9), we selected our reference point (the point at which the impedances were to be computed) on the centerline between Unit 1 and Unit 2, near the boundary between the auxiliary and turbine buildings. It was important to select the reference point minimizing these coupling terms when using and comparing with equivalent cylindrical or circular plate properties. Figure 4.11 shows our success in this regard. It compares the additional coupling terms (N-S translation/torsion and vertical translation/E-W rocking), which we desired to minimize as described above, with the more common E-W translation/E-W rocking and N-S translation/N-S rocking coupling terms, which are generally non-zero for the static solution. At low frequencies, below about 4 Hz, the additional coupling terms are very small. At higher frequencies their magnitudes increase, but they remain small relative to the horizontal/rocking coupling terms.

A second effect studied was differences in horizontal and rocking impedances between the two horizontal directions. These impedances will be identical for a cylindrical foundation with its reference point on the axis of

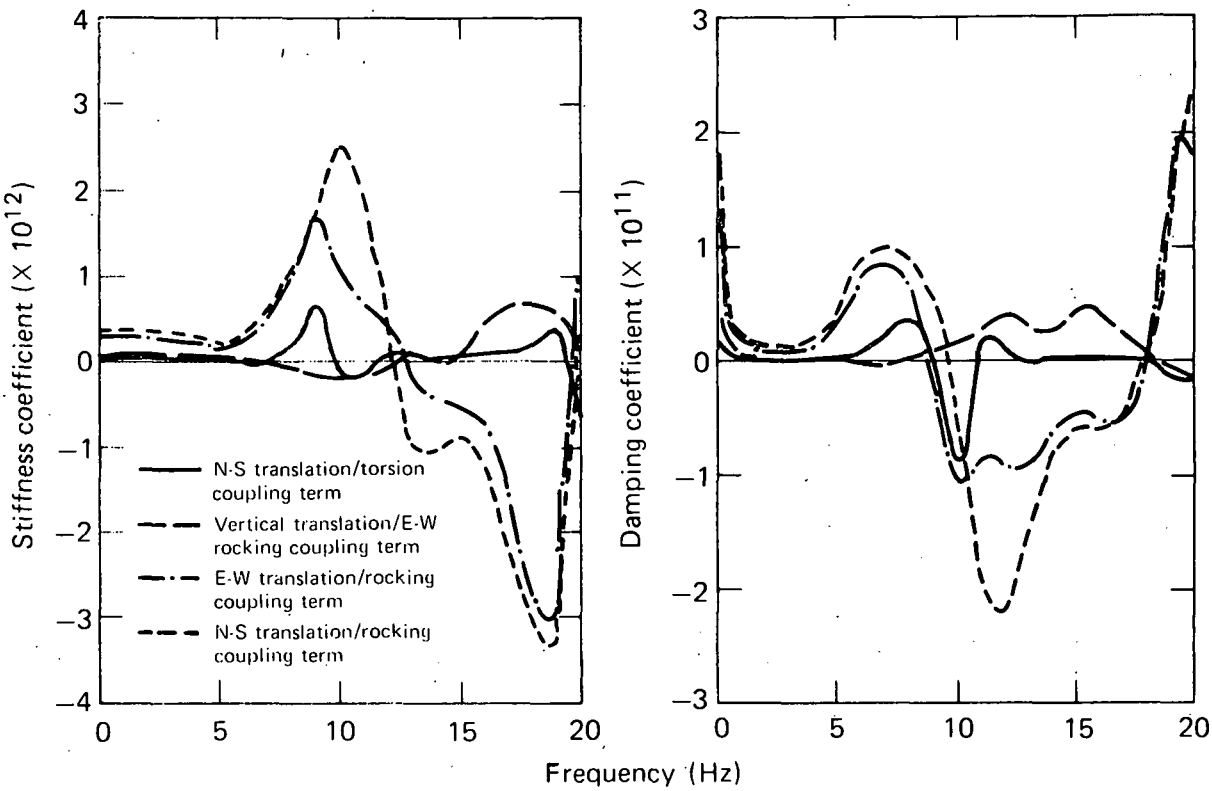

FIG. 4.11. Comparison of impedances for the flat T-shaped foundation of the AFT complex, showing the effect of shape on coupling terms.

symmetry, but not for an irregular configuration. The magnitude of the difference in rocking impedances depends on differences in rotational inertias of the foundation shape about the two horizontal axes. Figure 4.12 shows comparisons of the horizontal and rocking impedances for our T-shaped foundation, with the impedances for the flat circular plate overplotted. In Fig. 4.12a the horizontal impedances for the T-shaped case are quite similar and agree quite well with the flat circular plate case at all frequencies. Thus horizontal impedances do not appear to be affected much by foundation shape. The rocking impedances (Fig. 4.12b) show the greatest difference between the two directions. At almost all frequencies, rocking stiffness of the T-shaped foundation about the E-W axis (denoted here as N-S rocking) is three times as great as that about the N-S axis (identified as E-W rocking). The rocking stiffness for the circular plate lies between the two stiffnesses for the T-shaped foundation, being somewhat stiffer than the E-W rocking and significantly softer than N-S rocking.

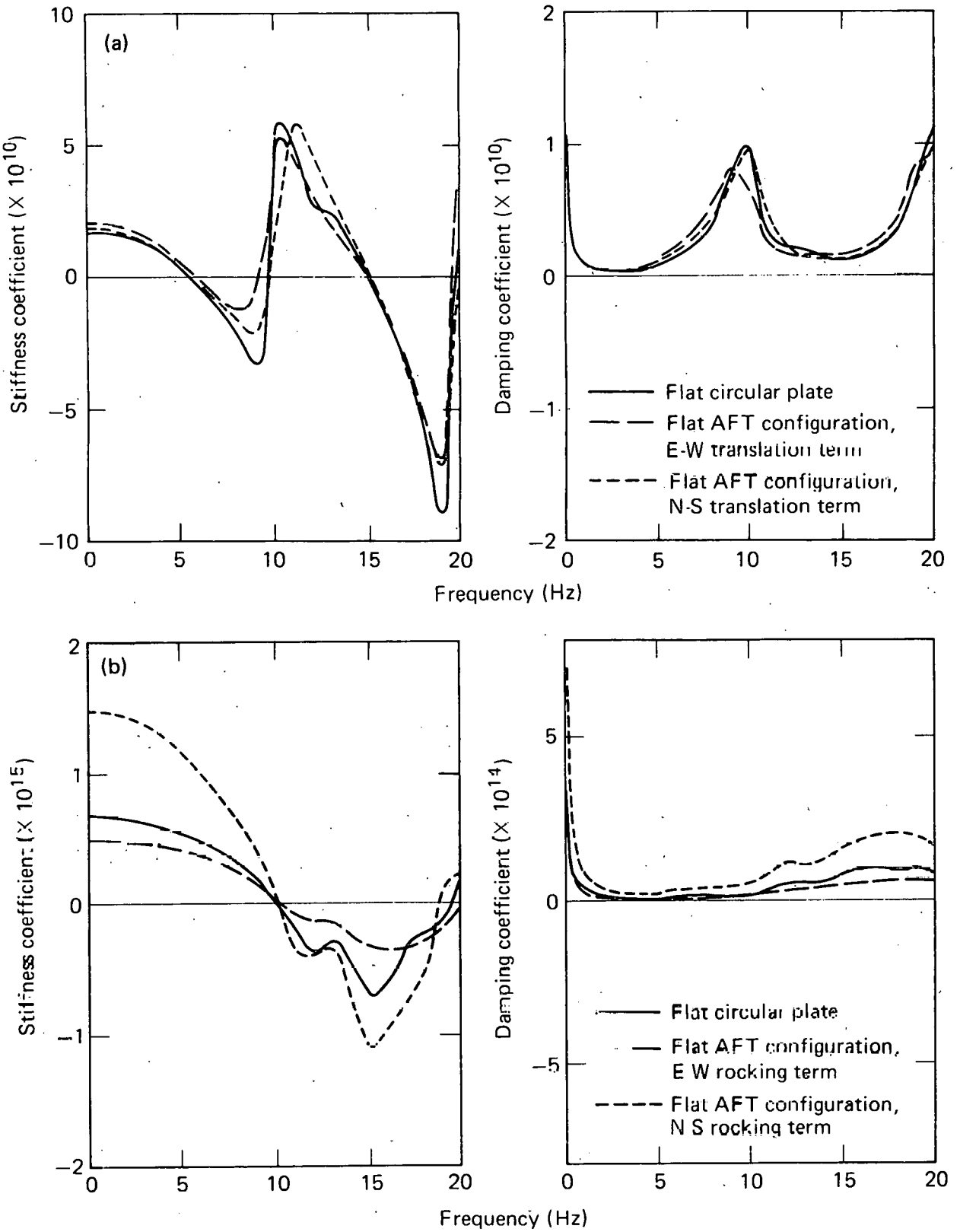

FIG. 4.12. Comparison of impedances for the flat circular plate and flat T-shaped configuration. (a) E-W horizontal term K_{11} and N-S horizontal term K_{22}, (b) E-W rocking term K_{55} and N-S rocking term K_{44}.

Corrected impedances for the AFT complex. Based on the studies described above, we concluded that the impedances for the AFT complex should include the effects of foundation shape and embedment. We accomplished this by using the impedances for the flat T-shaped surface foundation and applying a correction for embedment. This correction consisted of computing the differences, frequency by frequency, between the impedances for the equivalent embedded cylinder and the corresponding flat plate and adding these differences to the impedances for the T-shaped foundation. Figure 4.13 shows our final impedances, corrected for embedment.

4.4.2 Foundation Input Motion

"Foundation input motion" denotes the motion at the soil-foundation interface of a hypothetical massless structure and its foundation. This motion differs from the free-field ground motion in all cases, except for surface foundations subjected to vertically propagating waves. The two

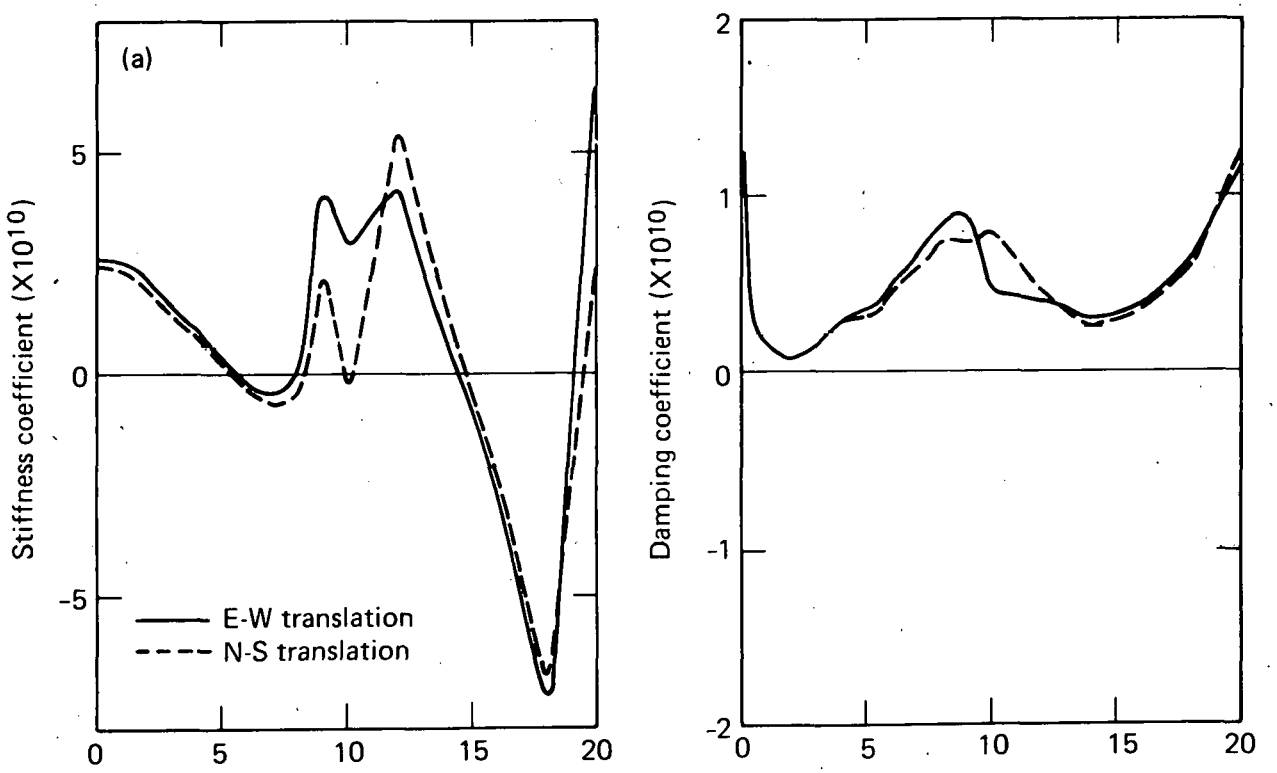

FIG. 4.13. Elements of the impedance matrix for the AFT foundation model corrected for embedment. Shown are (a) the horizontal components.

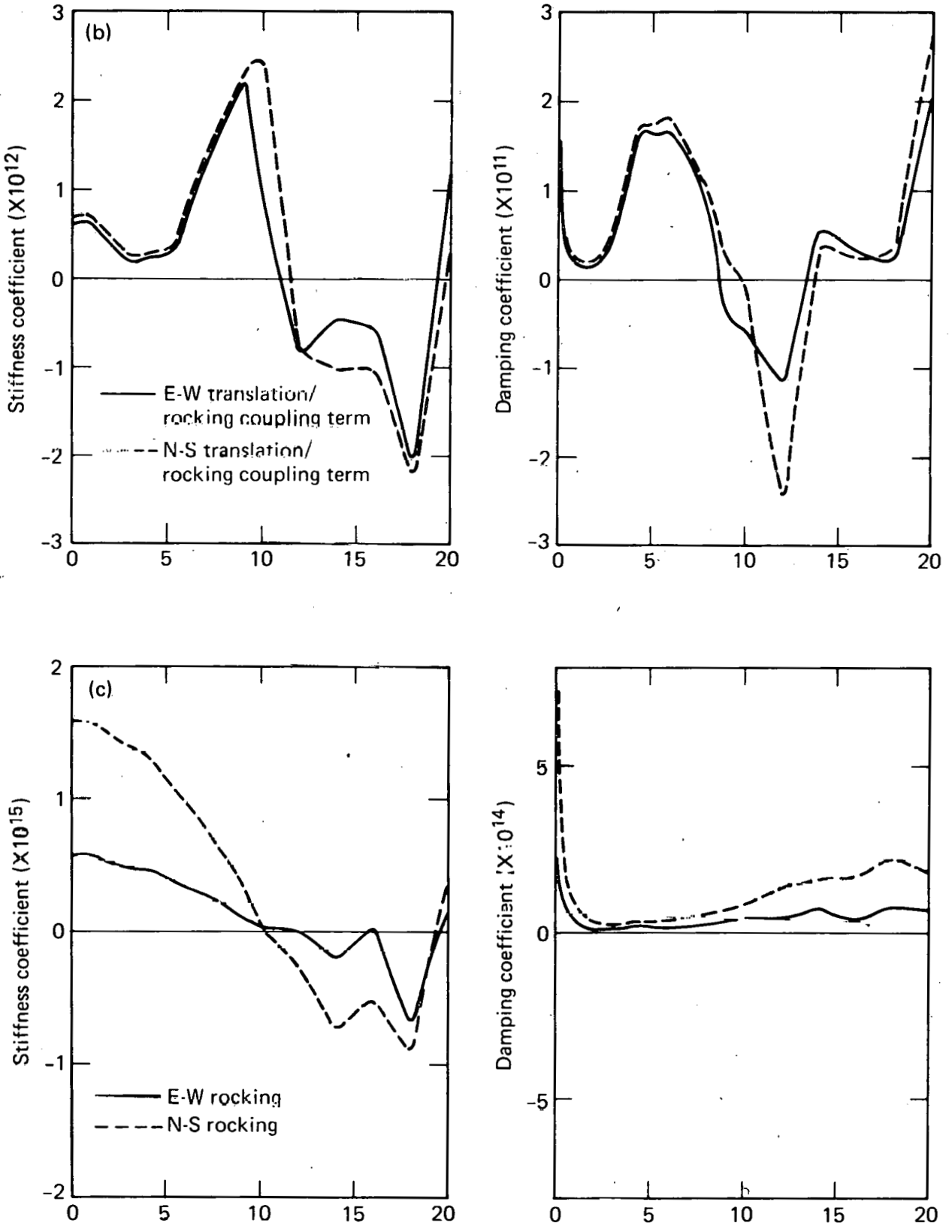

FIG. 4.13. (Continued). (b) the coupling impedances between horizontal and rocking components, (c) the rocking components.

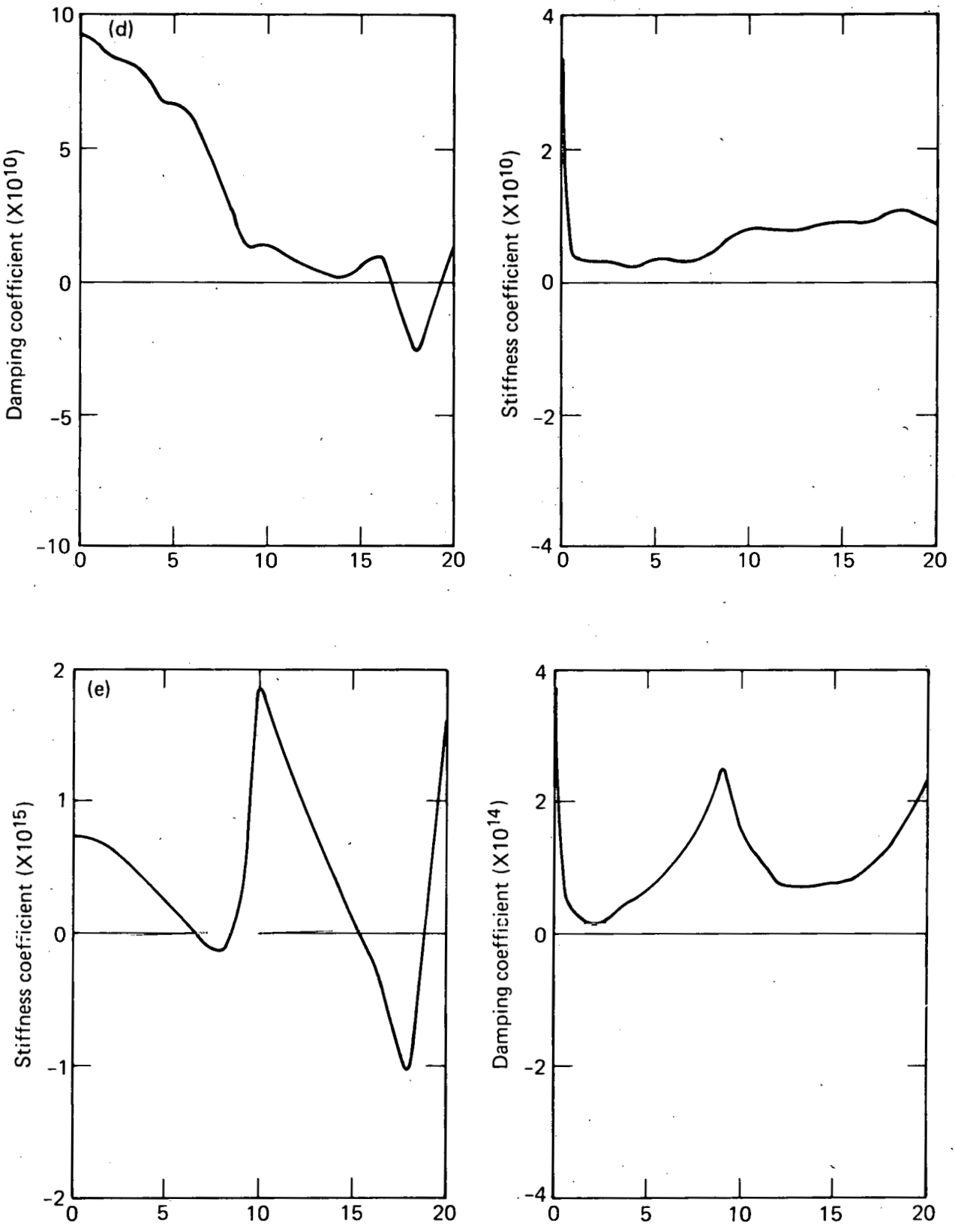

FIG. 4.13. (Continued). (d) the vertical component, and (e) the torsional component.

motions differ primarily for two reasons. First, the free-field motion varies with depth in the soil. Second, the soil-foundation interface scatters waves because points on the foundation are constrained to move according to the foundation's geometry and stiffness. When the effective stiffness of the foundation is large compared to that of the soil, rigid behavior can be assumed; the motion of the foundation is uniquely defined by six rigid-body degrees of freedom--three translations and three rotations. Foundation input motion is related to each component of free-field ground motion through a transformation defined by a complex-valued, frequency-dependent scattering vector. This relationship is defined at each frequency by a 6 x 3 scattering matrix reflecting the three components of free-field motion.

Reactor Building. Figure 4.14 shows components of the scattering matrix for the isolated reactor building. For our assumptions of vertically propagating

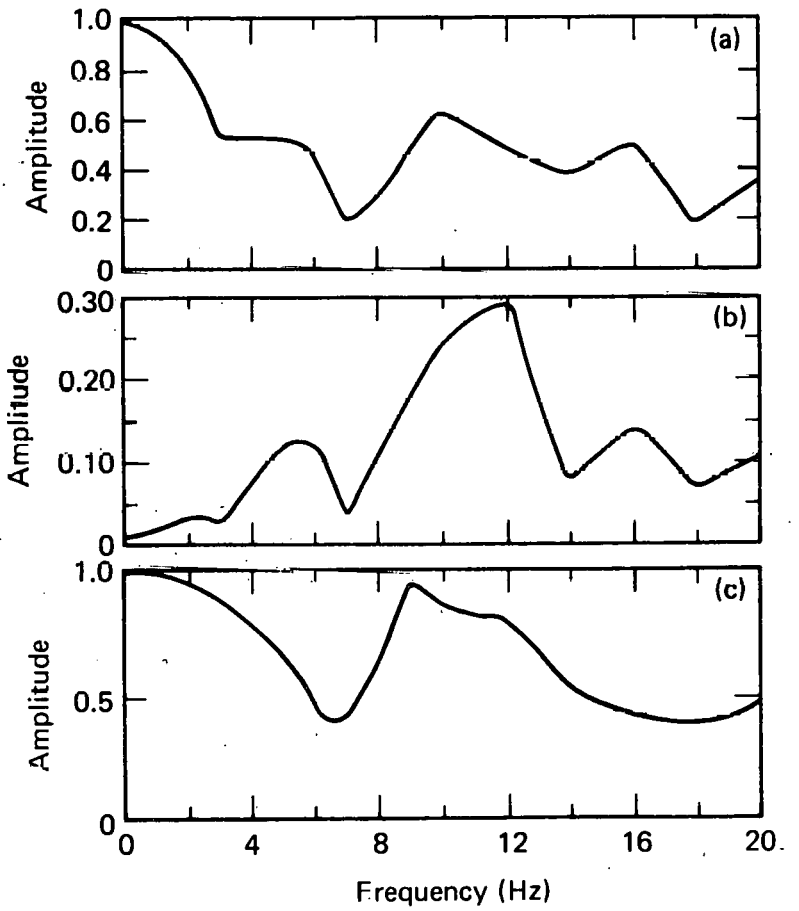

FIG. 4.14. Scattering matrix for the two reactor building foundations. Shown are (a) horizontal component caused by horizontal free-field motion, (b) rocking component caused by horizontal free-field motion, and (c) vertical component caused by vertical free-field motion.

shear and dilatational waves impinging on a rigid embedded circular cylinder, horizontal free-field motion produces coupled horizontal/rocking motion at the foundation. Because of symmetry, this effect is the same for both horizontal directions. Vertical free-field motion results in pure, decoupled vertical motion of the foundation. Torsional motion of the foundation is zero for vertically incident motions and axisymmetric foundations.

AFT Complex. For the AFT complex we used the scattering matrix for the equivalent embedded circular cylinder discussed previously. Wong and Luco[2] have shown that embedment effects can be significant for the foundation input motion. Figure 4.15 shows the horizontal, rocking and vertical scattering matrix components. Based on Wong and Luco's findings, we would expect the scattering matrix for the embedded cylinder to produce lower horizontal translation foundation input motions, at least at frequencies below about

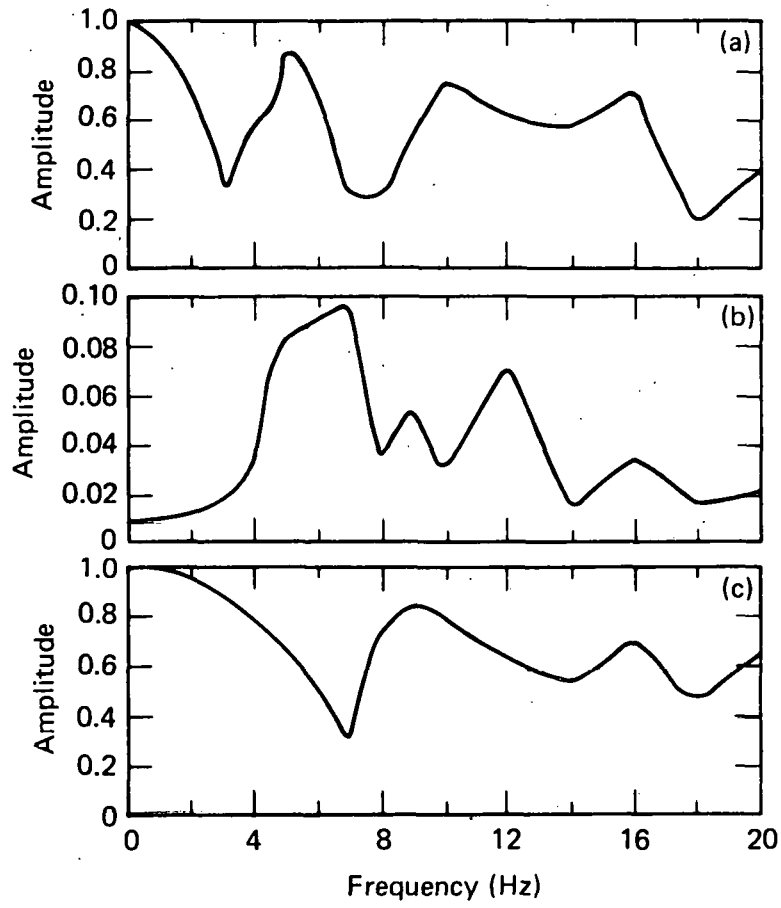

FIG. 4.15. Scattering matrix for the AFT foundation. Shown are (a) horizontal component caused by horizontal free-field motion, (b) rocking component caused by horizontal free-field motion, and (c) vertical component caused by vertical free-field motion.

5 Hz, than that which we would obtain by deconvolving the free-field motions to the elevation of the foundation. On the other hand, we would obtain rocking components from the embedded case that we would not obtain otherwise.

The complexity of the AFT foundation motivated us to study it using alternative techniques to gain more information concerning its behavior and the uncertainty in modeling its scattering effects. To accomplish this, we performed FLUSH analyses of N-S and E-W cross sections through the AFT foundation, assuming rigid massless properties for the structures and basemats. The cross sections correspond to Sections B-B and C-C of paragraph 4.5.

Transfer functions between free-field surface motions and foundation motions were computed with FLUSH to estimate components of the scattering matrix. Figure 4.16 compares the amplitudes of the scattering components for these two cross sections with those of the equivalent cylindrical foundation. Figures 4.16a and 4.16b show the horizontal and rocking terms caused by the horizontal free-field motion. Figure 4.16c shows the vertical term caused by vertical free-field motion. For horizontal free-field motion, the horizontal scattering terms (Fig. 4.16a) compare well for frequencies below 3 Hz. However, between 3 and 4 Hz, the horizontal terms from FLUSH fall well below that of the cylinder, and between 4 and 8 Hz they are significantly higher. Above 8 Hz the results for the embedded cylinder are higher than those from the FLUSH cross sections, especially in the range from 12 to 15 Hz. The rocking component (Fig. 4.16b) shows reasonably good agreement up to about 9 Hz, with FLUSH results generally higher where amplification occurs, and significantly higher at high frequencies. Thus, depending on the frequency content of the free-field motion and the resonant frequencies of the soil-structure system, we might expect higher horizontal and rocking foundation response from FLUSH or CLASSI in the ranges where their scattering values are higher.

There is a difference between the vertical scattering terms for vertical free-field excitation computed using FLUSH and CLASSI (embedded cylinder). This difference is in the frequency at which the minimum amplitude occurs (Fig. 4.16c). The CLASSI minimum occurs at about 7 Hz; the FLUSH at about 10 Hz. This difference also occurred for the reactor building scattering matrices. Additional studies initially indicate that this is not a result of

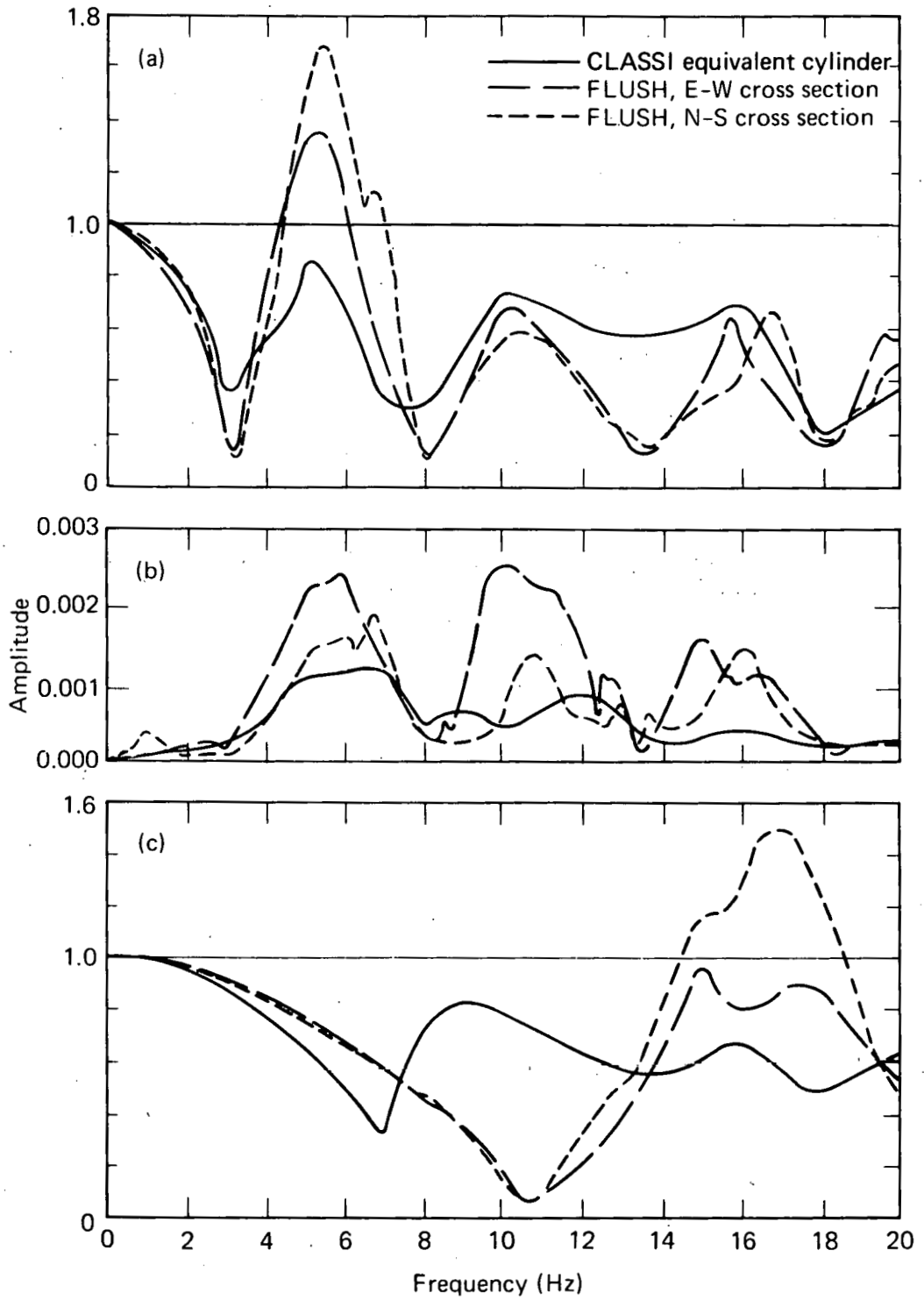

FIG. 4.16. Comparison of scattering matrix components for the CLASSI embedded cylinder and FLUSH models. Shown are (a) horizontal component caused by horizontal free-field motion, (b) rocking component caused by horizontal free-field motion, and (c) vertical component caused by vertical free-field motion.

the FLUSH assumption of a rigid boundary. Other possible causes, such as two- vs three-dimensional effects on soil stiffness, have yet to be studied. This is a subject that warrants further investigation.

Additional scattering terms resulted from the FLUSH analysis that do not occur for the embedded cylinder because of its symmetry. These terms are a vertical scattering term caused by E-W horizontal free-field motion and an E-W rocking term caused by vertical free-field motion. Both terms were obtained from the FLUSH E-W cross section, Section C-C (paragraph 4.5) and are a result of the asymmetry of that section. Because of the two-dimensional nature of the FLUSH analyses, we would expect these terms to be somewhat different for the T-shaped AFT foundation, and the vertical value would vary depending on its horizontal location in the cross section.

All of these analyses required simplifications. In the CLASSI analysis, a cylindrical shape was assumed. In the FLUSH case, plane strain analysis was performed, which does not duplicate three-dimensional behavior over the range of frequencies. In addition, our attempts to simulate a rigid foundation in the FLUSH analyses met with only partial success. Hence neither result can be considered exact, and differences are examples of uncertainty in SSI modeling.

4.4.3 Structure-Structure Interaction

We accounted for interaction between the foundations of the AFT complex and the two reactor buildings by computing impedances using flat, rigid surface foundations coupled only through the underlying soil layer. This was accomplished in much the same way as for the isolated AFT complex, except that the impedance matrix for each frequency was an 18 x 18 matrix, with the 6 x 6 off-diagonal blocks representing the coupling terms between the foundations. In the CLASSI algorithm, the compliance matrix is computed first and then inverted to obtain the impedance matrix. The 6 x 6 diagonal blocks of the compliance matrix were the same as those computed for the isolated foundations: the AFT foundation was modeled as a flat T-shaped foundation, corrected for embedment as described above, and the reactor building foundations were modeled as embedded cylinders. The coupling blocks were computed for multiple flat foundations. The inversion of the coupled compliance matrix results in an impedance matrix in which diagonal blocks have been modified from the isolated case to include approximate coupling effects.

Figure 4.17 shows a model of the coupled foundation system, including the discretization used in computing the impedances for the coupled foundations. Figures 4.18a-e show a comparison of isolated and diagonal block coupled impedances for the AFT complex. These comparisons show very little difference between the isolated and coupled foundations. The only significant difference occurs in the frequency range of 10 to 15 Hz. Figures 4.19a-e show the comparison for the reactor buildings. Again, with the exception of the horizontal/rocking coupling terms, the same observations can be made. The

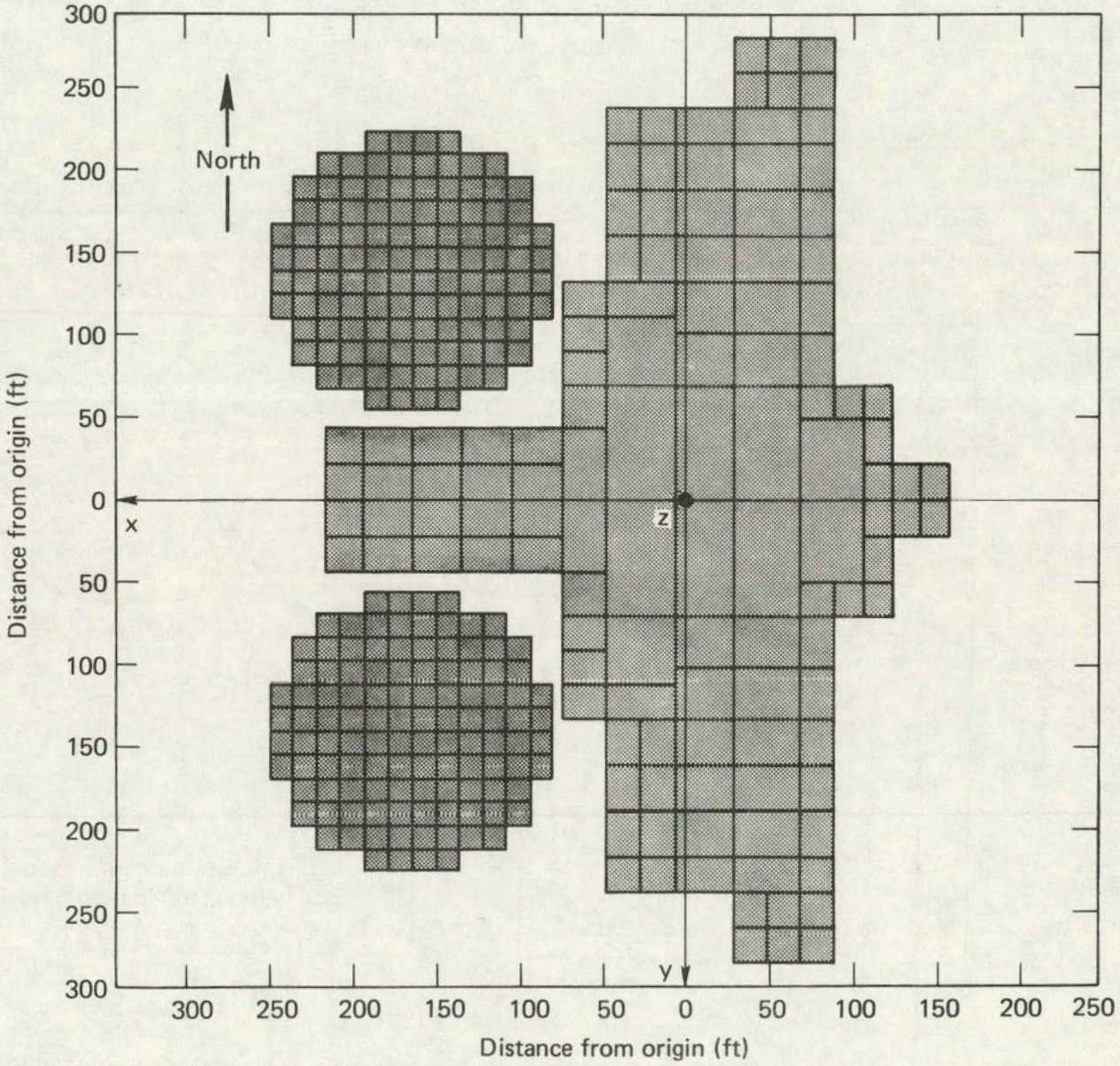

FIG. 4.17. CLASSI foundation model of the coupled AFT complex and reactor building foundations. The discretization used to compute impedance functions is shown.

horizontal/rocking terms, however, (Fig. 4.19b) are quite different, the isolated reactor foundation term being more than double the coupled foundation terms at low frequencies.

Figures 4.20a-b illustrate the coupling between foundations. Figure 4.20a shows the E-W horizontal terms for the AFT complex and the reactor building, compared with the term coupling the two foundations for the E-W translation. Figure 4.20b shows the same for the vertical translation. Note that, in general, the coupling terms for both components are significant when compared with the terms for the reactor building, but not when compared with the terms for the AFT complex. Thus we would surmise that, based on the soil impedances at least, structure-to-structure interaction would have a greater effect on the reactor buildings than on the AFT complex.

4.4.4 Dynamic Effects of Structures

Because of the way in which the substructure method is formulated, we were able to represent the dynamic effects of the structures on their

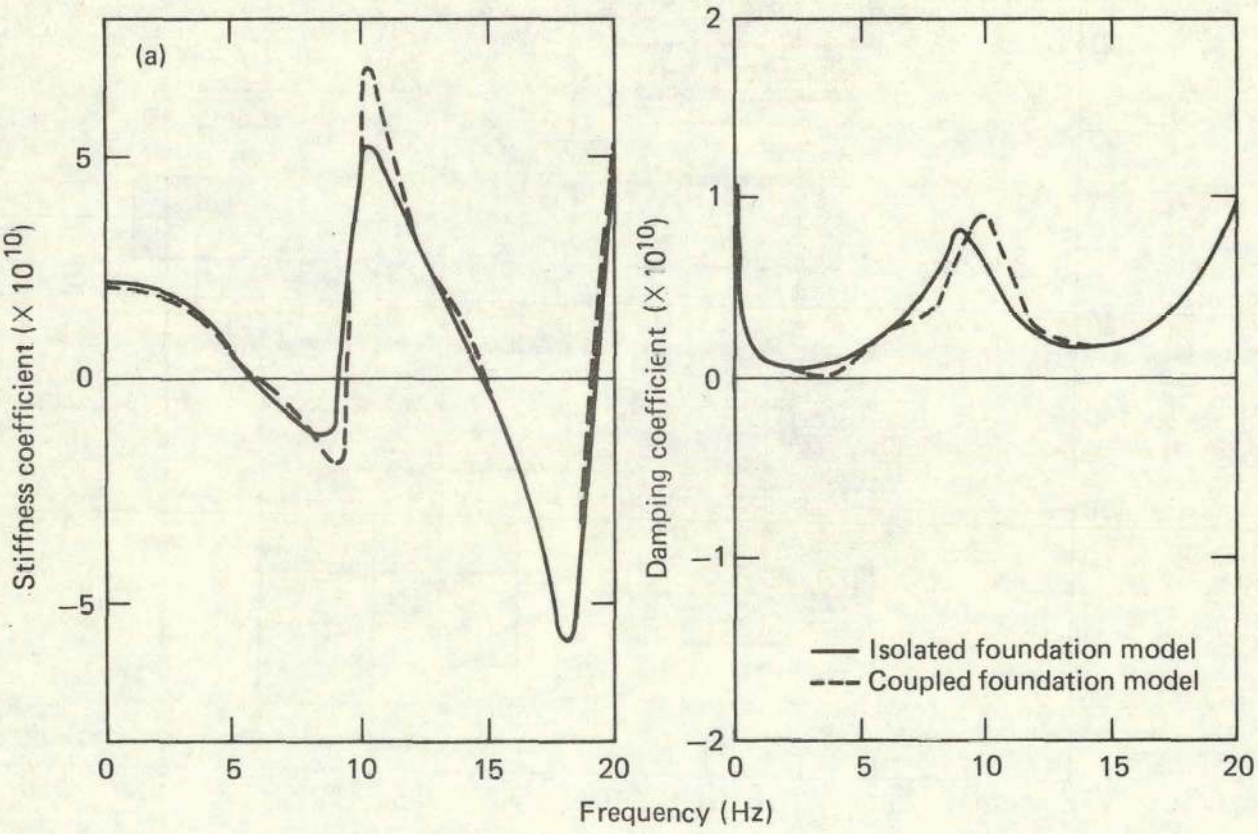

FIG. 4.18. Comparison of CLASSI impedance functions for isolated and coupled AFT foundation models. (a) E-W translation term K_{11}.

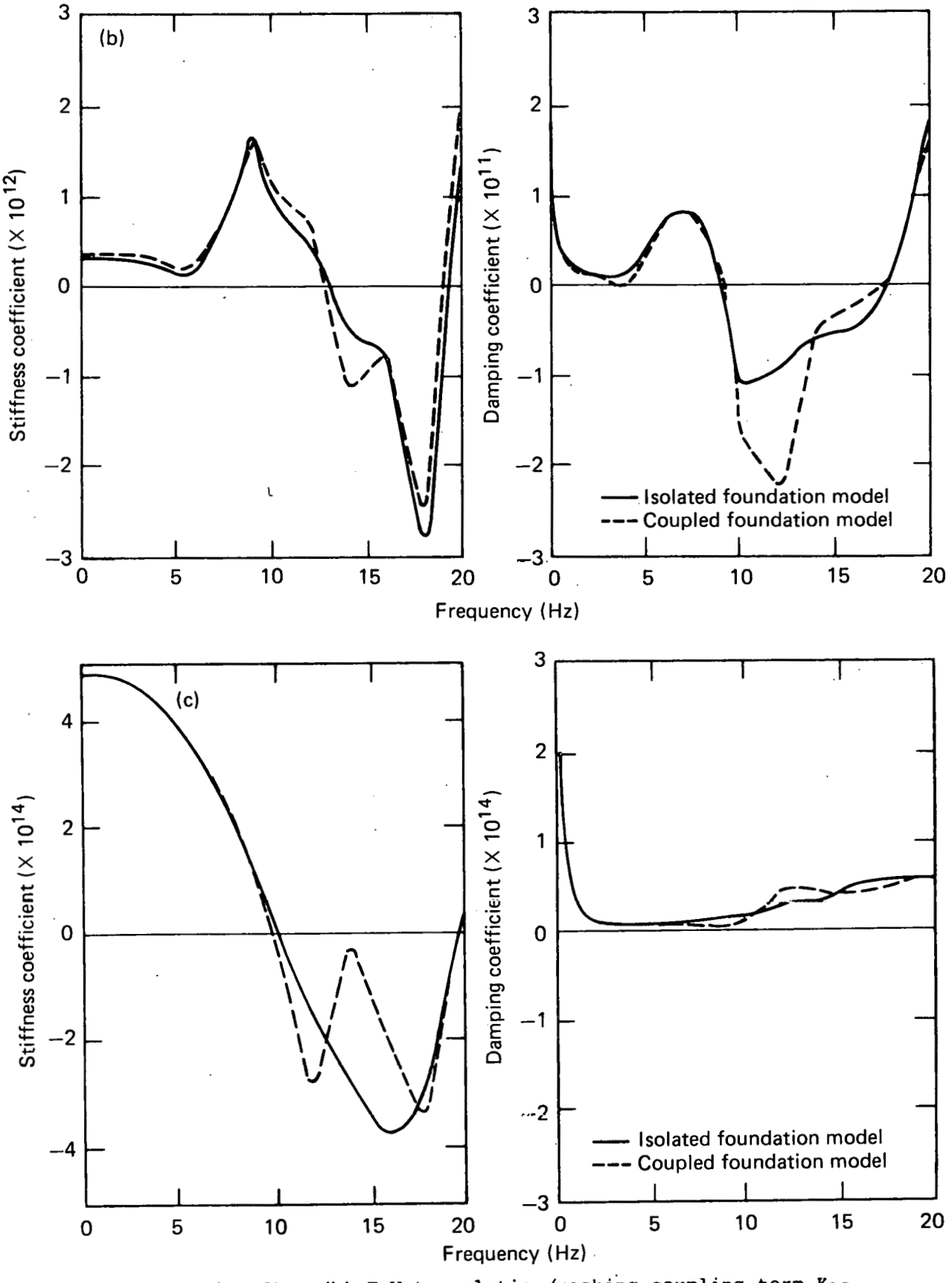

FIG. 4.18. (Continued). (b) E-W translation/rocking coupling term K_{15}, (c) E-W rocking term K_{55}.

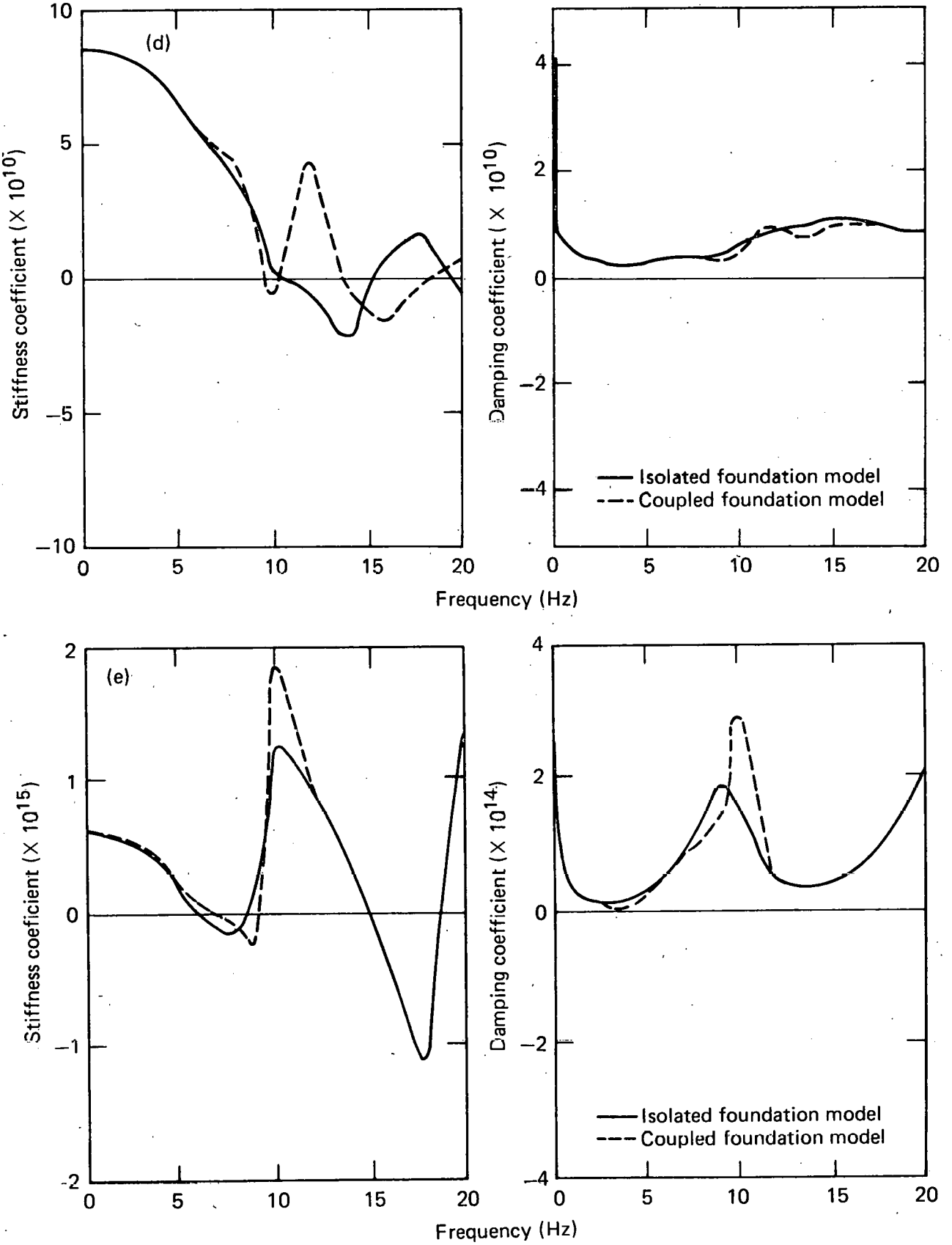

FIG. 4.18. (Continued). (d) vertical translation term K_{33}, and (e) torsional rotation term K_{66}.

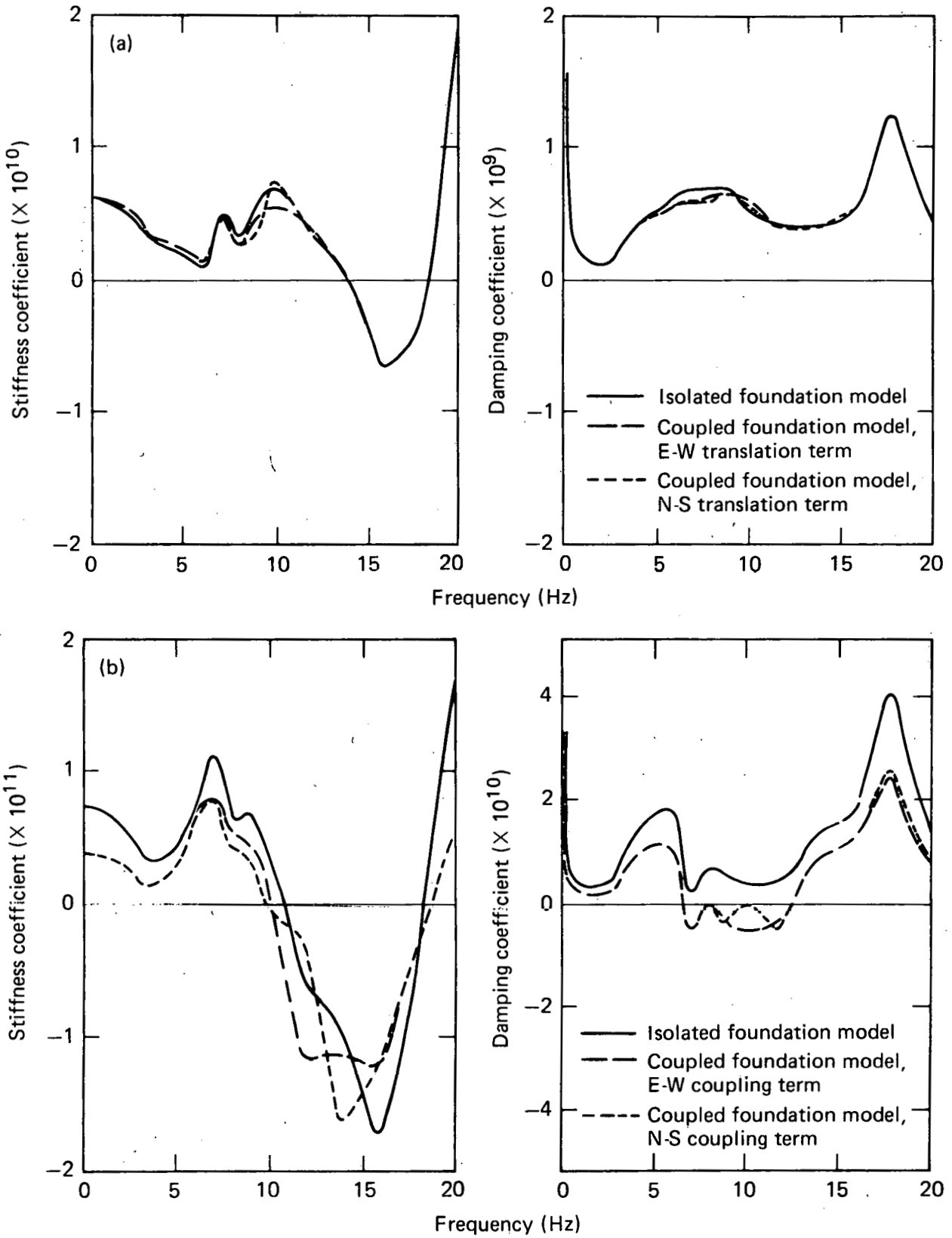

FIG. 4.19. Comparison of CLASSI impedance functions for isolated and coupled reactor building foundation models. (a) E-W horizontal translation term K_{11} and N-S horizontal translation term K_{22}, (b) E-W horizontal translation/rocking coupling term K_{15} and N-S horizontal translation/rocking coupling term K_{24}.

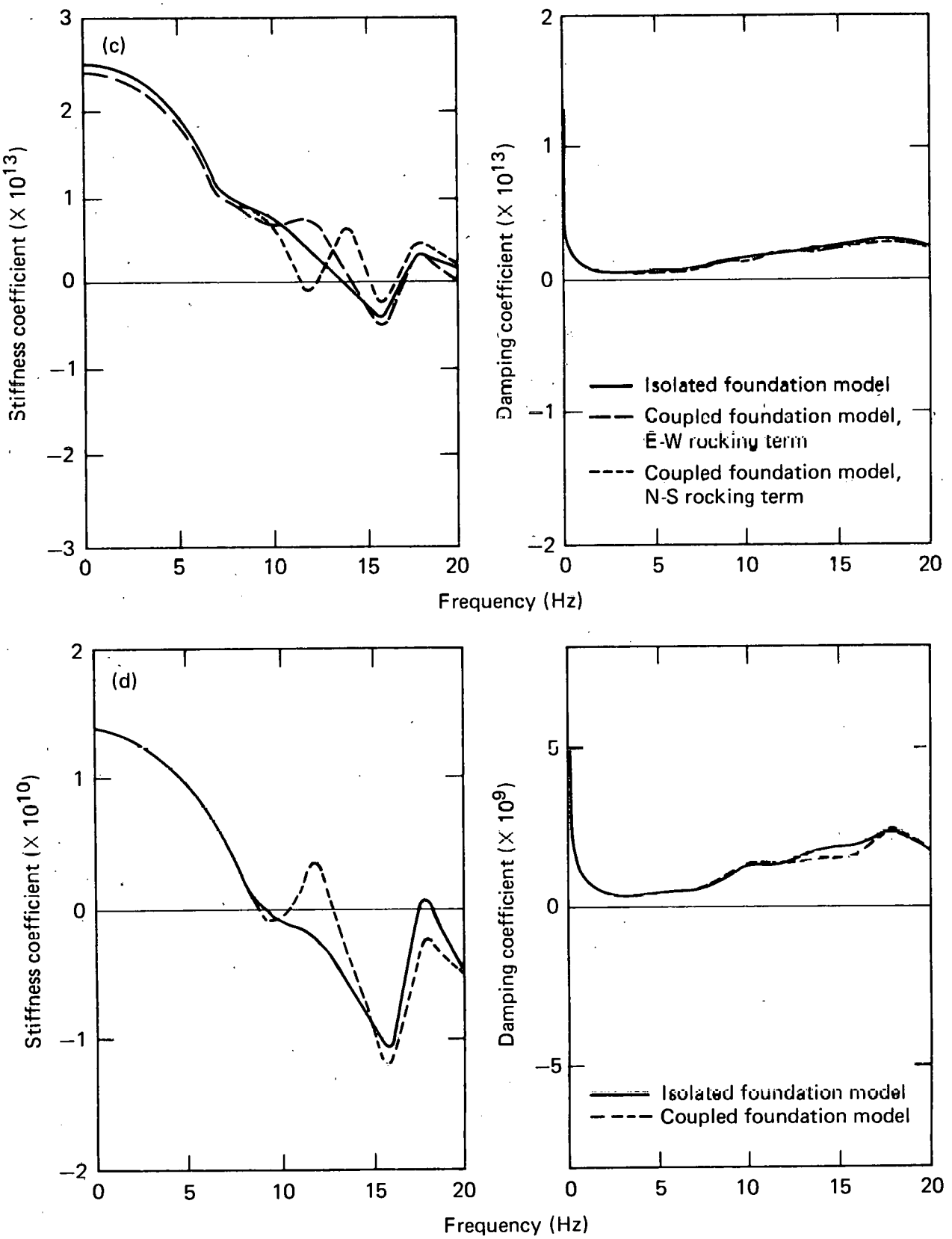

FIG. 4.19. (Continued). (c) E-W rocking term K_{44} and N-S rocking term K_{55}, (d) vertical translation term K_{33}.

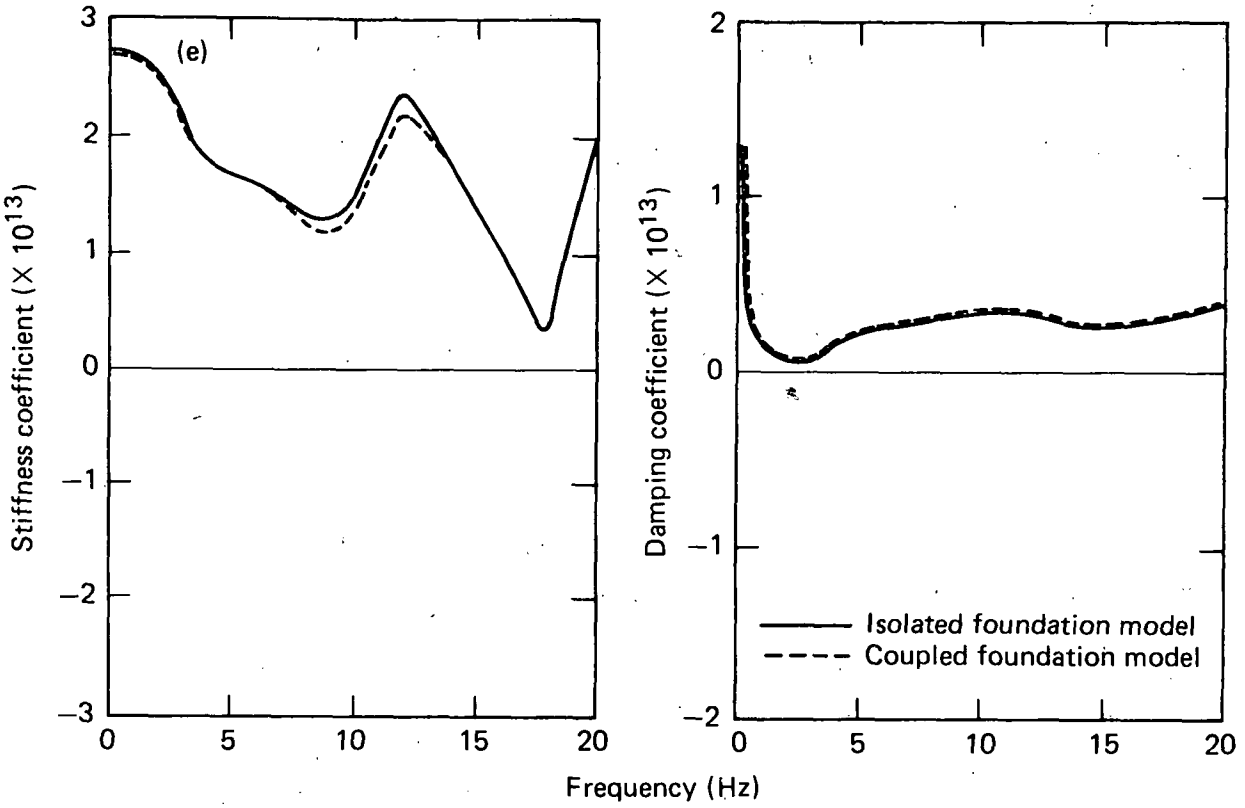

FIG. 4.19. (Continued). (e) torsional rotation term K_{66}.

foundations with the same degree of accuracy as in the detailed three-dimensional models. We also attained this accuracy in our model of the in-structure response. This was accomplished by projecting the dynamic characteristics of fixed-base structures--mode shapes and frequencies, and mass and spatial relationships--to a reference point on the foundation at which the foundation's SSI response was to be computed. Because the foundation was assumed to be rigid, the dynamic representation of the structure was reduced to six dynamic inertial parameters for each mode and a 6 x 6, rigid-body mass matrix of the structure about the reference point. Data may be similarly condensed for in-structure response, as the modal and spatial relationships are needed only for those degrees of freedom for which response is desired.

4.5 FLUSH ANALYSIS

Two SSI problems were addressed in our study--analysis of the Zion reactor building as an isolated structure and analysis of the entire Zion nuclear power plant. The first case represents a well defined problem for

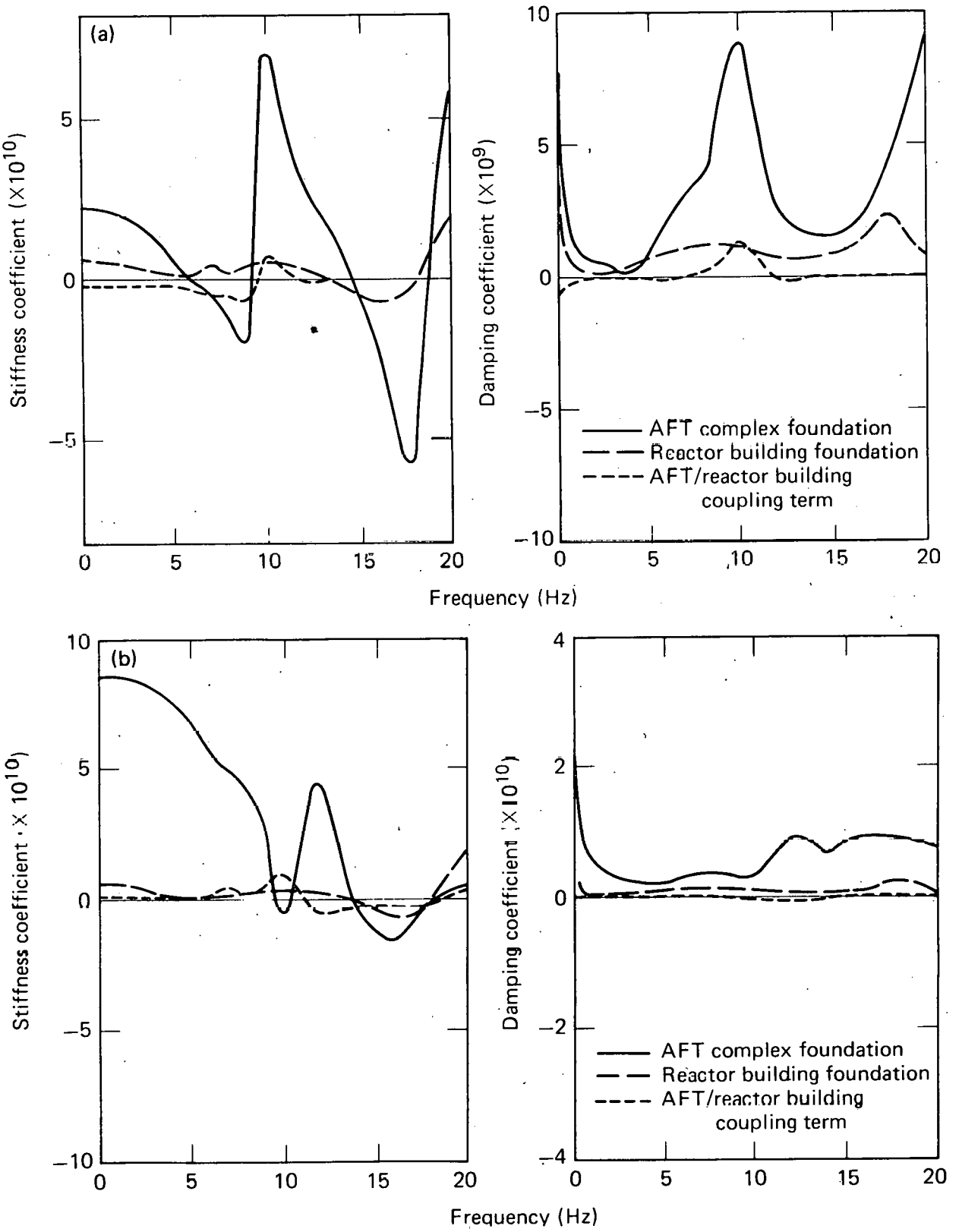

FIG. 4.20. CLASSI impedance functions for the coupled AFT complex and reactor building foundation system. Shown are the structure-to-structure coupling terms compared with diagonal terms for (a) the E-W translation coupling term and (b) the vertical translation coupling term.

which differences in the idealizations of the direct method and the substructure approach were minimal. The result serves as a benchmark for the two procedures. Analysis of the entire Zion plant, on the other hand, required significant simplifications for a FLUSH or CLASSI analysis. Many features of the FLUSH analyses were described in paragraphs 3.1, 4.1, and 4.2; the remainder are described here.

Our basic procedure was to identify slices or cross sections of the facility for analysis, to construct models for the soil and structures in each slice, and then to perform first-stage FLUSH analyses (horizontal and vertical) and second-stage structural analyses to obtain the detailed response necessary for comparison with the CLASSI results.

4.5.1 First-Stage FLUSH Analysis

The first step in the analysis was to specify the free-field motion (paragraph 4.1). In our studies, the control motion was always specified on the surface of the soil, and vertically propagating shear and dilatational waves were assumed to be the wave propagation mechanism at the site. In performing the FLUSH analysis, deconvolution was employed to determine the motion throughout the soil deposit in the free field corresponding to the lateral and bottom boundaries. The bottom boundary was located at the soil/rock interface (Fig. 4.5) and was assumed rigid. The lateral boundaries were assigned transmitting properties to simulate free-field conditions.

We performed iterative FLUSH analyses for the horizontal excitation acting in the plane of the cross section. Strain-compatible soil properties were iterated to convergence in each soil element of the model. Our initial soil property estimates were based on free-field values used in the CLASSI analysis. Using the strain-compatible soil properties obtained from the horizontal analysis, we analyzed the vertical excitation. Response time histories at selected locations on the basemat and in the structures were computed. The basemat response (translations and rotations) became the input for the second-stage analysis.

In general, depending on the symmetry of the foundation and the locations of response, the separate horizontal and vertical analyses resulted in horizontal, vertical, and rotational responses in the plane of the cross section. In our analysis the two earthquake components were assumed to occur simultaneously, and like responses were combined by linear superposition. At

basemat locations where two analysis cross sections intersected, we obtained estimates of three-dimensional response, excluding torsion. However, each cross section was analyzed for vertical excitations, leading to a nonunique prediction of vertical foundation motion. An additional uncertainty is introduced when parallel cross sections modeling the same structure lead to different foundation responses for all degrees of freedom. We considered both of these situations as sources of uncertainty within an analysis procedure.

4.5.2 Modeling Structural Foundations

To model the structures' foundations it was necessary to idealize their stiffness and geometry. In all of our analyses the foundations were assumed to behave rigidly. This is a very good assumption for the foundation of the reactor building, where effective stiffness is due to the foundation itself and to the stiffening effect of the containment shell and internal structure. The foundation of the AFT complex, however, was expected to behave in a flexible manner--especially with respect to rocking and vertical deformations. The procedure for determining the effective stiffness of the AFT's foundation, accounting for the stiffening effects of the numerous walls and floor slabs, and reducing this three-dimensional behavior to two dimensions is not straightforward. Our initial assumption, therefore, was to model it as being rigid. The reactor building's foundation was assumed to be a right circular cylinder embedded 36 ft. The foundation width and out-of-plane dimension (slice thickness) were chosen to provide soil shear and rocking stiffnesses approximately equivalent to those for a circular foundation shape. The geometry of the AFT's foundation for SSI analysis depended on the cross sections treated by FLUSH and is discussed later in this section.

4.5.3 Simplified Structural Models

In practice, the structural models used in a direct method of analysis represent only the overall dynamic behavior of the structure, and a second-stage structural analysis is usually performed using the results of the SSI analysis as excitation. The result of the second-stage analysis is the detailed three-dimensional response to two horizontal components of foundation motion, two rocking components and one vertical component. We followed this

procedure, using the structural models described in paragraph 4.3. In the first-stage analysis, the model for the reactor building's containment shell was identical to the model described in paragraph 4.3. Simplified models of the reactor building's internal structure and of the AFT complex were developed according to a modal equivalence principle.

There are several methods of developing simplified structural models for the SSI analysis. The modal equivalence principle permits modeling more modes than does a continuous beam or element representation. The basic procedure is to develop a series of single-degree-of-freedom (DOF) models, each designed to represent one mode of the structure. The frequency, mass, and mass location of each single-DOF model are selected to match the modal frequency, mass, and moment about the foundation as determined from the detailed model. Judged on the basis of their modal participation factors, only the most important modes are included. Any residual mass or rotational inertia not represented in the dynamic models is added to the foundation to ensure proper modeling of rigid body behavior. The resulting models for the internal structure and AFT complex are described in the next section.

4.5.4 Selection of Cross Sections for SSI Analysis

The principal objectives of our FLUSH SSI analyses were first, to obtain estimates of three-dimensional foundation response for use in detailed structural analysis and comparison with CLASSI and second, to analyze a relatively simple problem, with a minimum number of modeling assumptions, that could serve as a benchmark comparison between FLUSH and CLASSI. Effort toward meeting our first objective centered on the AFT complex, whereas achieving our second objective involved benchmark comparisons performed on a model of the reactor building, which assumed it to be an isolated structure.

The basic formulation in FLUSH is two-dimensional; hence, analyzing the entire Zion plant requires considering several slices through the layout. Each slice is analyzed independently, assuming structural response to be uncoupled in two orthogonal horizontal directions. The results are combined in the second-stage analysis. We selected three cross sections for FLUSH analysis, identified in Fig. 4.21 as A-A, B-B, and C-C. Elevation views showing the FLUSH model for each cross section appear in Fig. 4.22a-c. Figure 4.22d shows a FLUSH model of the reactor building as an isolated structure, as it was used for our benchmark case.

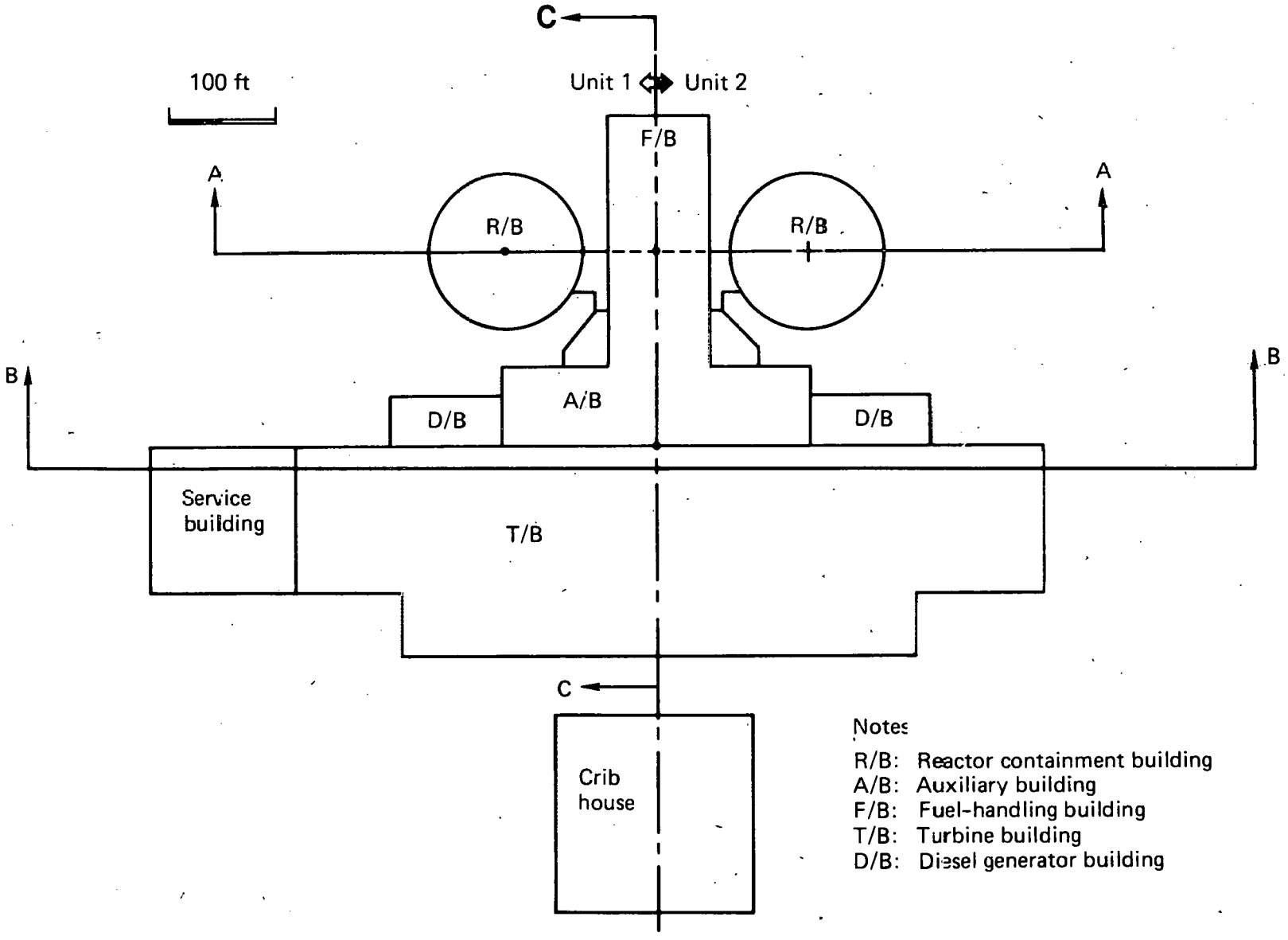

FIG. 4.21. Plan view of the Zion Nuclear Power Plant showing cross sections used for FLUSH analyses.

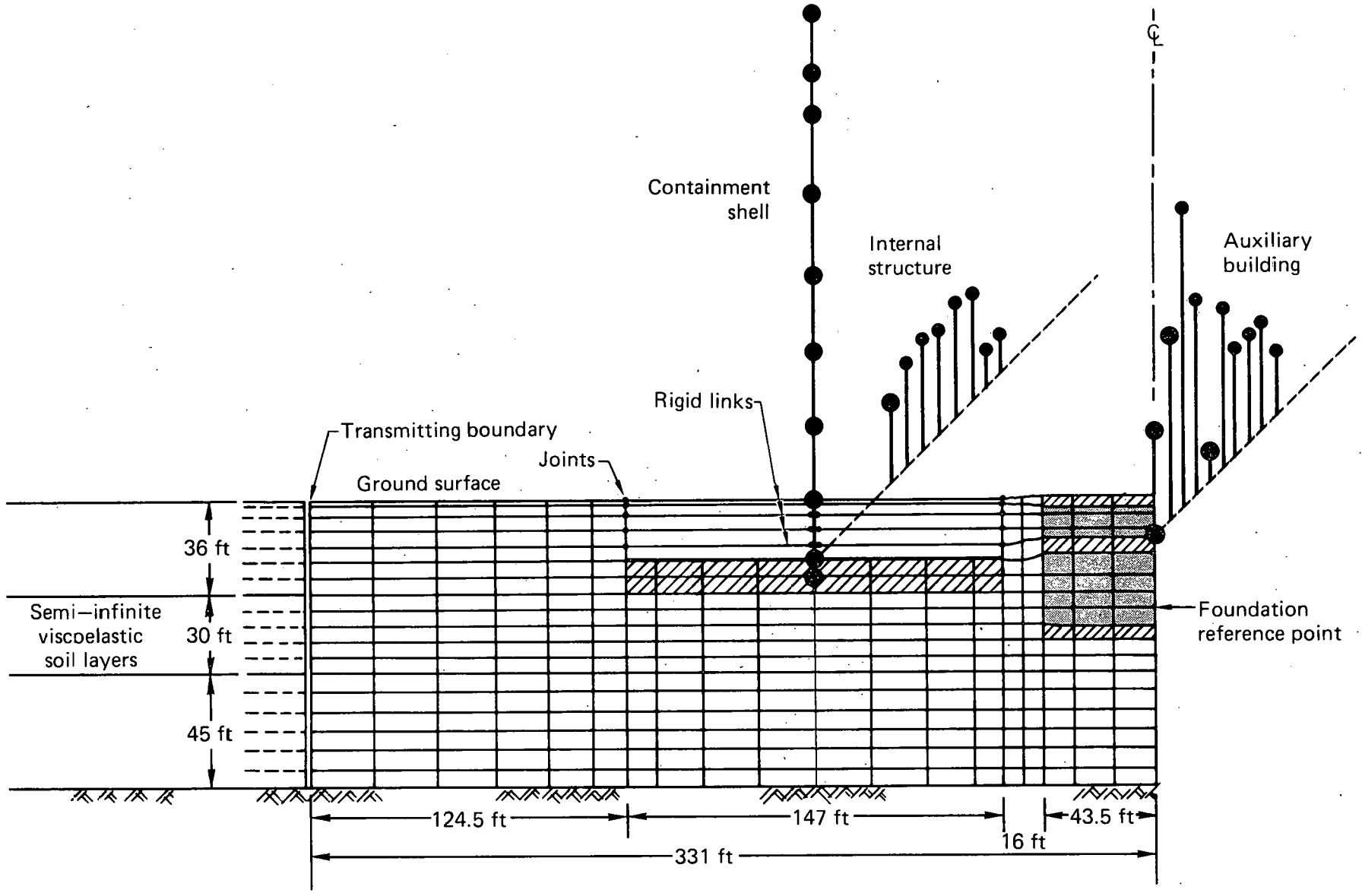

FIG. 4.22. Finite element model for FLUSH analyses showing (a) cross section A-A.

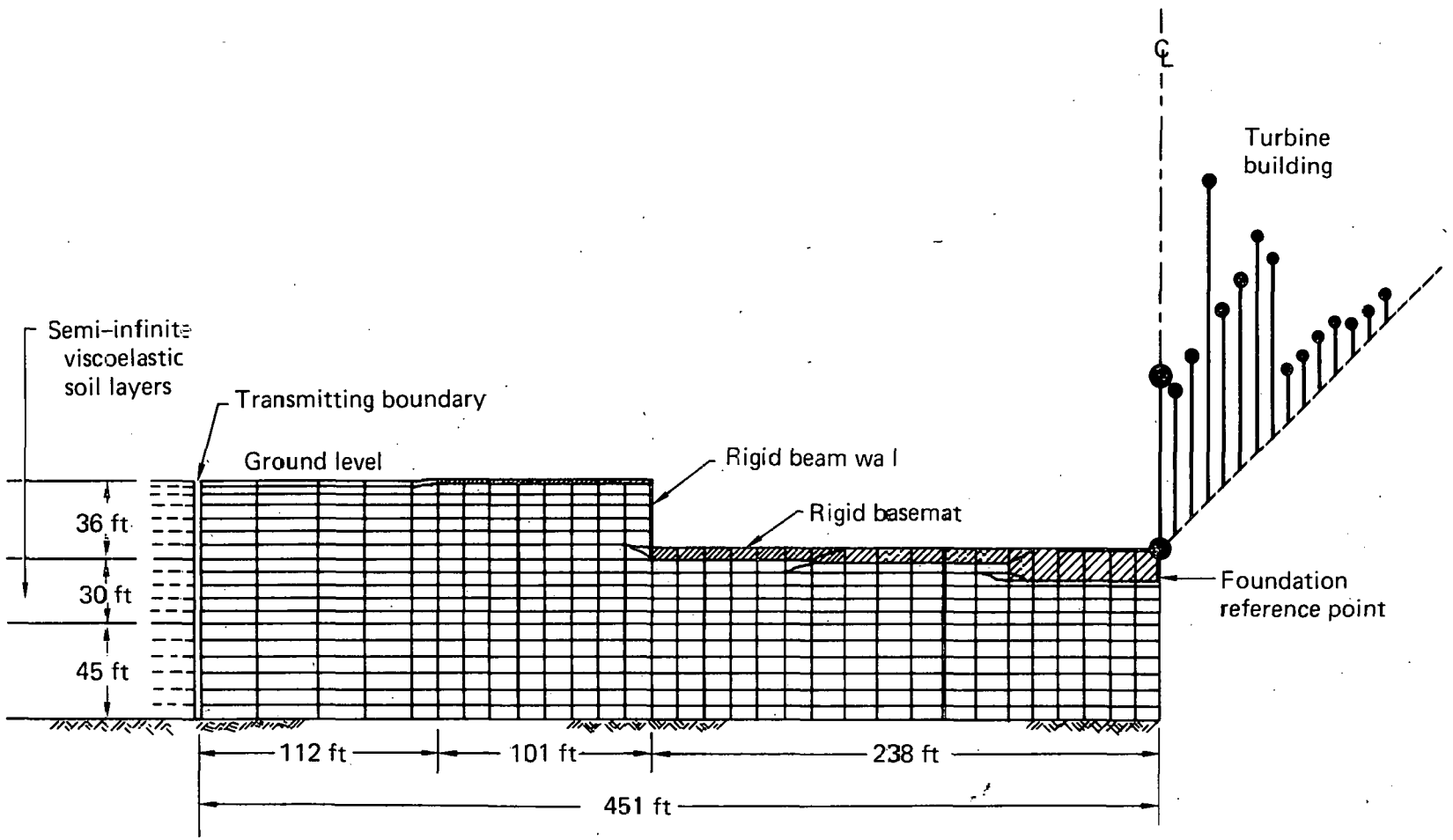

FIG. 4.22. (Continued). (b) cross section B-B.

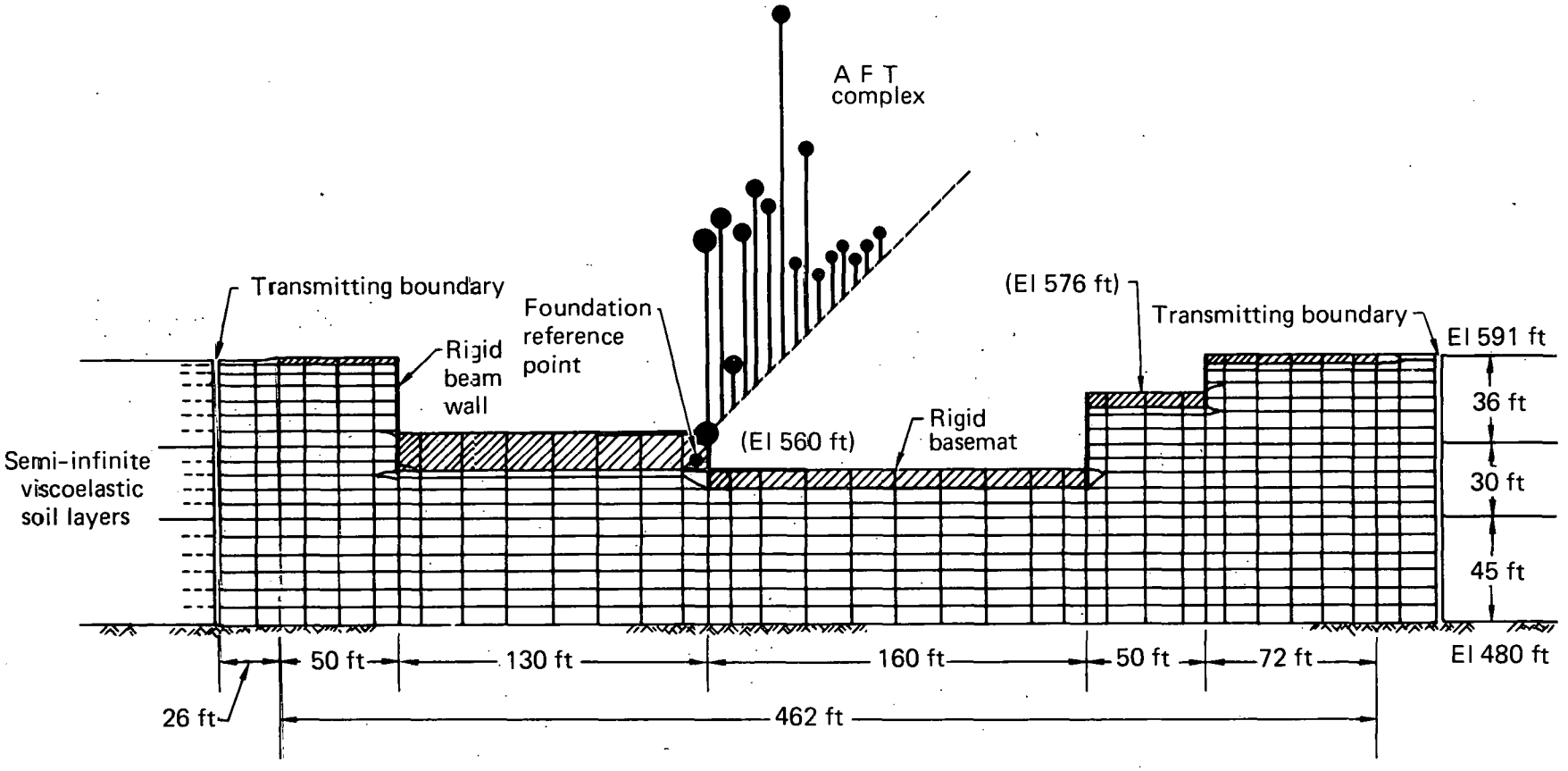

FIG. 4.22. (Continued). (c) cross section C-C.

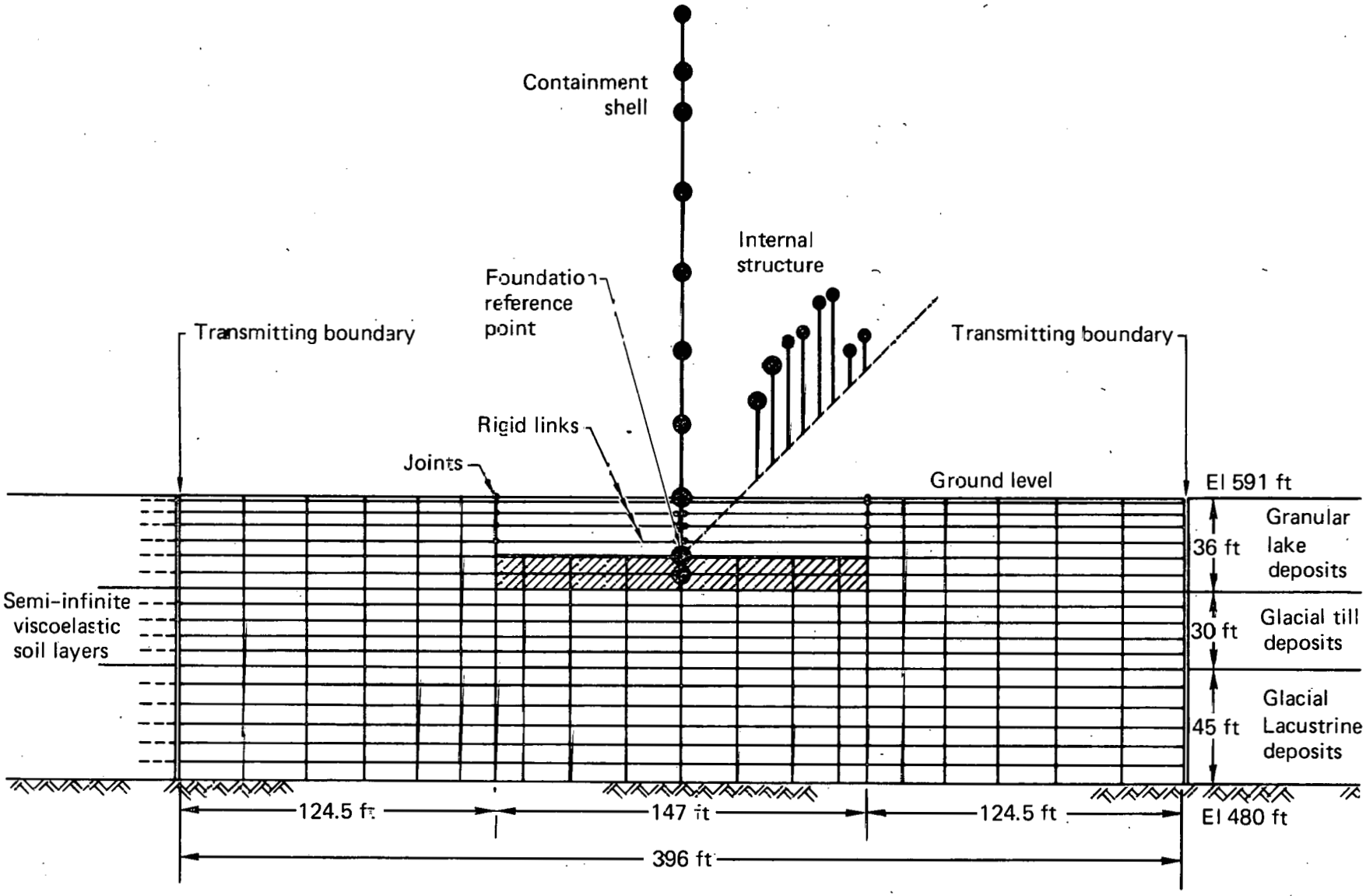

FIG. 4.22. (Continued). (d) Isolated reactor building through cross section A-A.

As mentioned in paragraph 4.5.2, we assumed the structural foundations to be rigid. Figure 4.21 illustrates this assumption by showing the idealized foundations as an assembly of rigid, plane strain, finite elements for horizontal portions, interconnected by rigid beam elements that simulate exterior walls. The dynamic effects of the structures were modeled using the modal equivalence principle or, as in the case of the reactor containment shell, using a lumped mass beam model. Residual structural mass not included in the model was distributed over the foundations. Loads from the structures (base shear and overturning moments) were distributed over the foundation model by means of rigid beam elements extending from the base connection points of the structural models to points on the foundation.

We analyzed each FLUSH model for horizontal and vertical free-field excitations. By computing horizontal, vertical, and rocking foundation motions at the point corresponding to the foundation reference point (Fig. 4.17), we combined the foundation motions for horizontal N-S and E-W and for vertical free-field excitations from intersecting pairs of cross sections. This enabled us to obtain three-dimensional motion of the AFT foundation. The following paragraphs describe each of the cross sections modeled. The models employed symmetry conditions and transmitting boundaries to the extent it was possible. The process of combining the foundation response from individual analyses and the description of the second stage analyses are contained in Section 5.0.

Cross Section A-A. Section A-A is a north-south slice taken through the center of the reactor buildings and through the western end of the auxiliary building. The model (Fig. 4.21a) is symmetrical about the right side, which is located at the centerline of the AFT complex. The reactor building foundation was modeled with a set of rigid, plane strain finite elements. The foundation horizontal and out-of-plane dimensions were selected so that the translational and rocking characteristics of the resulting rectangle resting on soil were close to those of the actual cylindrical shape. The reactor containment shell was modeled with a lumped-mass beam finite-element model that was, except for embedment, identical to the model used for the CLASSI analyses. Below grade this shell model was flexible and bonded to the soil horizontally by rigid links, whereas the CLASSI structure model was assumed horizontally rigid below grade. This was expected to introduce only small differences in response. The soil region between the containment shell and

auxiliary building was assumed to be void. Elements shown in this region are massless and of very low stiffness. The actual behavior in this region is difficult to predict.

In a two-dimensional representation, the relative configurations of the reactor building and AFT complex are significantly simplified--the separation between structures is assumed constant and infinite in length.

The reactor building internal structure was modeled using the modal equivalence method described in the previous section. The model contained eight modes, six representing N-S horizontal motion and two representing vertical motion. The modal mass of these eight modes represented 62% (horizontal) and 15% (vertical) of the total structural mass. This was about 80% of the effective modal mass for frequencies below 20 Hz. The remaining, or residual, mass was distributed over the basemat, accounting for rotational inertia and minimizing local deformations in the basemat. Both the containment shell and internal structure models were connected to the basemat at the center, and the resulting inertial loads were distributed throughout the basemat by means of rigid beam elements extending from this connection point.

We modeled the auxiliary building foundation with a block of rigid, plane strain elements. The structure was modeled using the modal equivalence principle. The single-DOF models comprising the structural model were connected to the foundation block at the centerline 15 ft below grade, and their inertial loads were distributed over the foundation in the same manner as they were for the reactor building. We selected the modes for the model from an eigenvalue analysis of a reduced AFT complex model, i.e., the auxiliary and fuel-handling buildings. We identified 10 N-S and 10 vertical modes having significant mass participation below 25 Hz. The resulting modal mass of these 20 modes represented 73% (horizontal) and 52% (vertical) of the total structural mass. The residual mass was distributed over the foundation as before. Because of constraints on the out-of-plane dimension imposed by modeling the reactor building foundation, the foundation area used for the auxiliary building model was about 22% of the actual area. All masses were factored by this value to maintain consistency with the actual bearing pressure of the structure on the soil.

We should note that in modeling the AFT complex through this cross section, we were faced with a difficult modeling issue--how to model the mass and stiffness of an irregularly shaped structure and foundation in two

dimensions and still maintain an appropriate relationship between it and other structures. This issue occurs whenever average properties for the structure cannot be established for the analysis slice. In particular the dilemma arises when considering structure-to-structure interaction, where the mass ratio between structures is an important parameter. In general, the more massive structure has the greatest effect on the neighboring structure. At Zion, the AFT complex is expected to affect the reactor building response. To capture this aspect of dynamic behavior, the mass ratio of the two structures is important. On the other hand, when modeling only a portion of the foundation, such as the Zion auxiliary building, including the entire mass of the structure will predict disproportionately high stress levels in the soil and distort structural response. This is especially true when nonlinear soil behavior is being approximated. To maintain reasonable levels of stress in the soil, a structure and foundation mass proportional to the foundation area is required. Hence, two alternatives arise--the mass of the structure and foundation model can be selected to yield the expected soil-bearing pressure, or the horizontal, vertical, and rotational inertia of the portion of structure within the analysis slice or the total mass of the structure including those portions outside the analysis slice can be included. The former case is deficient, especially in the prediction of structure-to-structure interaction effects. The latter approach overcomes this aspect but clearly leads to shifts in the amplitude and freguency content of the complicated structure--in our case, the AFT complex. We selected the first alternative. However, this aspect of the model clearly introduces a source of uncertainty.

Cross Section B-B. Section B-B is a north-south slice taken through the turbine building between the turbine pedestals and the auxiliary building. The FLUSH model (Fig. 4.21b) is symmetrical about the centerline of the AFT complex. The basemats were modeled with the rigid, plane strain finite elements and the exterior walls with rigid beam elements. The out-of-plane dimension was selected so that the foundation area corresponded to that of the turbine building. Similarly, the mass properties of the structure and foundation corresponded to those of the turbine building area of the AFT complex. The structural modes included in the model were identified with either response of the turbine building alone or significant overall AFT complex modes. In the latter case, the modal mass represented by single-DOF

models was in proportion to the turbine building relative to that of the total AFT complex. Residual structural mass was, again, distributed over the basemat. The single-DOF models representing the structure were connected to the basemat at the plane of symmetry and their dynamic loads distributed to the basemat by rigid beam elements.

Cross Section C-C. Section C-C extends east and west along the centerline of the AFT complex. The FLUSH model of the foundation (Fig. 4.21c) consists of a series of rigid, plane strain finite elements representing the basemats, which are connected by rigid beam elements representing the exterior walls of the foundation. The out-of-plane dimension was chosen to give the model the same area as that of the entire AFT complex. An equivalent modal model was used to represent the dynamic effects of the AFT structures below 20 Hz. The model used 15 horizontal modes, which accounted dynamically for about 70% of the structural mass in the E-W direction and about 50% of the rocking inertia. Fifteen modes were used to account dynamically for about 50% of the mass vertically.

5.0 DISCUSSION OF RESULTS

In the course of this study we performed numerous analyses using CLASSI and FLUSH to obtain estimates of the response of structures subjected to free-field earthquake motions, including the effects of soil-structure interaction. We used the CLASSI and FLUSH computer codes to analyze the Zion reactor buildings and AFT complex, first assuming them to be independent structures isolated from each other, and second including the effects of structure-to-structure interaction. We made a number of comparisons in an attempt to obtain estimates of the variability in response due to analysis methods, first for a well defined, easily idealized problem which serves as a benchmark reflecting optimum modeling conditions, and second for more complicated problems involving more and grosser assumptions.

Our first set of CLASSI vs FLUSH comparisons were made for our simplest problem--that of the isolated reactor building excited by one horizontal and one vertical component of free-field motion. Next we studied how structure-to-structure interaction affected the variability of the reactor building response using CLASSI and FLUSH. We then made similar comparisons for the AFT complex, first as an isolated structure, then including structure-to-structure interaction. Finally we studied how structure-to-structure interaction affected structural responses by comparing results from CLASSI analyses for isolated and multiple structures. Tables 5.1 and 5.2 summarize the analyses we performed and indicate the paragraphs where the results are discussed.

5.1 SSI ANALYSIS OF THE ISOLATED REACTOR BUILDING

To obtain an estimate of the best agreement we could expect from CLASSI and FLUSH, we performed SSI analyses of the Unit 1 reactor building, assuming it to be isolated from the other plant structures so that interaction between foundations did not occur. In terms of foundation geometry and other modeling assumptions, this represents the simplest problem available to us from our work on the Zion facility for the SSMRP.

We analyzed the reactor building for the N-S and vertical components of the synthetic and El Centro earthquakes, using both the FLUSH and CLASSI formulations. Our principal objective was to study the variability between

TABLE 5.1. Summary of Zion reactor building SSI analyses.

Analysis	Excitation: El Centro	Excitation: Synthetic	Results presented
CLASSI[a]			
● Isolated structure and foundation	x	x	5.1.
● Structure-to-structure interaction	x	x	5.2, 5.5
FLUSH[b]			
● Isolated structure and foundation--cross section of Fig. 4.21d			
● Iterated soil properties	x	x	5.1.1, 5.1.2, 5.1.3
● Free-field soil properties	x	x	5.1.3
● First-stage vs. second-stage	x	x	5.1.1
● Without foundation rocking input motion	x	x	5.1.2
● Structure-to-structure interaction		x	5.2

[a]All CLASSI analyses idealized the reactor building foundation to be embedded.

[b]All FLUSH results are from second-stage structure analysis unless otherwise stated.

TABLE 5.2. Summary of Zion AFT complex SSI analyses.

Analysis	Excitation: El Centro	Excitation: Synthetic	Results presented
CLASSI			
● Isolated structure and foundation		x	5.3
● Structure-to-structure interaction		x	5.4, 5.5
FLUSH			
● Isolated structure and foundation		x	5.3
● Structure-to-structure interaction		x	5.4

responses from the CLASSI analyses and from the two-stage FLUSH analyses, in which the second stage provided detailed structural response equivalent to that obtained directly by CLASSI. However, for the isolated reactor building study, we obtained results from the FLUSH analyses using several methods so that other comparisons could also be made. The responses that we computed included foundation motions at the top of the reactor building basemat on the axis of symmetry and in-structure response at the top of the containment shell dome at the centerline and on the operating floor, approximately 50 ft off the centerline. Table 5.3 summarizes the results of our principal analyses.

TABLE 5.3. Summary of reactor building peak accelerations obtained from CLASSI and FLUSH analyses for an isolated foundation. Translations are given in ft/sec^2. Rotations are given in rad/sec^2.

	Synthetic earthquake			El Centro earthquake		
	CLASSI	FLUSH method		CLASSI	FLUSH method	
Location	method	SSI	2nd stage	method	SSI	2nd stage
Top of foundation mat						
N-S translation	3.87	4.19	(4.19)	5.47	5.71	(5.71)
Vertical translation	3.44	3.75	(3.75)	2.67	3.18	(3.18)
N-S rocking	0.0344	0.0375	(0.0375)	0.0270	0.0281	(0.0281)
Top of containment shell						
N-S translation	12.69	12.31	12.19	10.94	10.84	10.65
Vertical translation	5.40	--	5.52	8.66	--	9.34
Operating floor at pressurizer						
N-S translation	4.52	NA	4.24	5.70	NA	6.12
Vertical translation	3.55	NA	4.34	2.72	NA	3.03
Free field						
N-S translation	7.33	7.33	--	6.49	6.49	--
Vertical translation	4.34	4.34	--	3.92	3.92	--

The foundation responses from the FLUSH and CLASSI analyses for the synthetic and El Centro earthquakes are shown in Figs. 5.1 and 5.2. The frequency content of the motion, as characterized by spectral accelerations, closely follows the free-field motion up to frequencies approaching those of the coupled soil-structure system. Above this frequency, foundation motions are reduced relative to the free field. An interesting observation pertains to the effect of the control motion on the character of the response. Compare the reduction in foundation motion relative to the free field for the El Centro (Fig. 5.1) and the synthetic (Fig. 5.2) earthquakes. The zero period amplitude (ZPA) for horizontal motions is reduced about 40% for the synthetic earthquake but only about 15% for the El Centro earthquake. Examination of the free-field response spectra reveals amplified spectral accelerations over a wider frequency range (1 to 10 Hz) for the El Centro earthquake. The broad-band nature of this motion leads to higher response than for the synthetic earthquake. Reduction in the ZPA for vertical motions is similar for each earthquake.

The comparison of foundation response spectra computed by CLASSI and FLUSH shows excellent agreement for horizontal motions. The greatest difference occurs between 3 and 4 Hz, where the CLASSI results show a dip not present in the FLUSH results. This frequency range coincides with the rocking frequency of the foundation. A difference of similar magnitude occurs at about 10 Hz. The response spectra of the rocking accelerations at the basemat (Figs. 5.1c and 5.2c) also agree quite well. This is due, at least in part, to the care taken in determining the FLUSH equivalent foundation dimensions, which resulted in equal moments of inertia for the two representations. This is an important consideration when reduced foundation and structure models (such as two-dimensional representations) are required. In those cases, foundation dimensions must be selected to match the expected dynamic behavior of the three-dimensional configuration.

At the top of the containment shell and on the operating floor, the comparison between the CLASSI results and second-stage FLUSH results was quite good for horizontal response but somewhat anomalous for vertical response. Table 5.3 summarizes peak accelerations, and Figs. 5.3 and 5.4 show response spectra at 2% damping. Peak horizontal accelerations compare well--within 2 to 8%. Horizontal response spectra match closely in frequency content, with some differences in amplitude at the resonant frequencies of the coupled soil-structure system. The largest difference approaches 40%, but in general

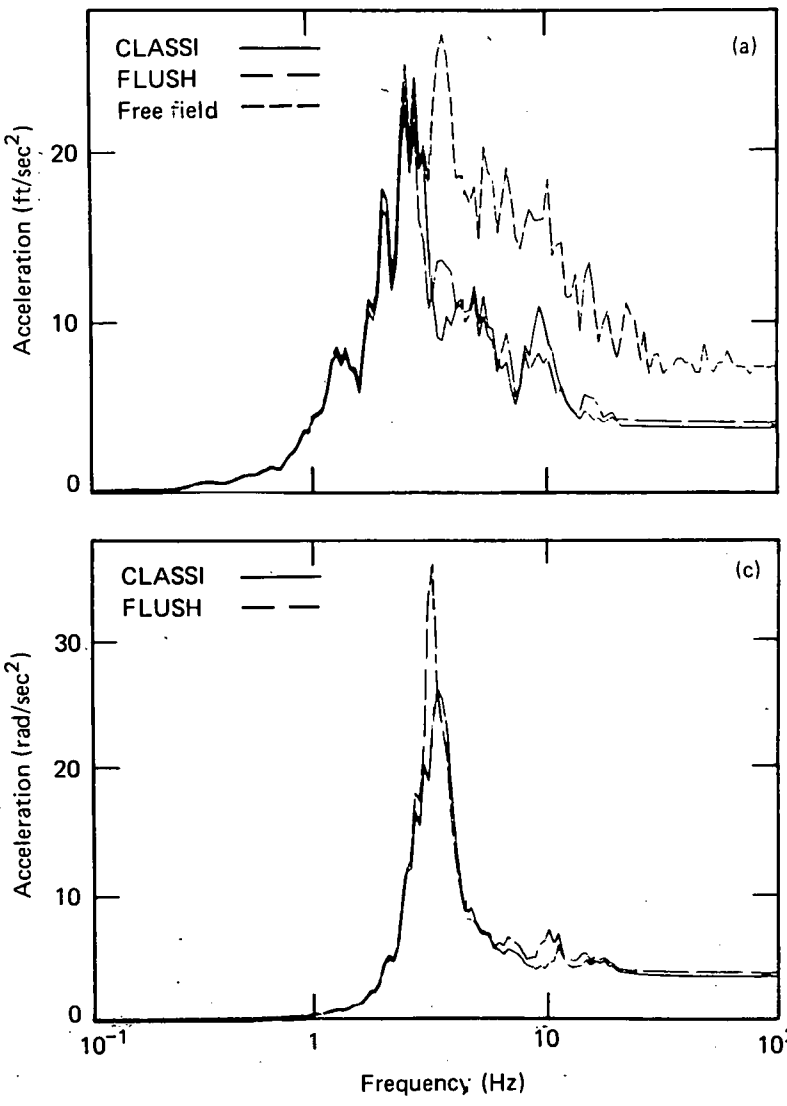

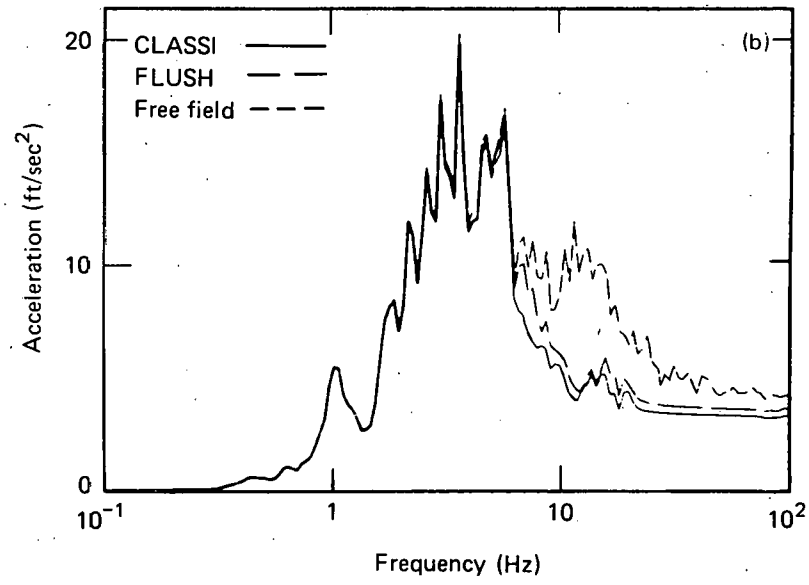

FIG. 5.1. SSI analysis of the isolated reactor building foundation using synthetic earthquake data. Shown are response spectra for (a) the N-S translation, (b) the vertical translation, and (c) N-S rocking.

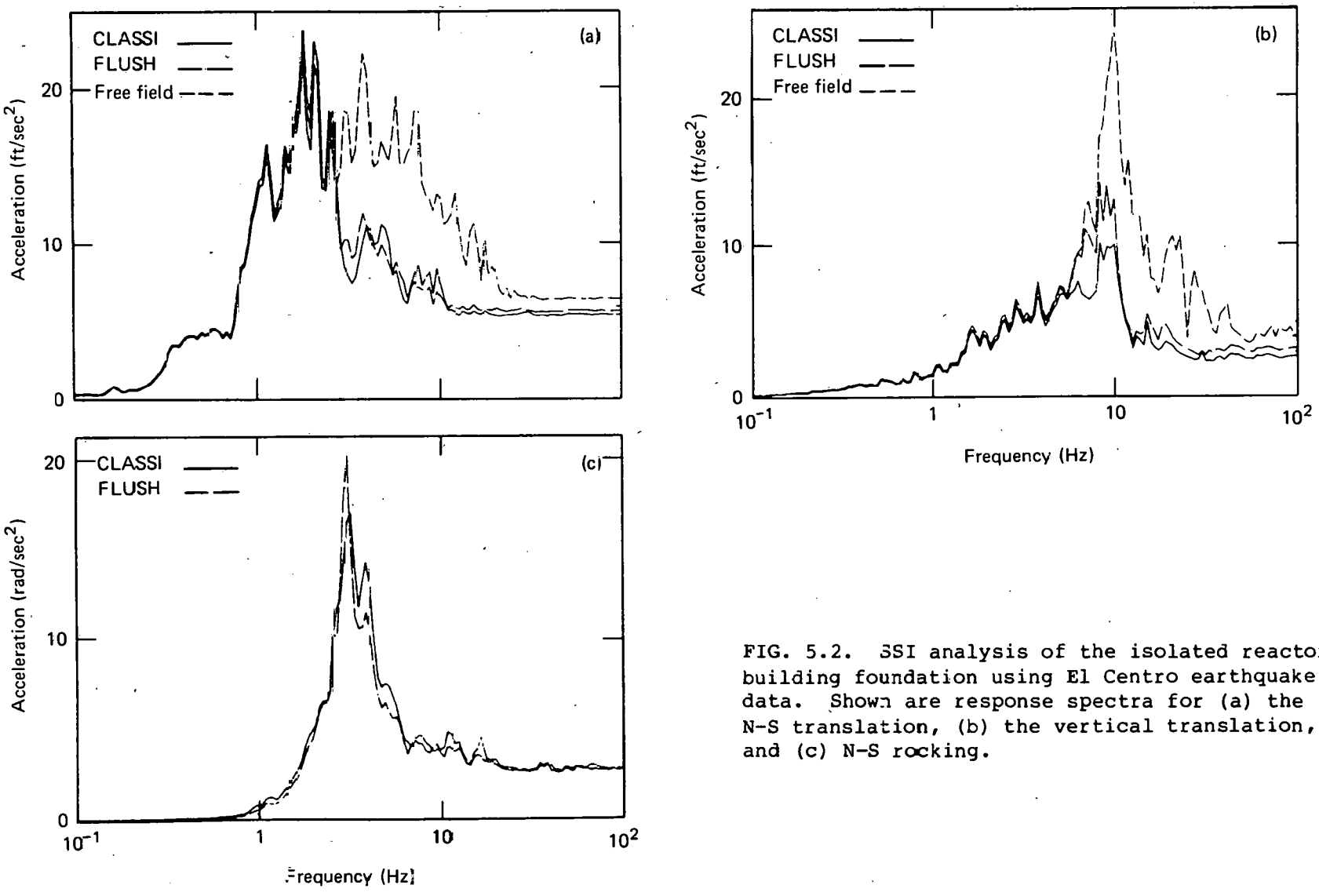

FIG. 5.2. SSI analysis of the isolated reactor building foundation using El Centro earthquake data. Shown are response spectra for (a) the N-S translation, (b) the vertical translation, and (c) N-S rocking.

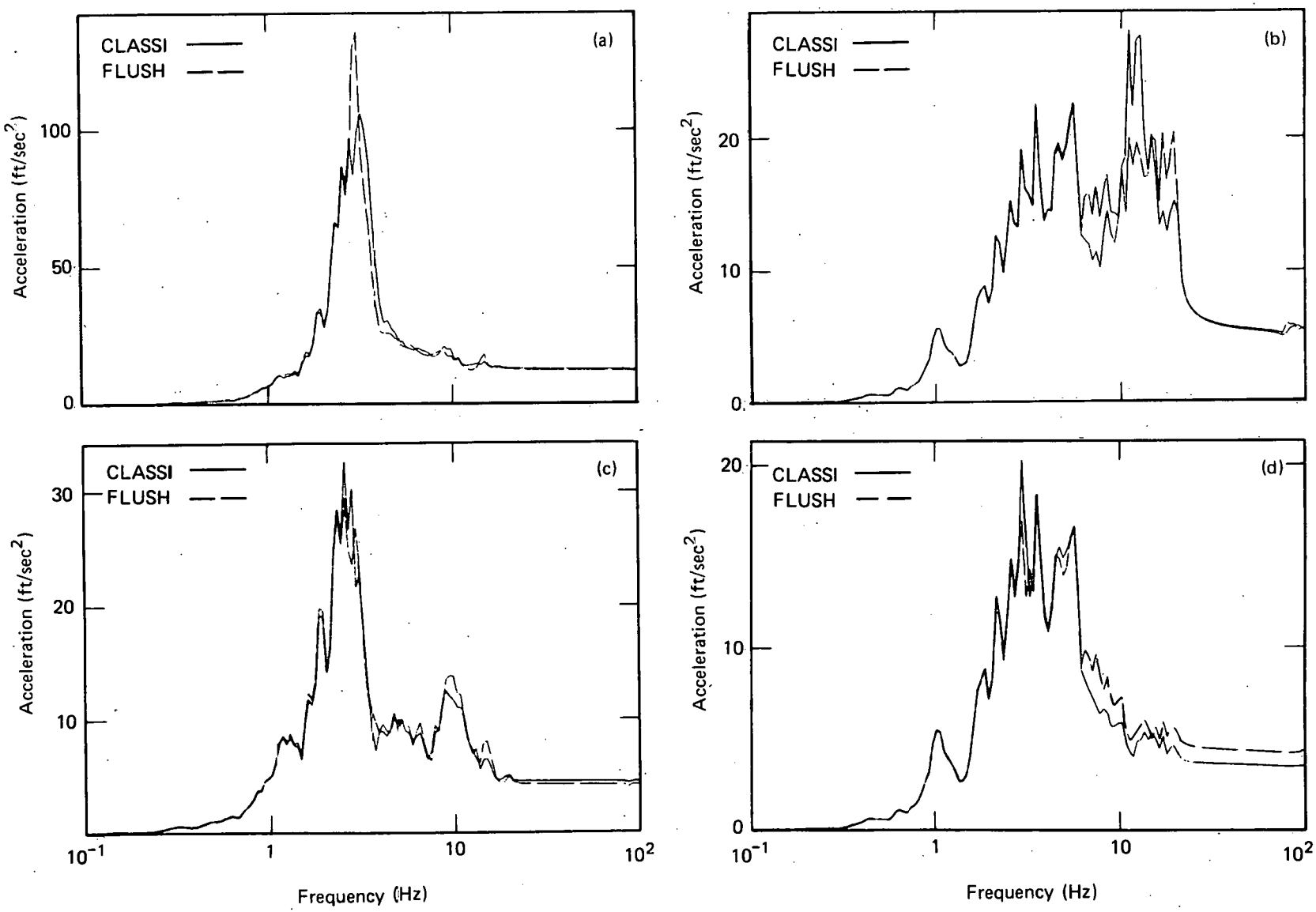

FIG. 5.3. Comparison of CLASSI and FLUSH analyses of the isolated reactor building using synthetic earthquake data. Response spectra and their locations are (a) the N-S translation at the top of the containment shell, (b) the vertical translation at the top of the containment shell, (c) the N-S translation on the operating floor at the pressurizer, and (d) the vertical translation on the operating floor at the pressurizer.

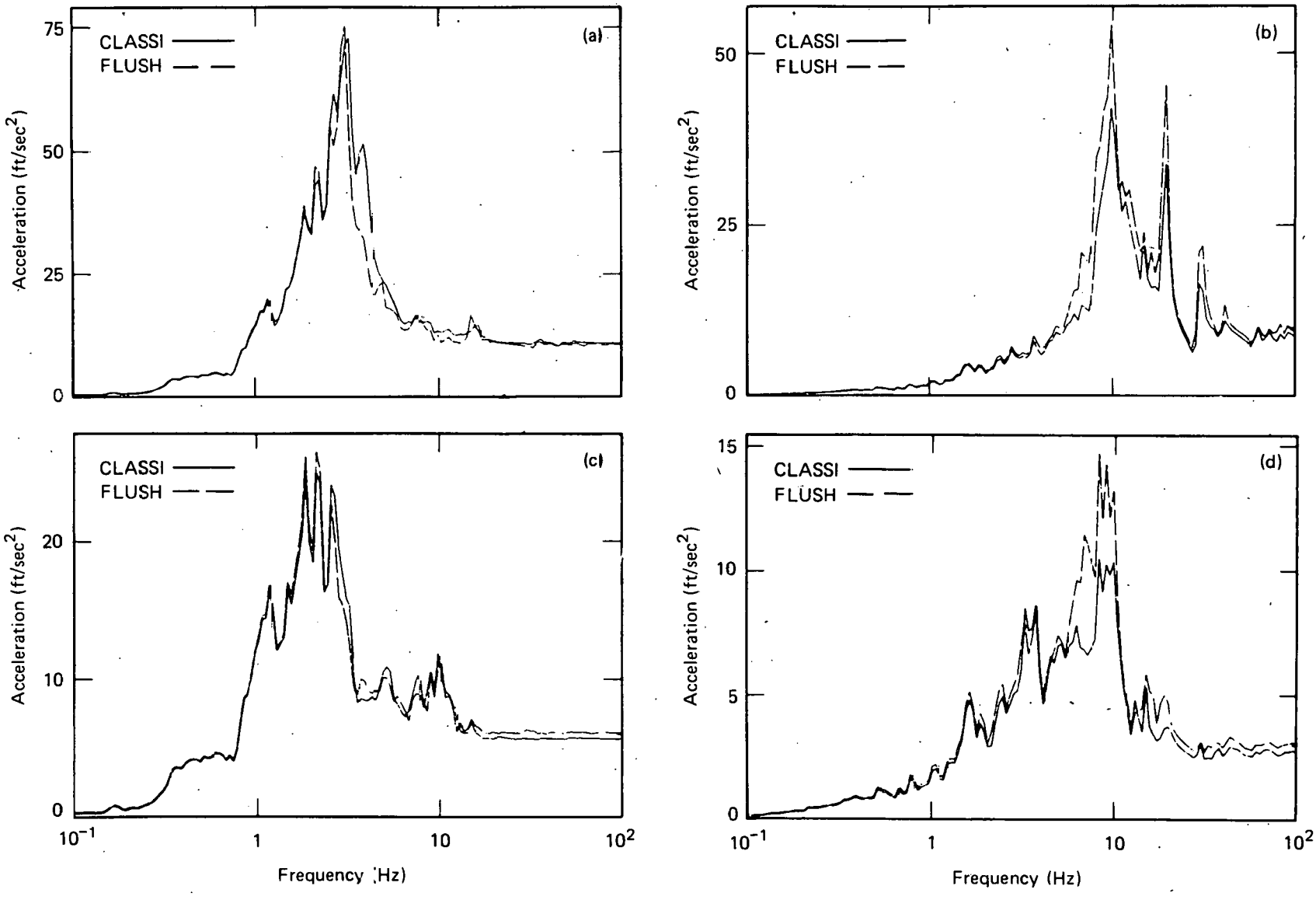

FIG. 5.4. Comparison of CLASSI and FLUSH analyses of the isolated reactor building using El Centro earthquake data. Response spectra shown are (a) N-S translation at the top of the containment shell, (b) vertical translation at the top of the containment shell, (c) N-S translation on the operating floor at the pressurizer, and (d) vertical translation on the operating floor at the pressurizer.

the match is much closer. The FLUSH results are shown for iterated soil properties, which account for secondary nonlinearities in the soil. When free-field soil properties corresponding to the CLASSI analysis are used, the agreement between CLASSI and FLUSH is even closer.

The comparison of vertical response predicted by FLUSH and CLASSI was inconsistent for the two control motions. Consider the El Centro earthquake. Figure 5.2b shows the foundation motion predicted by FLUSH and CLASSI compared to the free-field motion. The response spectra show a difference in amplitude of up to 40% in the 6 to 15 Hz range, with the shape being somewhat similar. This difference appears to propagate through the containment shell and internal structure, as shown in Fig. 5.4. The shapes of the resulting response spectra are similar--differences are mainly in the amplitude of response. Foundation motion predicted by FLUSH and CLASSI for the synthetic earthquake (Fig. 5.1b) compare well. However, in-structure vertical response (Fig. 5.3) differs in frequency content and amplitude, particularly at the top of the containment shell. These results were somewhat surprising in light of the good agreement for horizontal response and led us to investigate further.

- The results shown in Figs. 5.2 and 5.4 indicate greater energy dissipation in the CLASSI analysis than in FLUSH. One potential source of additional energy dissipation was the treatment of bedrock. In the CLASSI analysis, bedrock is modeled as a visco-elastic half-space, whereas in the FLUSH analysis, the bottom boundary of the model is assumed rigid, which is equivalent to a rigid half-space.

  Examination of the imaginary part of the vertical impedance for several assumed values of bedrock stiffness showed little variability; hence, we discounted this as a source of the differences.

- We obtained additional FLUSH results in a form compatible with the intermediate output of CLASSI. A vertical scattering matrix was computed from FLUSH and compared with CLASSI. Differences were clearly present--the CLASSI scattering matrix has a minimum at about 6 Hz, whereas the FLUSH results showed a corresponding minimum at about 10.5 Hz. This indicates a difference in basic behavior between the two models, a difference which requires further evaluation.

Table 5.4 summarizes the variations in acceleration response spectra over the entire frequency range.

5.1.1 Two-Stage Analysis vs Single-Stage FLUSH Analysis

We compared structural response from the first-stage (FLUSH) and second stage (FLUSH/CLASSI) analyses at the top of the containment shell to determine how well the two-stage method reproduced the results obtained directly from FLUSH. We would expect minimal differences because the structural models of the containment shell for both cases were virtually identical and adequate for modeling its expected dynamic behavior, i.e., uncoupled motion in two horizontal directions and the vertical. The only significant difference between the two models was their assumed behavior below grade--the CLASSI model was assumed rigid, whereas the FLUSH model was bonded to the soil at the exterior walls and included the bending flexibility of the shell. In addition, the second-stage of the two-stage analysis uses modal coordinates and the FLUSH analysis does not. A comparison of response spectra of the horizontal accelerations at the top of the shell for the synthetic and El

TABLE 5.4. Variations in acceleration response spectra (2% damping) for the reactor building, assuming an isolated foundation. Differences are given in percent.

	Horizontal			Vertical		
		Amplified frequency range			Amplified frequency range	
Location	ZPA	Typical	Extreme	ZPA	Typical	Extreme
Top of foundation	<10	<10	35	<20	<20	40
Operating floor at pressurizer	<10	<10	20	<25	<20	60
Top of containment shell	<5	<10	40	<10	<10	40

Centro earthquakes is shown in Fig. 5.5. In both cases the response from the two-stage analysis agreed very well with that from the single-stage analysis. However, similar analyses using free-field soil properties showed spectral differences of about 20%. Spectra of vertical accelerations were virtually indistinguishable.

For more complicated structures such as the Zion AFT complex, uncertainty introduced by the two-stage process was expected to be considerably greater.[8] When simplified structural models are required to perform SSI analysis, the inability to include many modes and coupled dynamic behavior between various coordinate directions leads to differences in structural response determined by first-stage vs second-stage analyses. Although our modal equivalent structural models for the AFT complex represented as accurate a first-stage model as possible, we would expect differences between first-stage and second-stage results to appear. To assess their magnitude, significant post-processing of the FLUSH results would be required. This was not done but would be a valuable task for future consideration.

5.1.2 Effect of Foundation Rocking on Structural Response

Many two-stage analyses performed in the past have ignored foundation rotation as an excitation in the second stage. However, it is important to include if one hopes to produce consistent results. To demonstrate the necessity of including both translations and rotations in the second-stage analysis, we performed our second-stage analyses with and without rotations and then compared the results.

The quantity of interest was horizontal response at the top of the containment shell and on the operating floor. Figure 5.6 shows the comparison. At the top of the containment shell (Fig. 5.6a), the resonant frequency for the analyses without foundation rocking shifted from near the rocking frequency (about 3 Hz) to the fixed-base fundamental frequency of the shell (about 5 Hz). Note that omitting basemat rocking reduced the peak spectral response for the synthetic earthquake by about 10%, but it increased response for the El Centro earthquake dramatically. This graphically illustrates the effect that frequency characteristics of different earthquakes can have on response. Similar differences are seen in the response spectra of the horizontal accelerations on the operating floor (Fig. 5.6b). The differences are not quite as pronounced here, probably because the location is

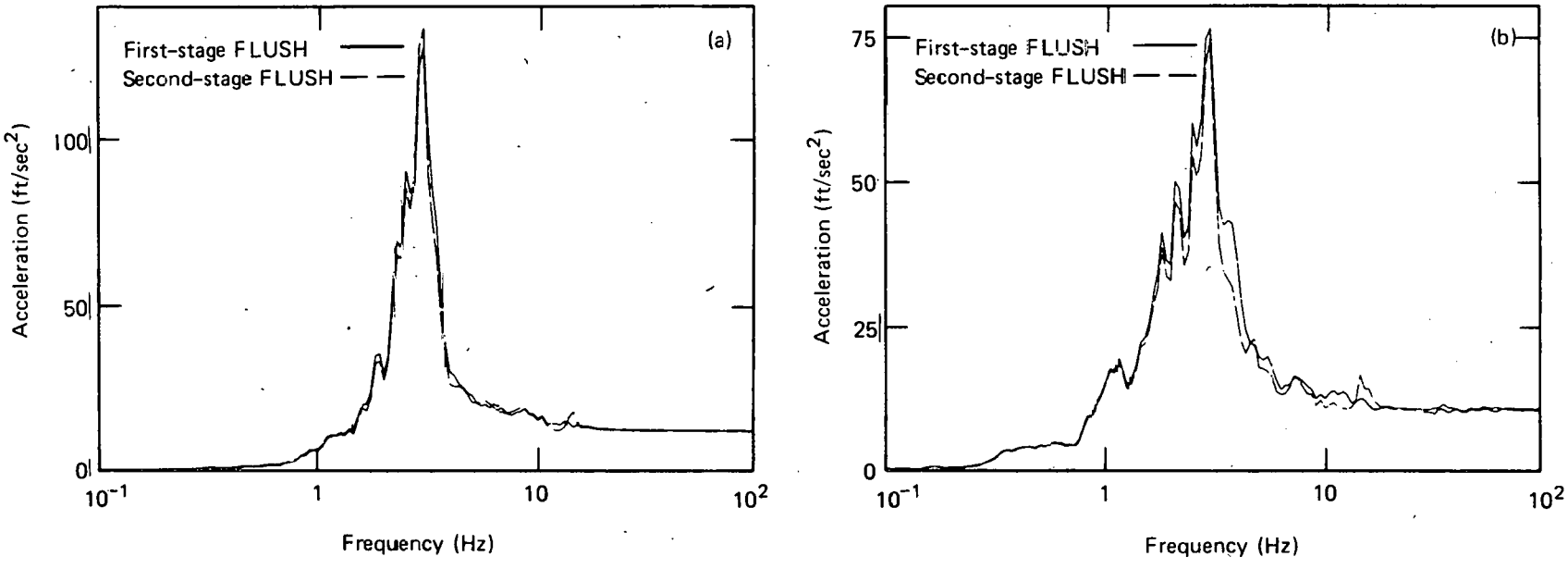

FIG. 5.5. Comparison of first- and second-stage FLUSH response to horizontal acceleration at the top of the containment shell. (a) shows response to the synthetic earthquake, while (b) shows response to the El Centro earthquake.

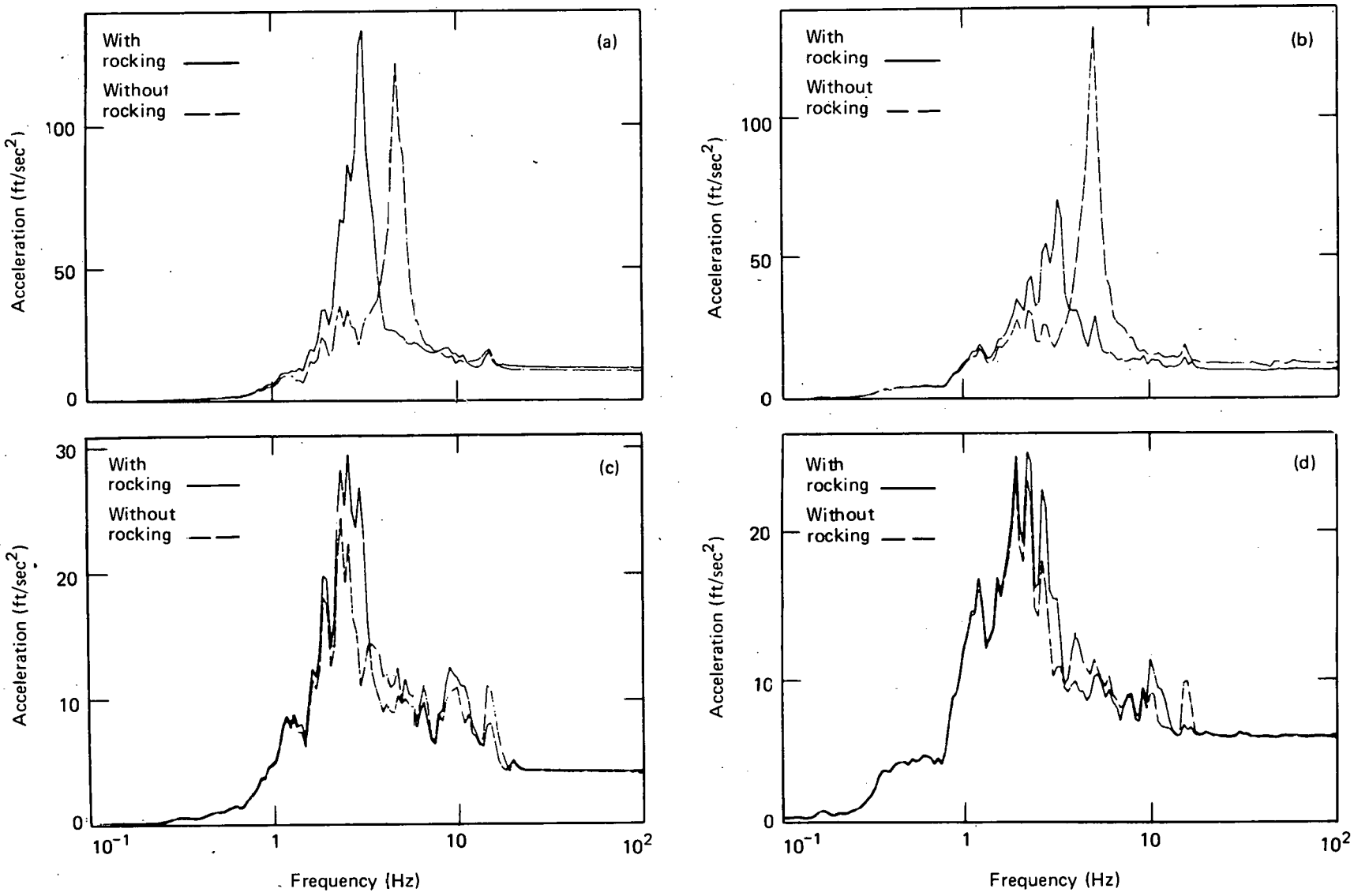

FIG. 5.6. Comparison of FLUSH analyses of the reactor building with and without basemat rocking. Shown are N-S translations for (a) synthetic earthquake motions at the top of the containment shell, (b) El Centro earthquake motions at the top of the containment shell, (c) synthetic earthquake motions on the operating floor at the pressurizer, and (d) El Centro earthquake motions on the operating floor at the pressurizer.

lower in the structure and because the response of the internal structure is essentially high frequency and is not dominated by any single mode. Differences in peak accelerations varied by less than 25% at both locations, in contrast to the marked differences in spectra.

These results clearly show the importance of including foundation rocking in the second-stage analysis. In addition, translation and rocking have a definite phase relationship; treating each independently and combining the results without maintaining this relationship produces erroneous results. The effect of ignoring foundation rotations shifts the frequencies of in-structure spectra from the coupled soil-structure system frequencies to the fixed-base structural frequencies. The implication of this effect for subsystem and equipment design is clear.

Figure 5.6 illustrates the frequency shifts and differences in amplitude. Note that no consistent trend is apparent, such as one case always predicting higher results. Other factors such as the properties of the soil, fixed-base structure, and input motion can influence the results.

5.1.3 Effects of Adjusting Free-Field Soil Properties for Secondary Nonlinearities

As we stated earlier, our principal comparisons were based on FLUSH analyses that had been iterated to obtain spatial variations in soil properties within a given soil layer, reflecting the secondary effects of structure response on soil properties. By comparing two-stage FLUSH analyses that assumed free-field properties with our iterated FLUSH analyses, we examined how these secondary soil nonlinearities affected structural response. Figures 5.7 and 5.8 show results for the synthetic earthquake. Differences are generally quite small. This is no doubt due to the small difference between iterated and free-field soil properties, which was generally less than about 20%. The El Centro earthquake results were similar. These variations appear to result from differences in the rocking motion of the basemat and its subsequent effect on in-structure response. The differences in basemat rocking may be attributable to changes in soil bulk stiffness caused by assuming proportional bulk and shear modulus. Note that rocking is reduced for the free-field properties, bringing it closer to the CLASSI result (Fig. 5.1c). Vertical response is minimally affected.

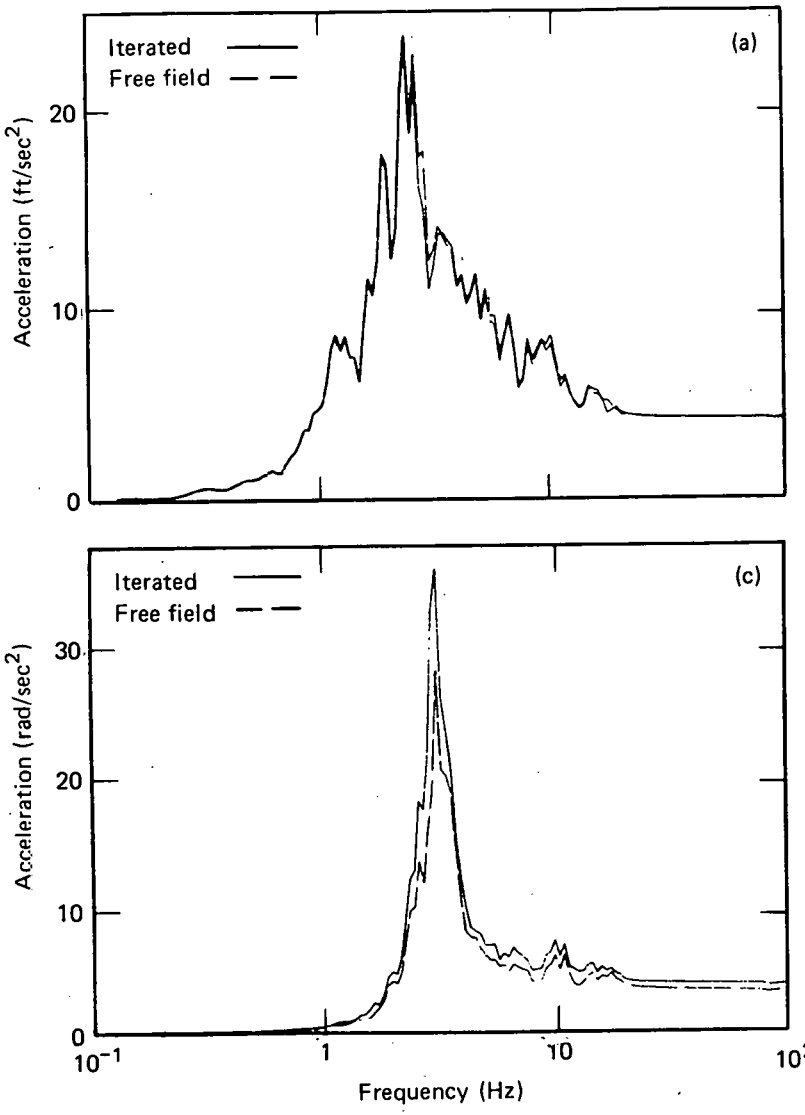

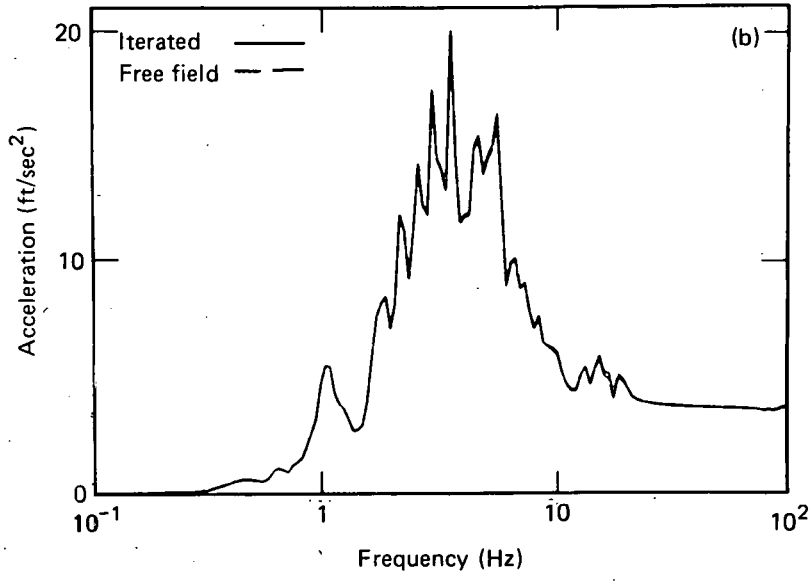

FIG. 5.7. Comparison of iterated and free-field FLUSH analyses at the top of the reactor building foundation mat. Shown are (a) the N-S translation, (b) the vertical translation, and (c) N-S rocking responses to the synthetic earthquake.

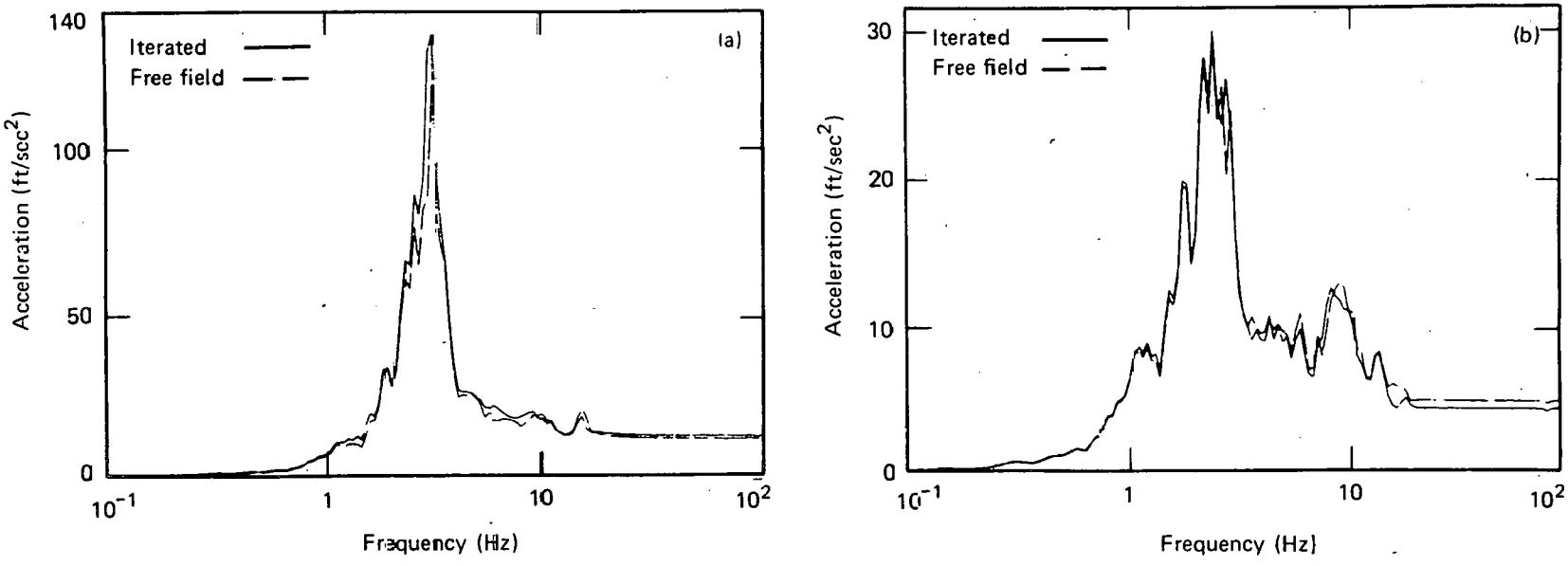

FIG. 5.8. Comparison of free-field and iterated FLUSH analyses for the synthetic earthquake. Figure (a) shows horizontal response at the top of the containment shell, and (b) shows horizontal response on the operating floor at the pressurizer.

5.2 RESPONSE OF REACTOR BUILDING PREDICTED BY CLASSI AND FLUSH, INCLUDING STRUCTURE-TO-STRUCTURE INTERACTION

We next compared the response of the Zion Unit 1 reactor building, including structure-to-structure interaction as predicted by CLASSI and FLUSH. Again, two components of free-field motion were included--the N-S and vertical--but only the synthetic earthquake was considered. A summary of peak accelerations is shown in Table 5.5. On the average, the FLUSH results are about 30% less than the CLASSI responses, varying from about 90% of the CLASSI vertical foundation acceleration to 50% of the CLASSI rocking acceleration. A comparison of the accelerations with those of Table 5.3 for the isolated foundation shows the CLASSI results increased by over one-third for the coupled foundations while the FLUSH results actually decreased for most responses.

Figures 5.9 and 5.10 show comparisons of response spectra on the foundation and at the top of the containment shell. On the foundation the

TABLE 5.5. Comparison of CLASSI and FLUSH analyses of coupled foundations for the reactor buildings. Table shows a summary of peak accelerations in the reactor buildings. Translations are given in ft/sec^2. Rotations are given in rad/sec^2.

Location and component	CLASSI analysis	FLUSH analysis
Foundation at reference point		
N-S translation	4.92	3.82
Vertical translation	4.10	3.76
N-S rocking	.0438	.0233
Top of containment shell		
N-S translation	15.79	9.38
Vertical translation	6.40	5.83
Operating floor		
N-S translation	6.51	4.73

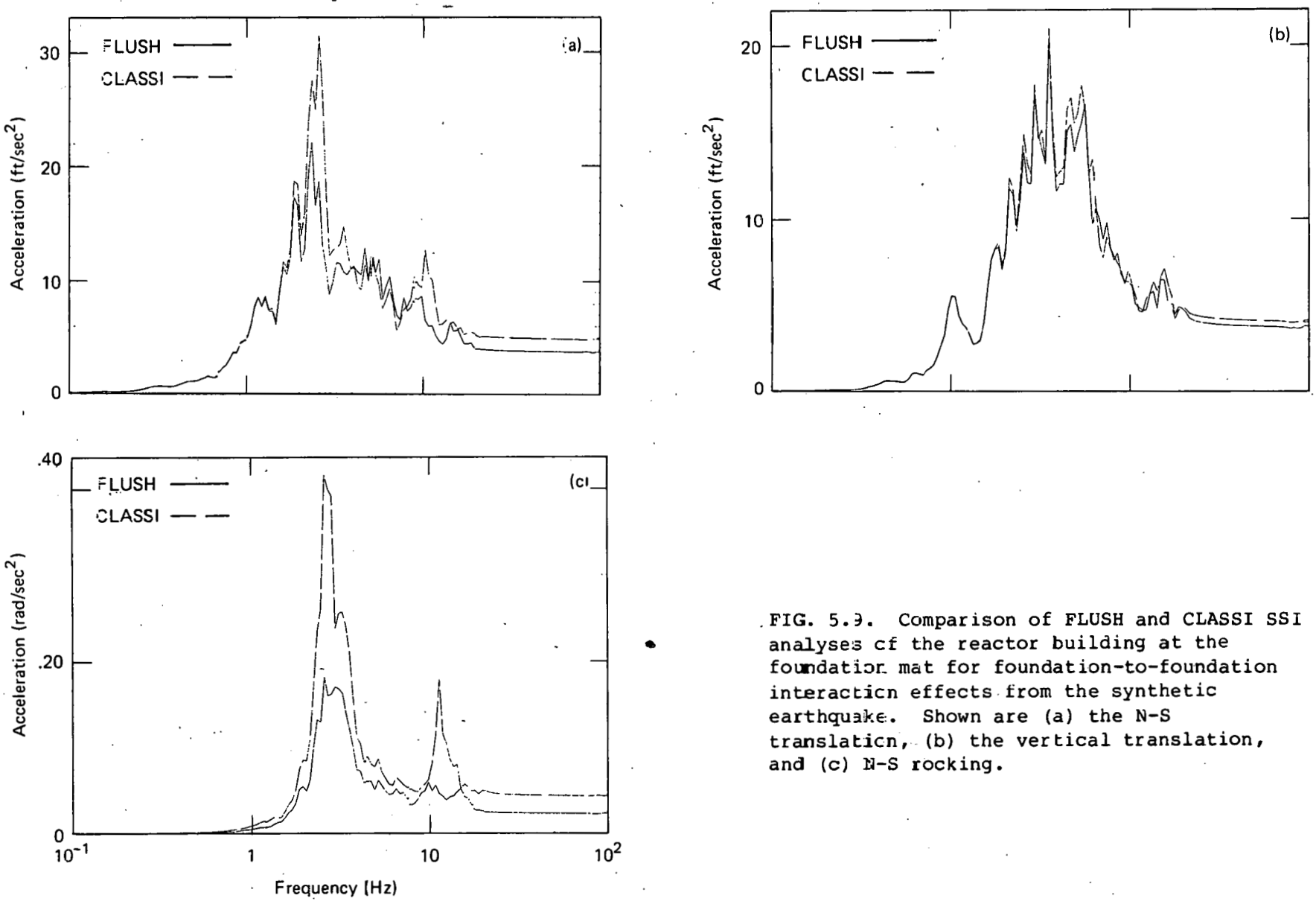

FIG. 5.9. Comparison of FLUSH and CLASSI SSI analyses of the reactor building at the foundation mat for foundation-to-foundation interaction effects from the synthetic earthquake. Shown are (a) the N-S translation, (b) the vertical translation, and (c) N-S rocking.

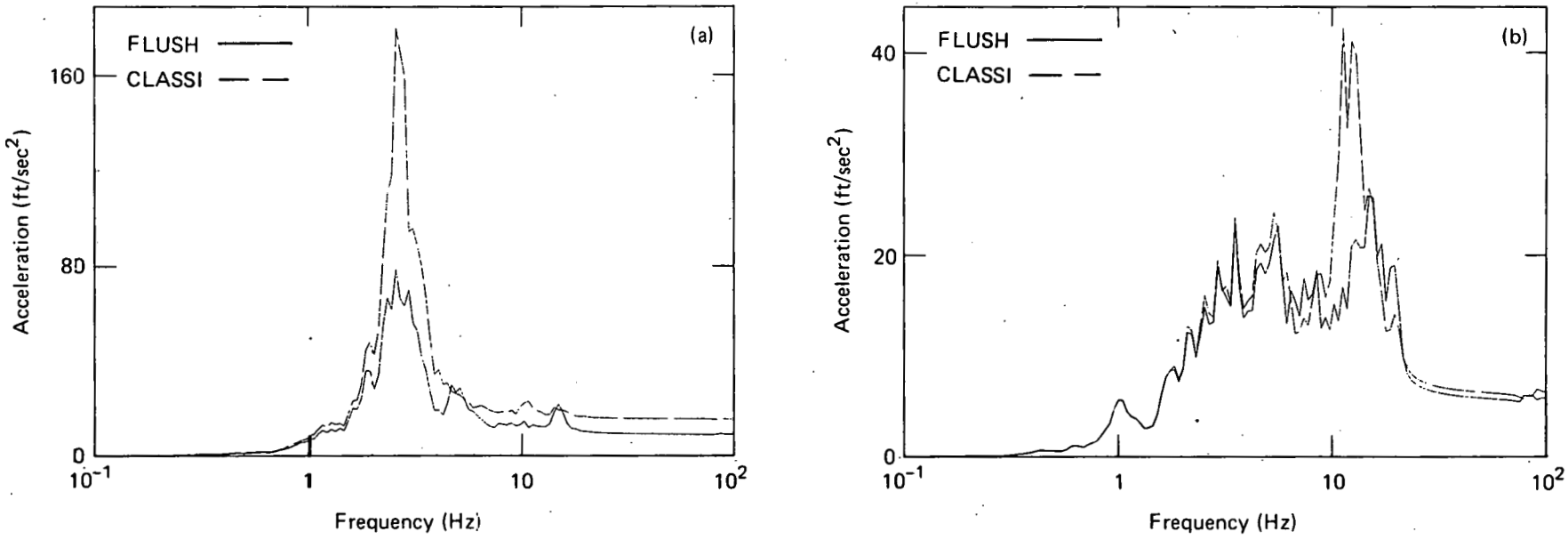

FIG. 5.10. Comparison of FLUSH and CLASSI SSI analyses of the reactor building at the top of the containment shell for foundation-to-foundation interaction effects from the synthetic earthquake. (a) shows the N-S and (b) the vertical translations.

CLASSI spectral peaks for the N-S translation (Fig. 5.9a) are up to 50% higher than those from FLUSH in the frequency range between 2 and 4 Hz. For rocking (Fig. 5.9c) the CLASSI response is over 150% higher at the primary rocking frequency (2.5 to 3.5 Hz). Vertical response on the foundation (Fig. 5.9b) appears to agree fairly well. At the top of the containment shell, spectral accelerations for the N-S translation (Fig. 5.10a) reflect the differences seen in the foundation N-S translation and rocking. Here the CLASSI spectral peak is about 135% higher than the FLUSH value. For vertical response (Fig. 5.10b), there is a high peak in the CLASSI response spectrum at about 10 to 15 Hz which does not exist for FLUSH. This peak is a result of structure-to-structure interaction between the reactor buildings and the AFT complex. It is not present in the FLUSH results for reasons given below.

If we compare Figs. 5.9 and 5.10 with Figs. 5.1 and 5.3 for the isolated foundation we see that most of the differences on the foundation are results of the modeling of the coupled foundation system. On reviewing the modeling assumptions of CLASSI and FLUSH in Section 4.0, we see that these differences do not seem surprising. The mass of the AFT complex is about five times that of either reactor building. CLASSI assumes the entire foundation to be rigid, thereby mobilizing all of AFT mass to drive the reactor buildings. On the other hand, FLUSH used a structural model for the AFT complex which contained the mass of only that portion of the structure which lay within the slice selected for the problem, while assuming a rigid foundation in the plane of motion; therefore, the mass of the reactor building was about twice as large as that of the AFT model. Thus, for the FLUSH problem, the reactor building was not driven by the AFT complex. This is discussed further in paragraph 5.4.

5.3 SSI ANALYSIS OF THE ISOLATED AFT COMPLEX

In addition to the isolated reactor buildings, we also studied the variability in response of the AFT complex as an isolated structure. In this case we compared the results from a CLASSI SSI analysis of the AFT complex with those from two-stage FLUSH analyses. Analyses were made for the synthetic earthquake only. Three components of free-field motion were included.

The CLASSI analysis was straightforward, using the soil impedances and wave-scattering effects for the isolated foundation described in paragraph 4.4

and performing the analysis for the three free-field components simultaneously. For the FLUSH analyses we first performed separate SSI analyses of cross sections B-B and C-C (Fig. 4.22), using the appropriate horizontal and vertical free-field motions. The foundation motions obtained were combined according to Table 5.6, resulting in five components: three translations and two rocking components. No torsional input motion was obtained. Note that two sets of foundation motions were calculated, varying only in the vertical component. In one case (denoted FLUSH analysis 1) this component was obtained from the vertical analysis of cross section B-B and in the other case (denoted FLUSH analysis 2) from the horizontal and vertical

TABLE 5.6. FLUSH analyses of the AFT complex. Table shows the method of combining foundation motions from individual FLUSH analyses to obtain input motions for three-dimensional detailed structural analysis.

E-W translation	Algebraic sum (time-step by time-step) of horizontal foundation translations from analyses of E-W cross section for horizontal and vertical free-field motions.
E-W rocking	Algebraic sum (time step by time step) of foundation rocking from analyses of E-W cross section for horizontal and vertical free-field motions.
N-S translation	Horizontal foundation translation from analysis of N-S cross section for horizontal free-field motion.
N-S rocking	Foundation rocking from analysis of N-S cross section for horizontal free-field motion.
Vertical translation	Vertical foundation translation from analysis of N-S cross section for vertical free-field motion.
	Algebraic sum (time-step by time-step) of vertical foundation translations from analyses of E-W cross section for horizontal and vertical free-field motions.

analyses of cross section C-C. During this process, the motions were calculated at locations in each cross section which correspond to the reference point on the foundation for the second-stage analysis. Two second-stage analyses were performed, one for each set of foundation motions. Each of the above cases are represented in Figs. 5.11 to 5.15 by two sets of vertical response spectra denoted "FLUSH"; the horizontal spectra, being virtually identical for both FLUSH cases, are represented by one set of spectra. Response was calculated at locations in the structure selected to illustrate the effects of all six components of foundation motion on structural response.

Response spectra on the AFT foundation obtained from the CLASSI and FLUSH first stage (SSI) analyses are shown in Fig. 5.11. Peak accelerations are summarized in Table 5.7. Differences in the amplitudes of spectral peaks are summarized in Table 5.8. In general, the translational motions from FLUSH agree well with those from CLASSI. Differences in peak accelerations were on the average about 5%. The largest differences in peak spectral accelerations occurred in narrow frequency ranges; about 40% near 10 Hz for the E-W translation (Fig. 5.11a); about 25% near 10 Hz for the N-S translation (Fig. 5.11b); about 30% between 6 and 10 Hz for the vertical translation. Response spectra for rocking in the E-W direction (about the y-axis) and N-S direction (about the x-axis) have distinct differences. For E-W rocking (Fig. 5.11e) the frequency content was similar, but amplitudes differed by as much as 100%, and the ZPAs differed by almost 50%. The spectra for N-S rocking (Fig. 5.11d) differed in the frequency of the spectral peak. The CLASSI result had its largest amplification in the range between 5 and 7 Hz, while the FLUSH value occurred at about 10 Hz. This difference may be a result of some unavoidable flexibility in the foundation of the FLUSH model of cross section B-B, because while the response spectrum shown in Fig. 5.11d was representative of the motion near the plane of symmetry of the model, typical motions at the foundation's far ends had spectral peaks at about 3.5 Hz. Thus the CLASSI result lies between the two FLUSH results. Interestingly, the ZPAs were within 5% of each other. Torsional foundation response predicted by the CLASSI analysis is shown in Fig. 5.11f. No corresponding FLUSH result exists. Note that the torsional response from CLASSI is of the same magnitude as the N-S rocking.

The differences in the response on the foundation are a result of the differences in modeling assumptions used for each analysis, both for modeling

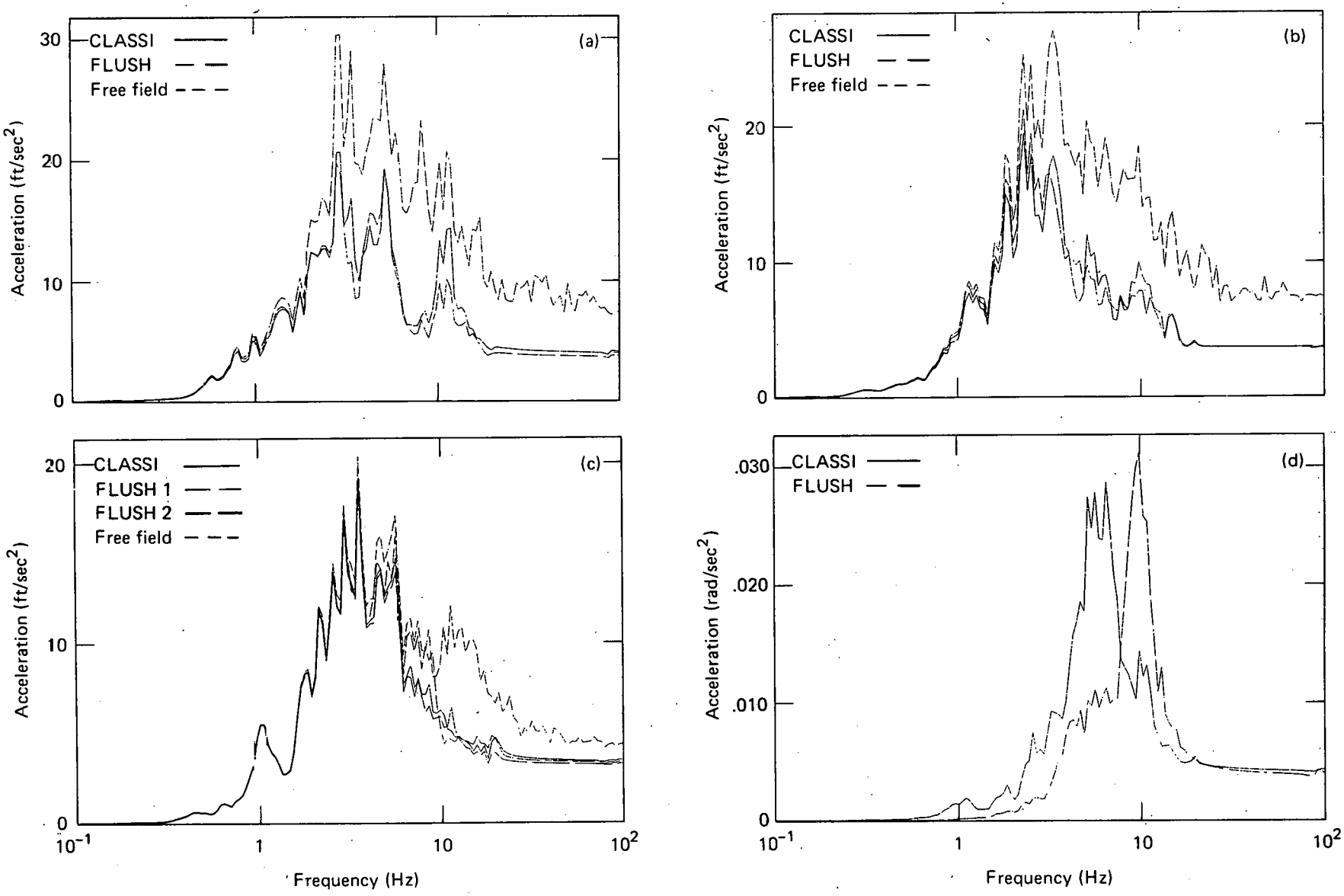

FIG. 5.11. Comparison of CLASSI and FLUSH analyses of the isolated AFT complex at its foundation. Shown are (a) E-W translation, (b) N-S translation, (c) vertical translation, (d) N-S rocking.

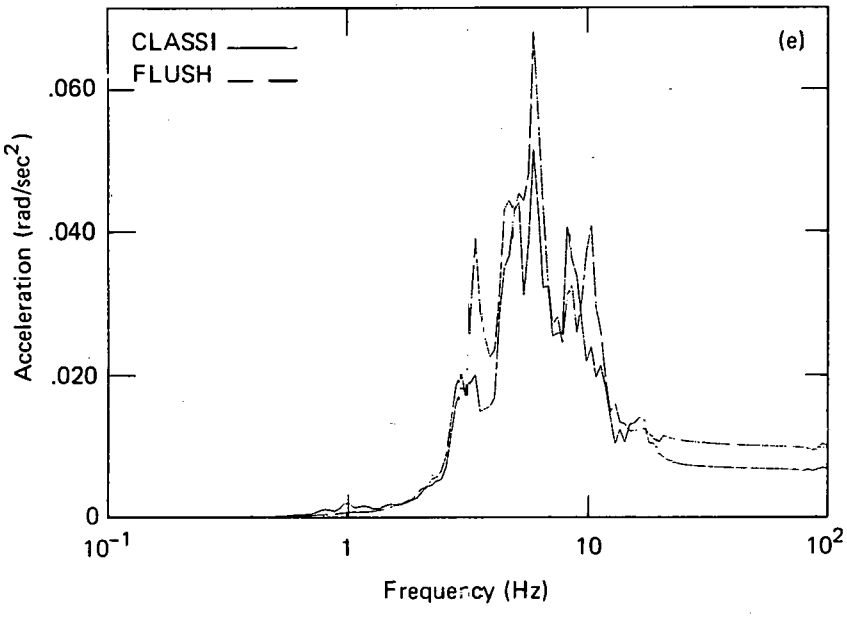

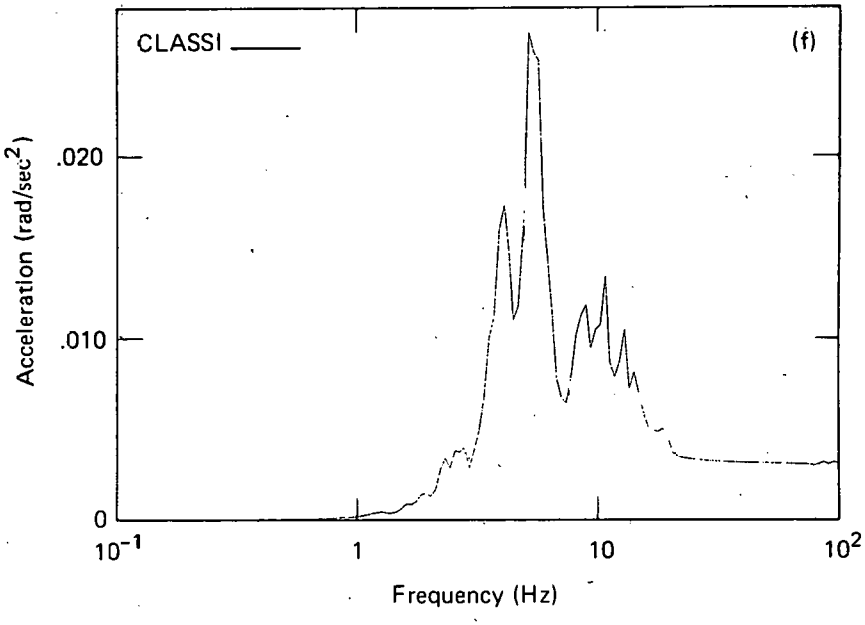

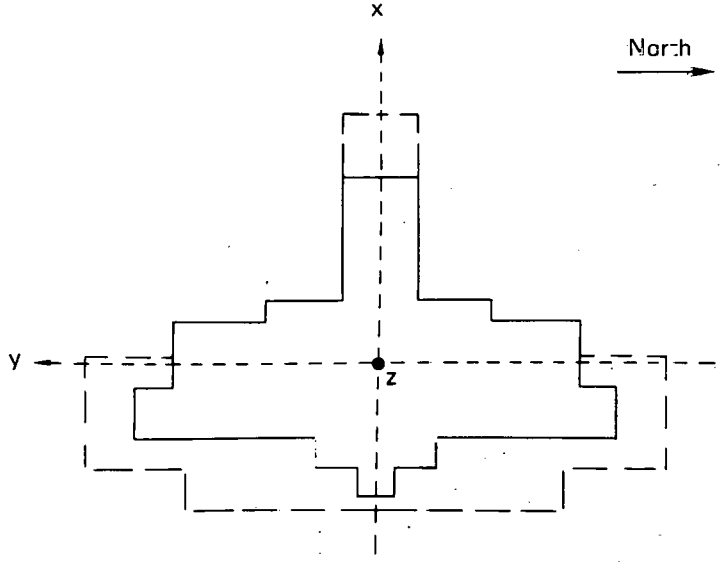

FIG. 5.11. (Continued). (e) E-W rocking, and (f) torsion.

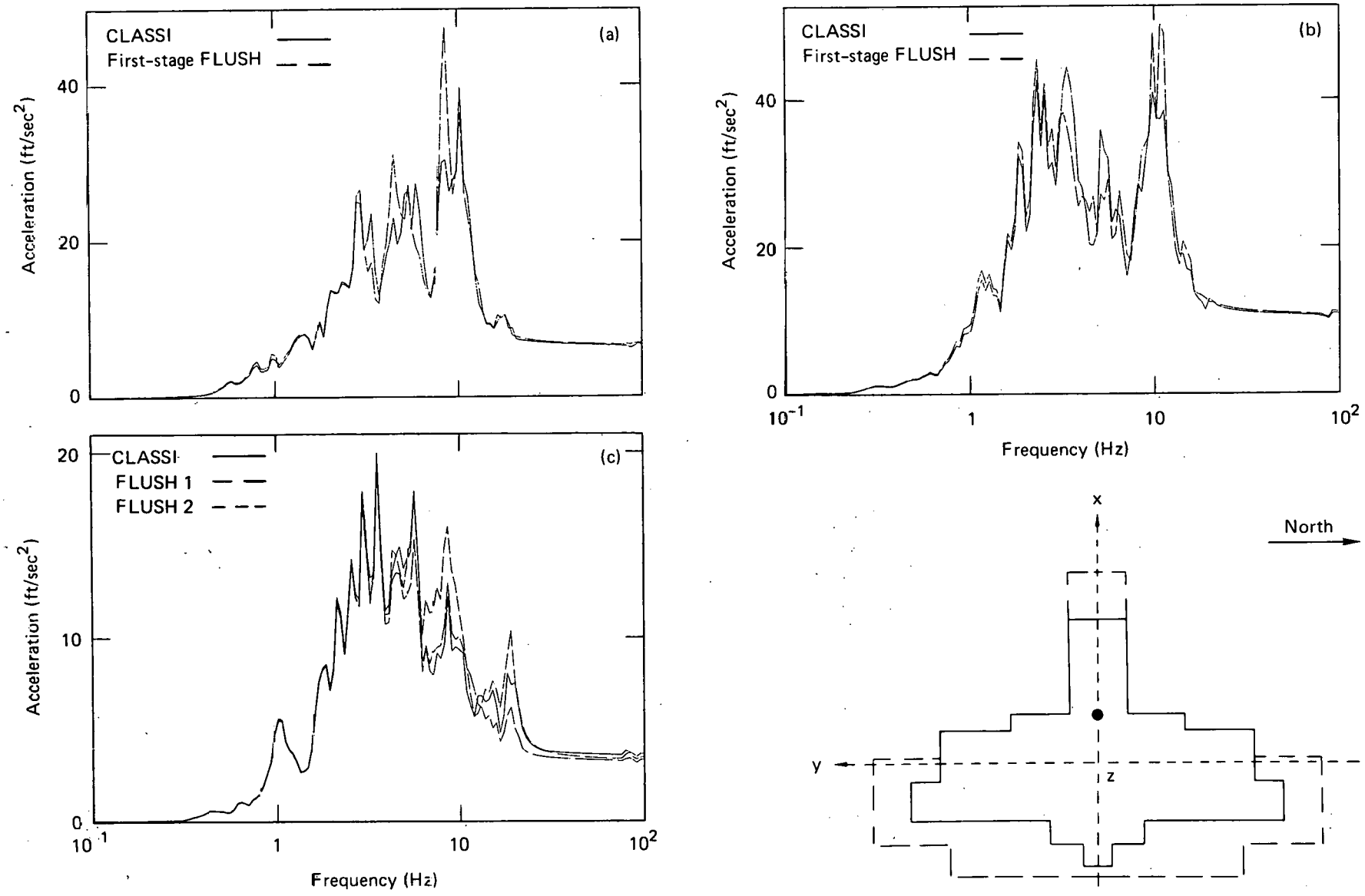

FIG. 5.12. Comparison of CLASSI and FLUSH analyses of the isolated AFT complex in the control room. Shown are (a) E-W translation, (b) N-S translation, and (c) vertical translation.

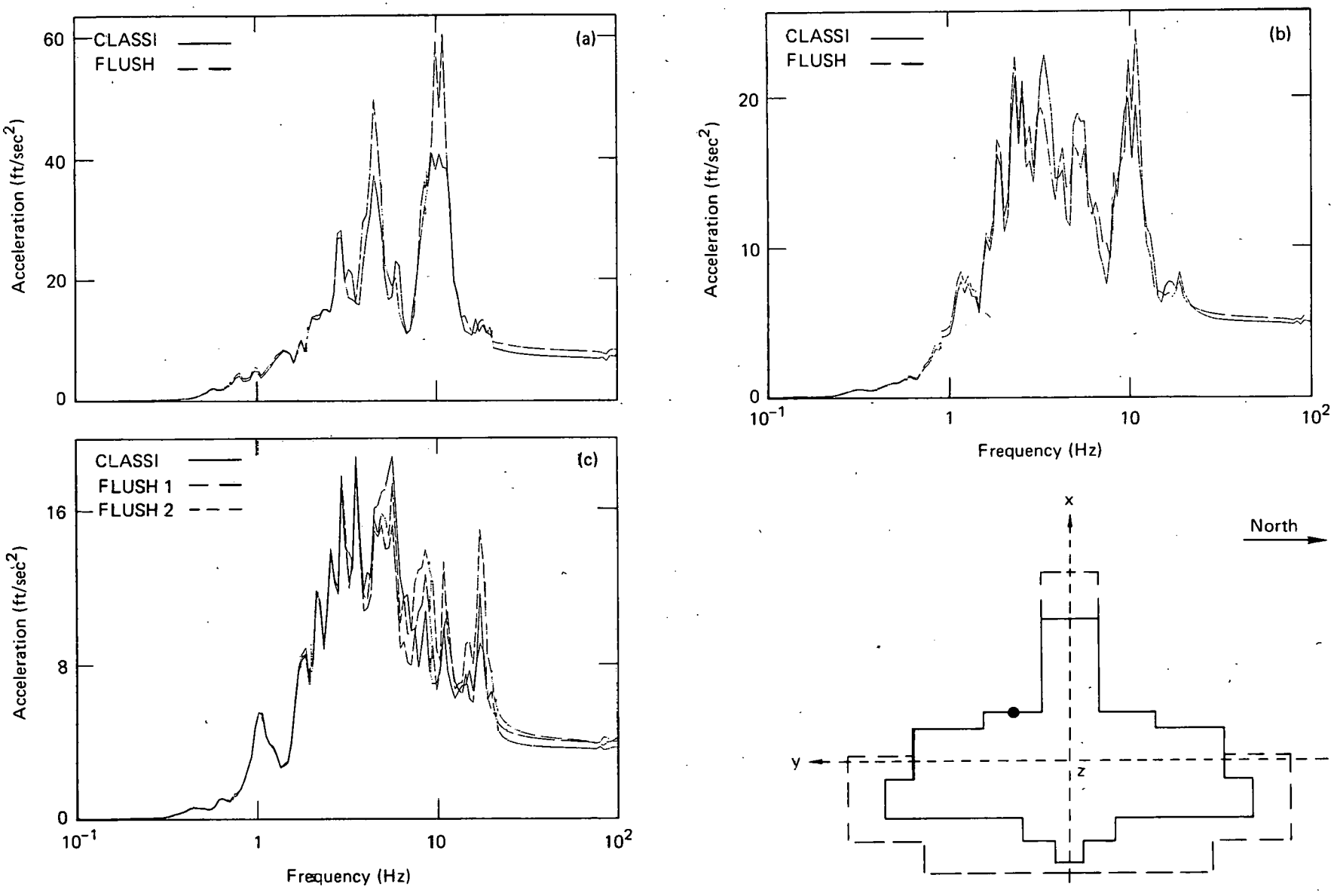

FIG. 5.13. Comparison of CLASSI and FLUSH analyses of the isolated AFT complex near the south end of the auxiliary building roof. Shown are (a) E-W translation, (b) N-S translation, and (c) vertical translation.

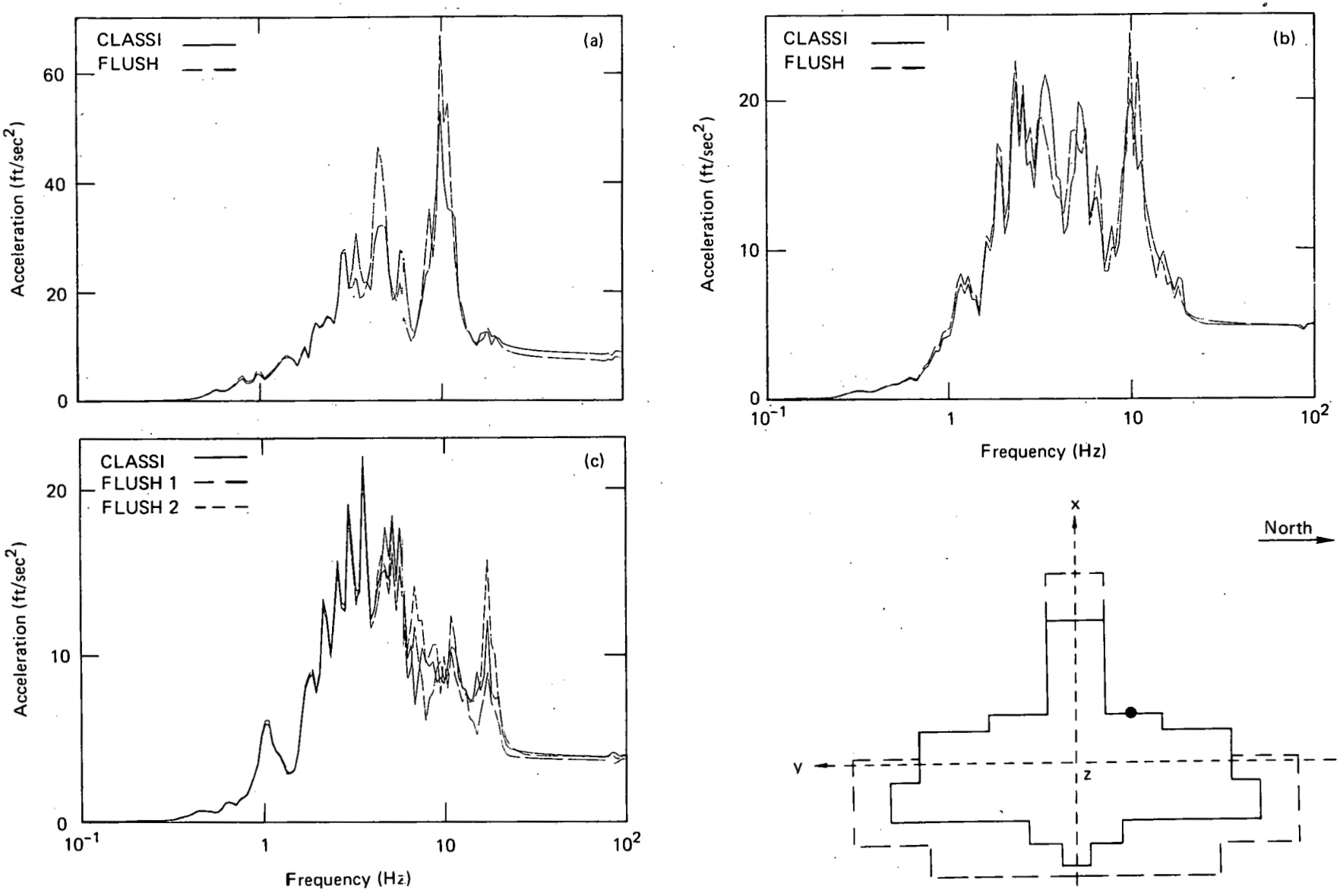

FIG. 5.14. Comparison of CLASSI and FLUSH analyses of the isolated AFT complex near the north end of the auxiliary building roof. Shown are (a) E-W translation, (b) N-S translation, and (c) vertical translation.

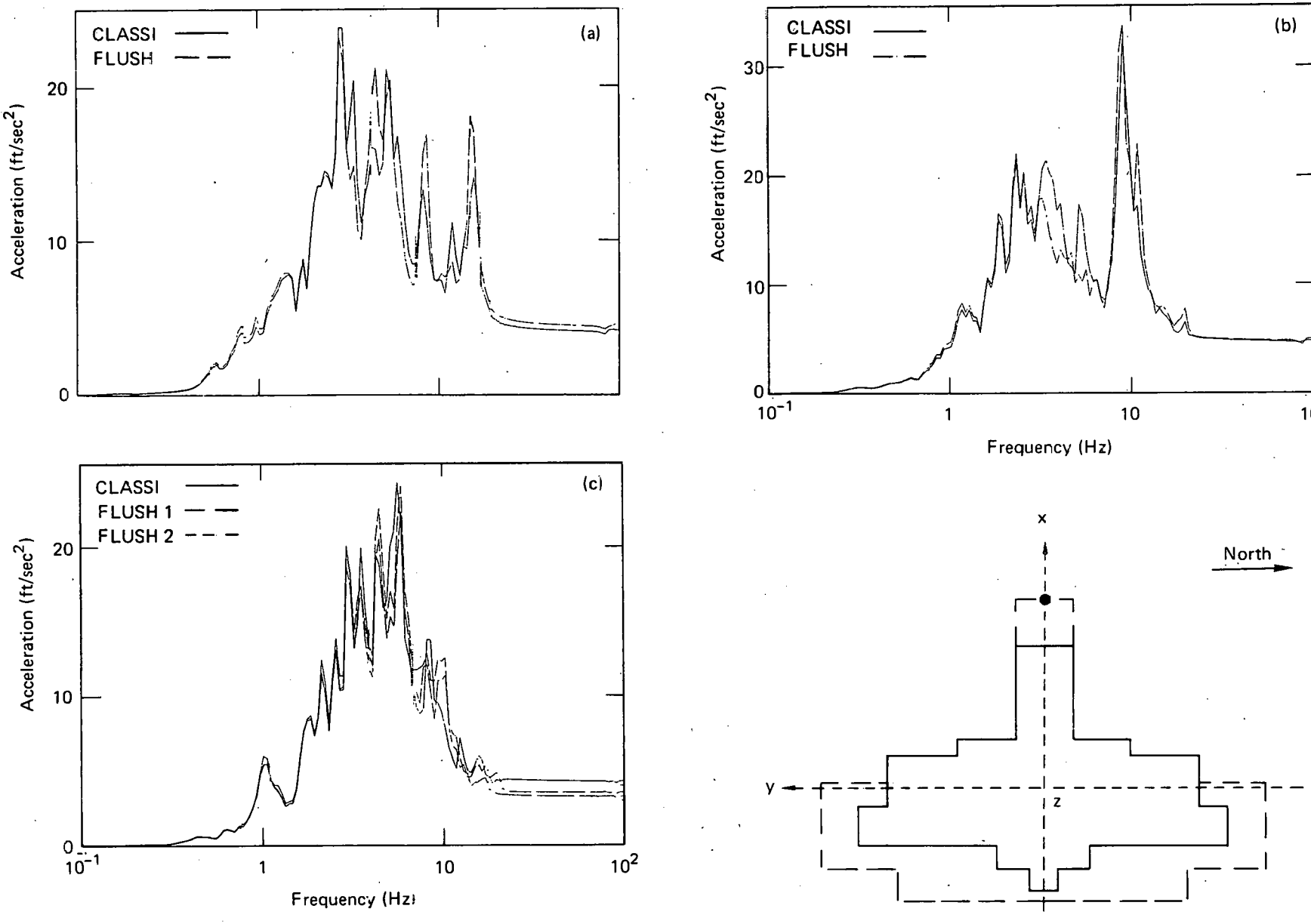

FIG. 5-15. Comparison of CLASSI and FLUSH analyses of the isolated AFT complex at the west wall. Shown are (a) E-W translation, (b) N-S translation, and (c) vertical translation.

TABLE 5.7. Comparison of CLASSI and FLUSH analyses of isolated AFT complex. Table shows a summary of peak accelerations. Translations are given in ft/sec^2. Rotations are given in rad/sec^2.

Location and component	CLASSI analysis	FLUSH second-stage analysis	
Foundation at reference point			
E-W translation	4.10	3.76	3.76
N-S translation	3.68	3.65	3.65
Vertical translation	3.45	3.25	3.37
N-S rocking	.0042	.0040	.0040
E-W rocking	.0070	.0102	.0102
Torsional rotation	.0032	--	--
Control room			
E-W translation	6.70	6.84	6.86
N-S translation	5.40	5.49	5.49
Vertical translation	3.68	3.36	3.48
Auxiliary building roof, south end			
E-W translation	7.23	8.29	8.65
N-S translation	5.02	5.31	5.36
Vertical translation	3.68	4.04	4.12
Auxiliary building roof, north end			
E-W translation	8.82	7.69	7.57
N-S translation	4.89	4.95	4.92
Vertical translation	3.68	3.45	3.63
West wall of fuel-handling building			
E-W translation	4.16	4.51	4.73
N-S translation	4.78	4.88	4.88
Vertical translation	4.31	3.28	3.55

TABLE 5.8. Variations in acceleration response spectra (2% damping) for the AFT complex, assuming an isolated foundation. Differences are given in percent.

Location	Horizontal			Vertical		
		Amplified frequency range			Amplified frequency range	
	ZPA	Typical	Extreme	ZPA	Typical	Extreme
Foundation	<10	<25	40	<10	<15	30
Control room	< 5	<30	60	<10	<15	35
Auxiliary building roof	<20	<25	50	<10	<20	40
West wall of fuel handling building	<15	<30	50	<25	<20	50

the soil behavior and for idealizing the structure. Without further study, however, we are not able to determine the contribution from each.

We obtained in-structure peak accelerations response spectra in the control room, about 50 ft above grade, on the roof near the north and south ends of the auxiliary building, about 75 ft above grade, and about two-thirds of the way up the west wall of the fuel-handling building. These are shown in Figs. 5.12 through 5.15 and Table 5.7. Differences are summarized in Table 5.8. In general, the differences between the CLASSI and second-stage FLUSH analyses are somewhat larger than on the foundation. Variations in peak accelerations at the different locations average about 12% for the E-W and vertical directions, while the N-S direction shows better agreement, with an average variation of about 3%. The differences between the in-structure response spectra show the same general pattern as the differences in the corresponding translational foundation spectra, increasing in some narrow

frequency bands by up to about double that on the foundation. In the E-W direction (Figs. 5.12a-5.15a), the FLUSH results show a marked amplification near 4-5 Hz and 8-12 Hz that is not nearly as pronounced in the CLASSI results. This pattern occurs at all our locations and the frequency bands are close to the frequencies of the predominant E-W structural modes of the AFT complex. These changes from the differences on the foundation are results of differences in FLUSH and CLASSI E-W foundation rocking, including the phase relationships with the foundation translations. In the N-S direction (Fig. 5.12b-5.15b), the differences at the control room and on the auxiliary building roof are about the same as on the foundation. At the west wall, the CLASSI response shows a spectral peak at 5.5 Hz, which is about 50% higher than the FLUSH response. This is probably caused by the torsional foundation motion from the CLASSI analysis. In the vertical direction the 30% difference in the foundation motion between 6 and 10 Hz is also present in the control room and auxiliary building roof, but not at the west wall. The amplification at 19 Hz at the control room and auxiliary building roof is caused by a local vertical roof mode, while the amplification of the FLUSH response on the roof at about 10 Hz appears to be caused by the differences in the N-S foundation rocking.

5.4 COMPARISON OF CLASSI AND FLUSH ANALYSES OF AFT COMPLEX INCLUDING STRUCTURE-TO-STRUCTURE INTERACTION EFFECTS

To study differences in calculated response of the AFT complex when structure-to-structure interaction effects were included, we compared the results from the FLUSH second-stage analyses that used foundation motions from Sections A-A and C-C (Fig. 4.22) with the CLASSI analysis of the coupled foundation system. As with our study of the isolated AFT complex, this comparison was made for the synthetic earthquake only, using all three components of free-field motion. For the FLUSH analyses, the foundation motions were assembled from the individual SSI analyses in the manner specified in Table 5.6, where Section A-A is the north-south section, and Section C-C is the east-west. Note that Section C-C was used to develop the foundation motions for both the isolated case and this case; hence, we would not expect much change in the FLUSH E-W building response. Any change is most likely a result of torsional response of the structure due to eccentric north-south loading.

A summary of peak accelerations is shown in Table 5.9, and response spectra of motions on the foundation and in the structure are shown in Figs. 5.16 through 5.20. The locations where response was obtained are the same as those used for the isolated case (paragraph 5.3), and again, two sets of vertical spectra denoted "FLUSH" are shown. Table 5.10 summarizes the variations between the FLUSH and CLASSI results. In general, peak accelerations agreed within about 10 to 20%, with the notable exception of the N-S rocking component of the foundation motion and its consequent effects on N-S translations at upper levels in the structure and vertical motions at locations north and south of the AFT centerline. Here, the FLUSH rocking component was an order of magnitude higher than that from CLASSI. This is not surprising when one considers the modeling assumption made for each analysis. The CLASSI formulation assumes that the AFT foundation is rigid, greatly increasing the N-S rocking resistance of the extreme northern and southern portions of the turbine buildings (the distance from the plane of symmetry to extreme ends is 280 ft). In the FLUSH formulation, the foundation is modeled as rigid in the plane of the model, but no constraint exists to limit the differential rotations between parallel slices. Because of this, the effective rocking resistance of the AFT complex as modeled in Section A-A is determined for a resisting arm of only 43.5 ft. Thus, we would expect the CLASSI model, much stiffer in N-S soil rocking impedance, to produce much lower foundation rocking than FLUSH.

The effects of the differences in the foundation N-S rocking components is evident in the response spectra of all of the N-S translations in the structure, as well as in the spectra of the vertical translations at the north and south ends of the auxiliary building roof. The spectral amplification of the FLUSH results frequency (3-4 Hz) is from 2-1/2 to almost 6 times that of the CLASSI results at the rocking frequency (3-4 Hz). This appears to be responsible for the large differences in the ZPAs of the vertical motions, although not for the horizontal motions. The difference in the N-S ZPAs at the north and south ends of the auxiliary building appears to be caused by the spectral peak at about 18 Hz, suggesting that the first stage FLUSH structural model did not include a N-S mode that is present in the detailed model.

TABLE 5.9. Comparison of CLASSI and FLUSH analyses of coupled foundations for the AFT complex. Table shows a summary of peak accelerations in the AFT complex. Translations are given in ft/sec^2. Rotations are given in rad/sec^2.

Location and component	CLASSI analysis	FLUSH second-stage analysis	
Foundation at reference point			
E-W translation	4.20	3.76	3.76
N-S translation	3.85	3.24	3.24
Vertical translation	3.57	3.50	3.37
N-S rocking	.0045	.0440	.0440
E-W rocking	.0073	.0102	.0102
Torsional rotation	.0047	--	--
Control room			
E-W translation	6.06	6.83	6.86
N-S translation	5.59	5.82	5.82
Vertical translation	3.64	3.51	3.48
Auxiliary building roof, south end			
E-W translation	7.73	7.34	7.31
N-S translation	5.23	6.70	6.78
Vertical translation	3.79	11.14	10.95
Auxiliary building roof, north end			
E-W translation	9.45	6.63	6.57
N-S translation	5.01	7.28	7.15
Vertical translation	3.87	9.45	9.44
West wall of fuel-handling building			
E-W translation	4.08	4.67	4.73
N-S translation	5.34	5.93	5.93
Vertical translation	4.09	3.25	3.55

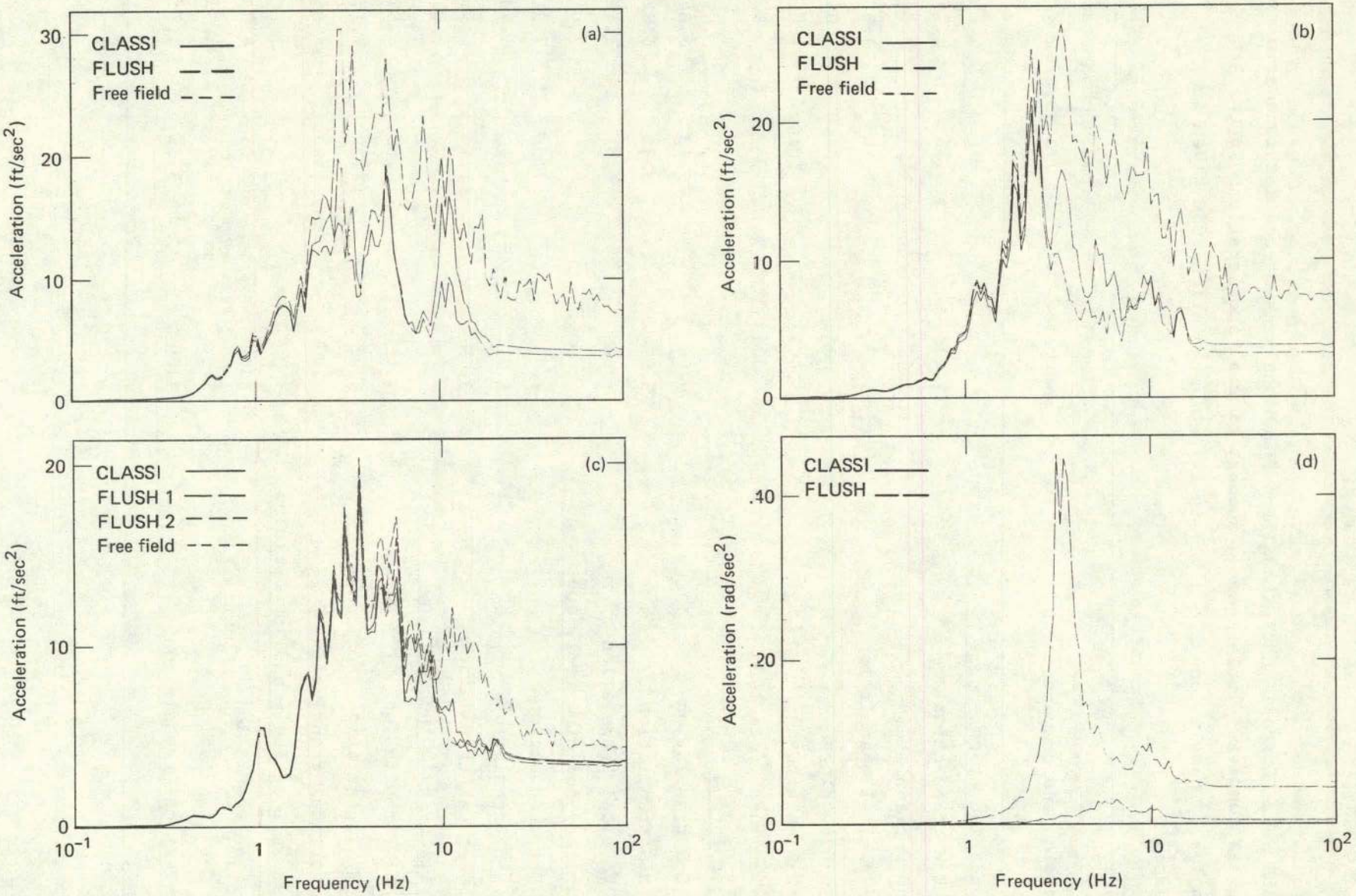

FIG. 5.16. Comparison of CLASSI and FLUSH coupled foundation analyses on the AFT complex foundation. Shown are (a) E-W translation, (b) N-S translation, (c) vertical translation, (d) N-S rocking.

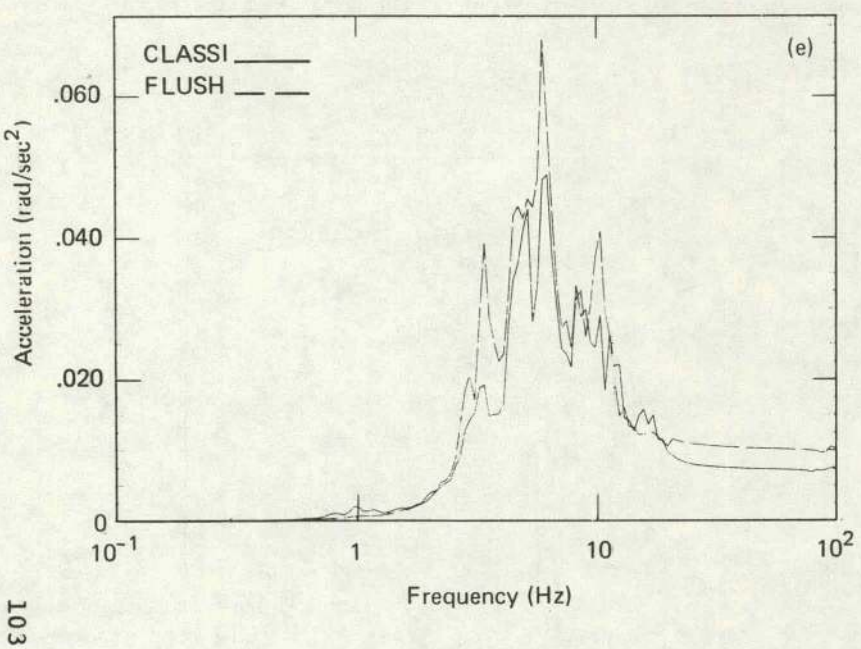

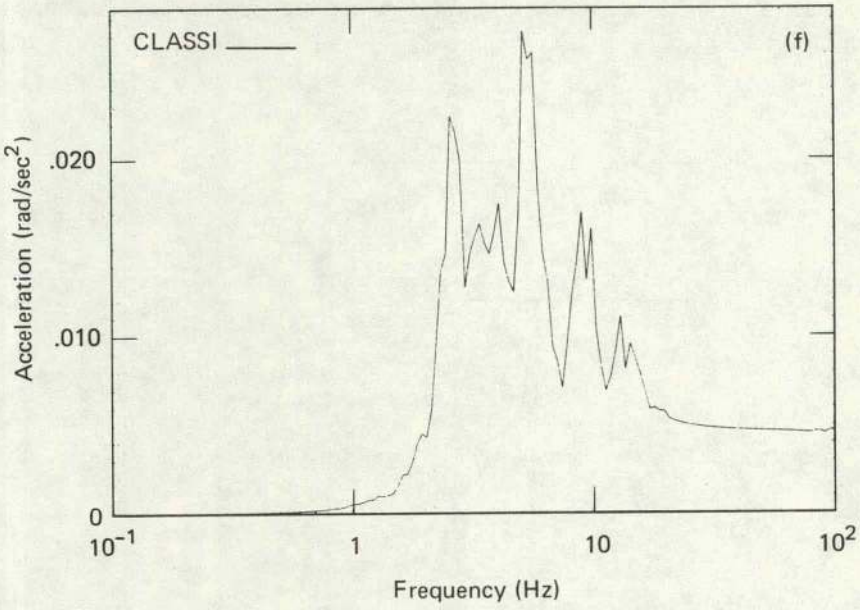

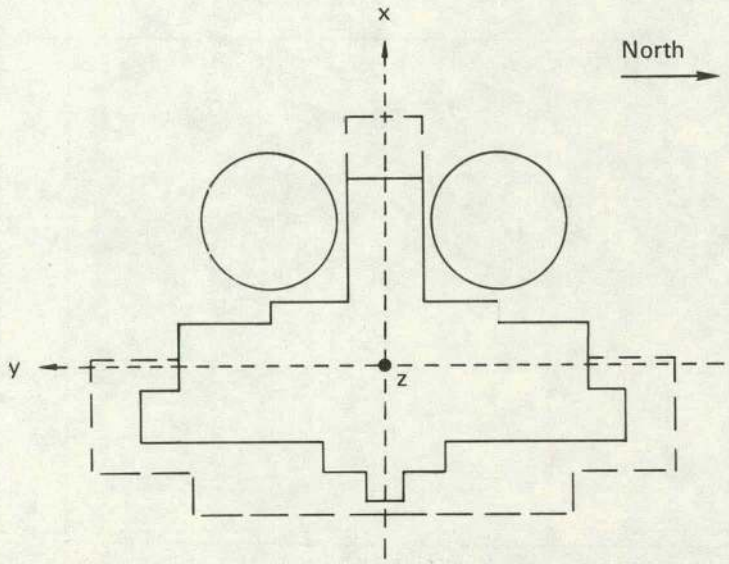

FIG. 5.16. (Continued). (e) E-W rocking, and (f) torsion.

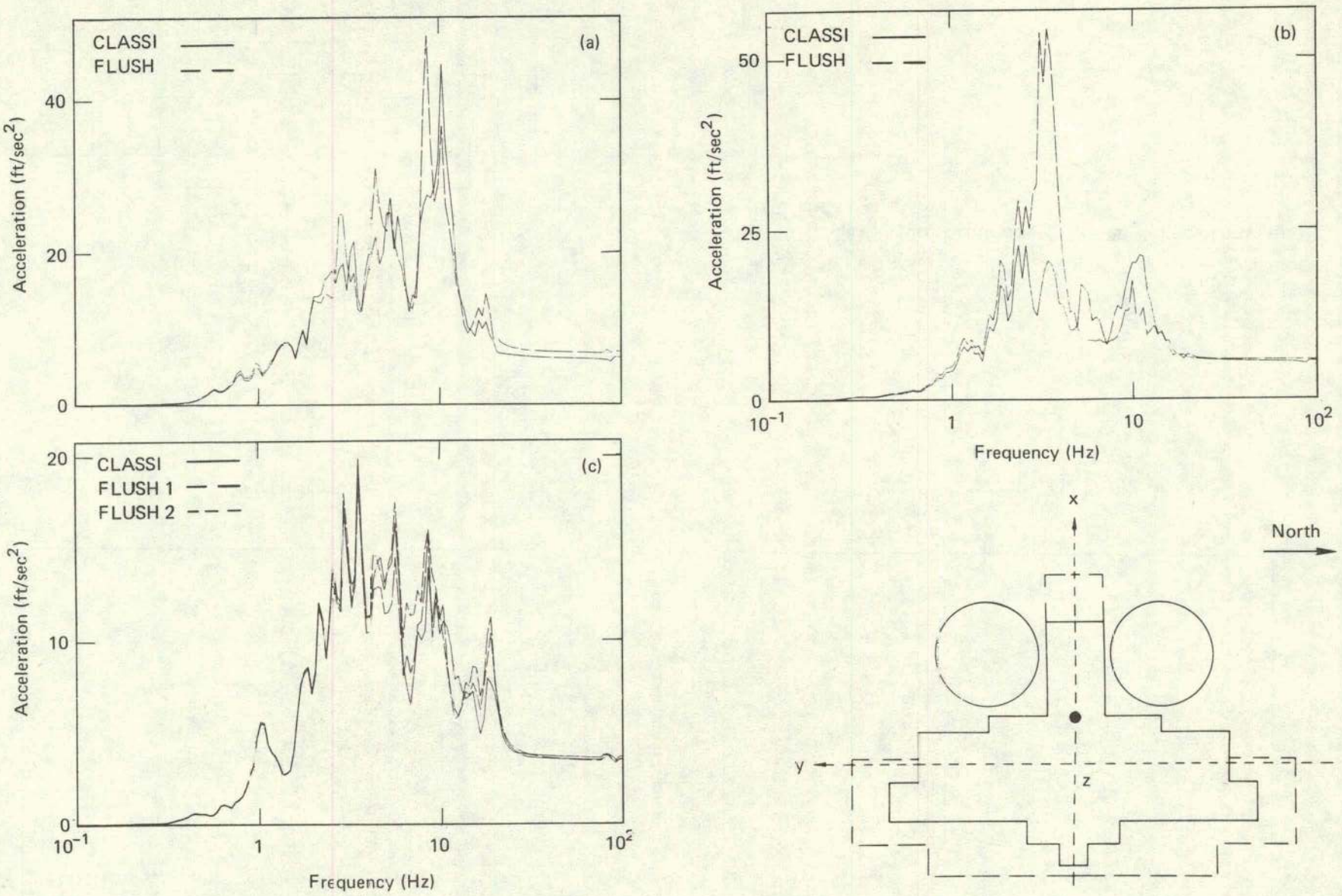

FIG. 5.17. Comparison of CLASSI and FLUSH coupled foundation analyses in the AFT complex control room. Shown are (a) E-W translation, (b) N-S translation, and (c) vertical translation.

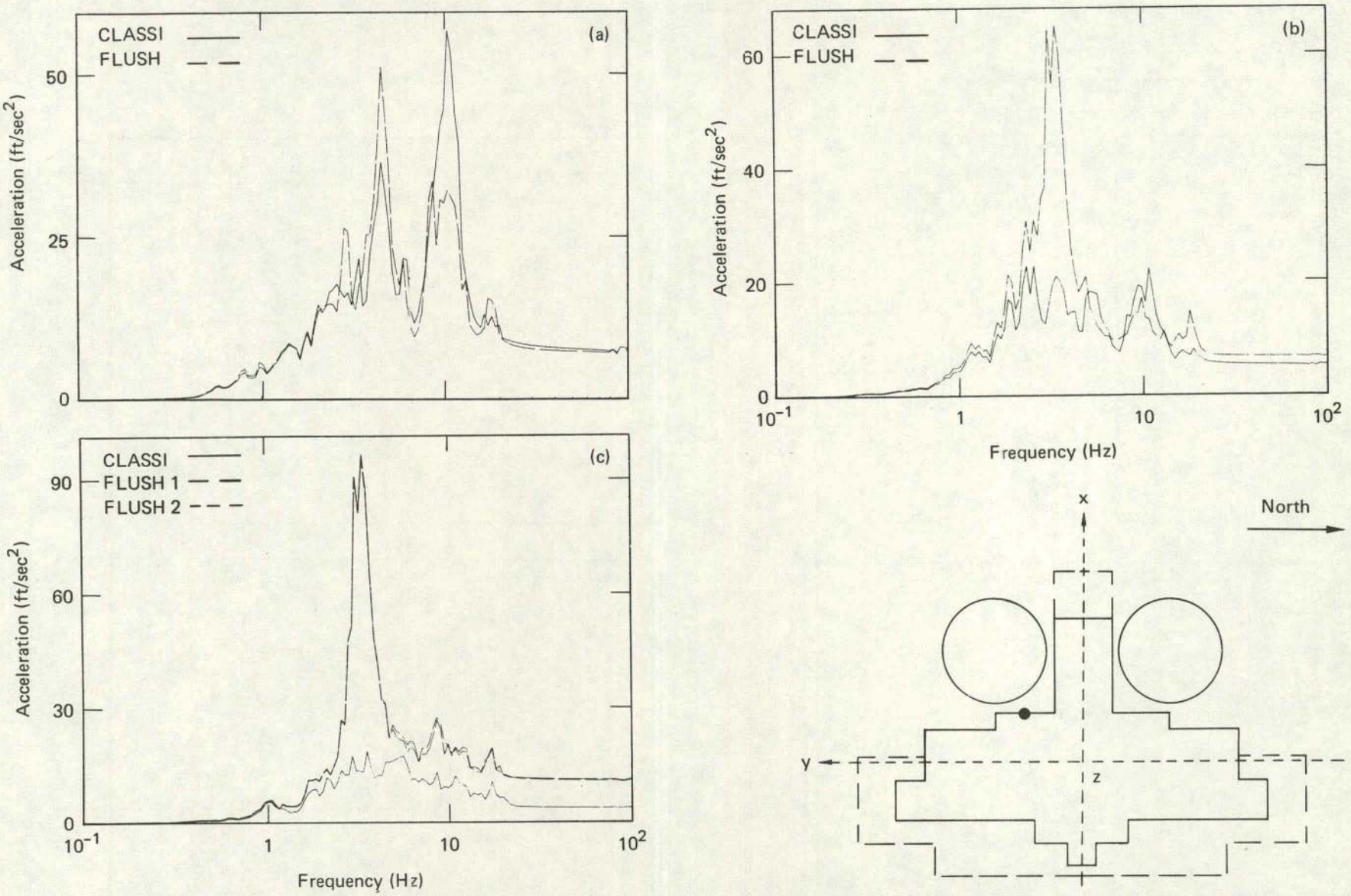

FIG. 5.18. Comparison of CLASSI and FLUSH coupled foundation analyses near the south end of the auxiliary building roof. Shown are (a) E-W translation, (b) N-S translation, and (c) vertical translation.

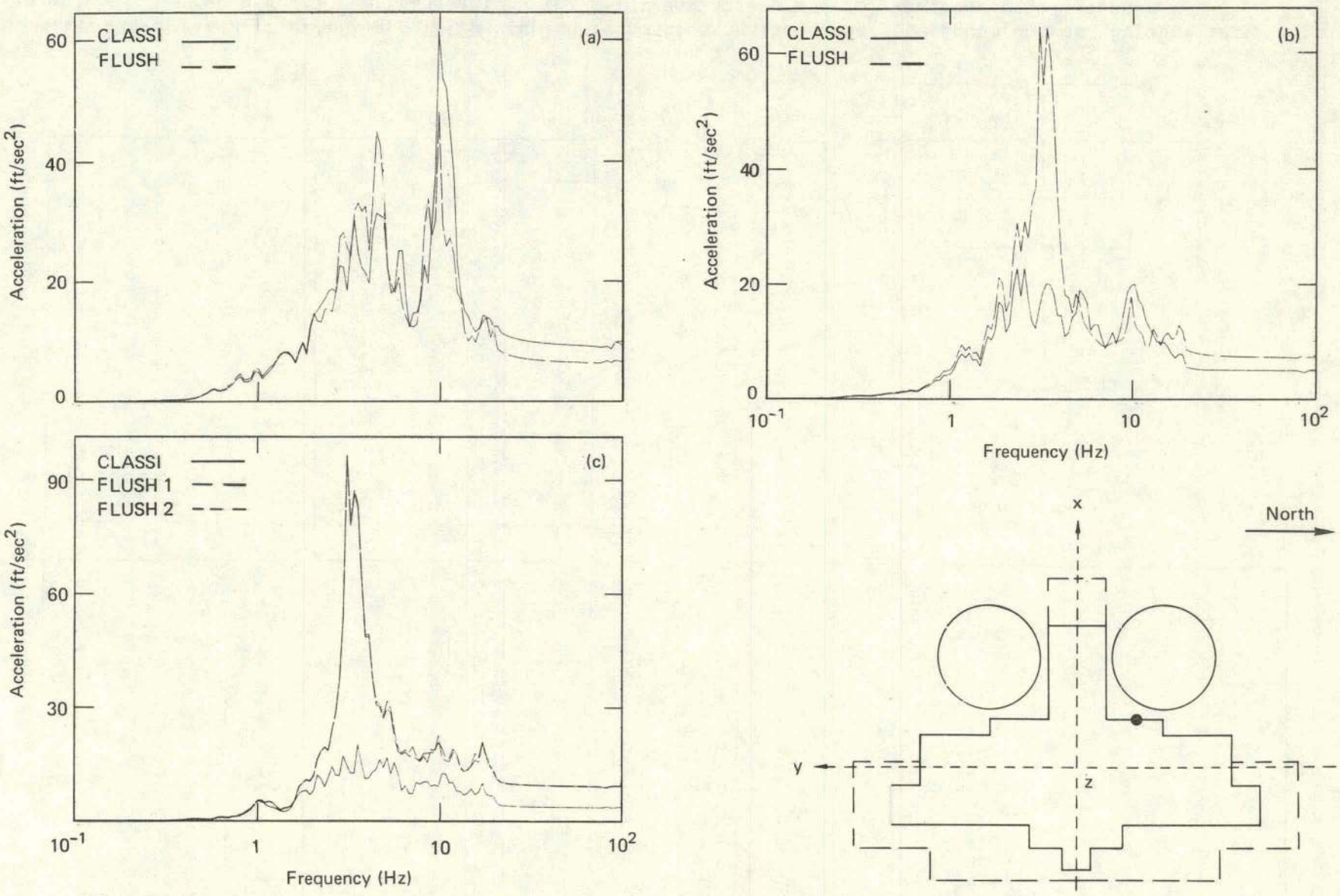

FIG. 5.19. Comparison of CLASSI and FLUSH coupled foundation analyses near the north end of the auxiliary building roof. Shown are (a) E-W translation, (b) N-S translation, and (c) vertical translation.

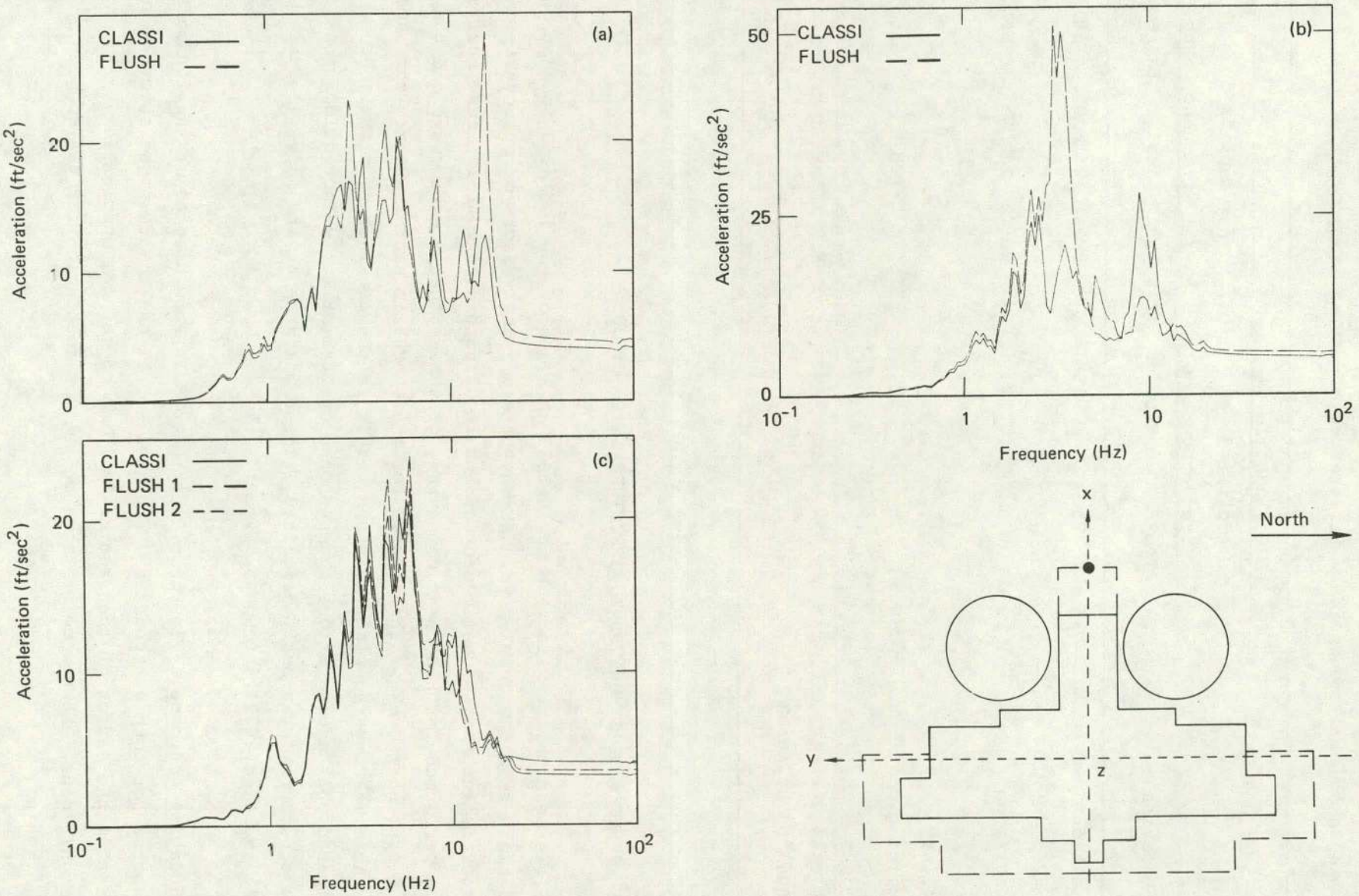

FIG. 5.20. Comparison of CLASSI and FLUSH coupled foundation analyses at the west wall of the AFT complex. Shown are (a) E-W translation, (b) N-S translation, and (c) vertical translation.

TABLE 5.10. Variations in acceleration response spectra for the AFT complex, assuming a coupled foundation. Differences are given in percent.

Location	Horizontal			Vertical		
		Amplified frequency range			Amplified frequency range	
	ZPA	Typical	Extreme	ZPA	Typical	Extreme
Foundation	15	35	65	5	25	50
Control room	10	35	170	5	20	80
Auxiliary building roof	30	35	225	150	125	450
West wall of fuel handling building	15	40	150	20	20	75

5.5 EFFECTS OF STRUCTURE-TO-STRUCTURE INTERACTION

We used the results from the CLASSI analyses of the isolated foundations and those from the coupled foundations to study the effects of structure-to-structure interaction on foundation and in-structure response. These analyses were performed for all three components of the synthetic earthquake and the El Centro earthquake. The results for the synthetic earthquake are the same as those we compared with the FLUSH result in the previous sections. We compared peak accelerations and response spectra at the selected locations in the structures previously described. These comparisons are shown in Table 5.11 and Figs. 5.21 through 5.30.

Foundation Response. Figures 5.21 through 5.24 show spectra of the foundation response for both earthquakes. From Table 5.11 and the response spectra, we see that the effect of the reactor building on the AFT complex is insignificant. Peak accelerations on the AFT foundation for the coupled

TABLE 5.11. Comparison of CLASSI analyses for isolated and coupled foundations. Table shows a summary of foundation and in-structure peak accelerations.

	Synthetic earthquake		El Centro earthquake	
Location and component	Isolated foundation	Coupled foundations	Isolated foundation	Coupled foundations
AFT complex				
Foundation at reference point				
E-W translation	4.10	4.20	3.30	3.45
N-S translation	3.68	3.85	5.34	5.30
Vertical translation	3.45	3.57	2.91	3.04
N-S rocking	.0042	.0045	.0040	.0043
E-W rocking	.0070	.0073	.0052	.0051
Torsional rotation	.0032	.0047	.0034	.0041
Control room				
E-W translation	6.70	6.06	4.64	5.82
N-S translation	5.40	5.59	5.82	5.67
Vertical translation	3.68	3.64	3.63	4.33
Auxiliary building roof, south end				
E-W translation	7.23	7.73	5.61	6.11
N-S translation	5.02	5.23	5.82	5.53
Vertical translation	3.68	3.79	3.34	3.51
Auxiliary building roof, north end				
E-W translation	8.82	9.45	5.84	6.16
N-S translation	4.89	5.01	5.90	5.84
Vertical translation	3.68	3.87	3.82	3.90
West wall of fuel-handling building				
E-W translation	4.16	4.08	3.69	3.88
N-S translation	4.78	5.34	5.51	5.38
Vertical translation	4.31	4.09	2.89	3.04

TABLE 5.11 (cont'd)

Location and component	Synthetic earthquake			El Centro earthquake		
	Isolated foundation	Coupled foundations		Isolated foundation	Coupled foundations	
		Unit 1	Unit 2		Unit 1	Unit 2
Reactor building						
Foundation at reference point						
E-W translation	3.61	3.41	3.80	3.55	3.87	3.84
N-S translation	3.87	4.92	4.52	5.47	5.56	5.71
Vertical translation	3.44	4.10	3.87	2.67	2.89	2.97
N-S rocking	.0344	.0438	.0388	.0270	.0362	.0360
E-W rocking	.0412	.0546	.0547	.0148	.0251	.0258
Torsional rotation	--	.0062	.0051	--	.0041	.0041
Top of containment shell						
E-W translation	16.29	19.17	19.75	6.89	9.30	9.25
N-S translation	12.69	15.97	15.28	10.94	14.86	14.80
Vertical translation	5.40	6.40	6.00	8.66	10.30	10.23
Operating floor						
E-W translation	5.66	6.08	6.29	4.23	5.04	5.18
N-S translation	4.52	6.51	6.07	5.70	6.92	6.98
Vertical translation	3.55	6.23	6.25	2.72	3.09	4.05
Free field						
E-W translation	7.33			3.99		
N-S translation	7.33			6.49		
Vertical translation	4.34			3.92		

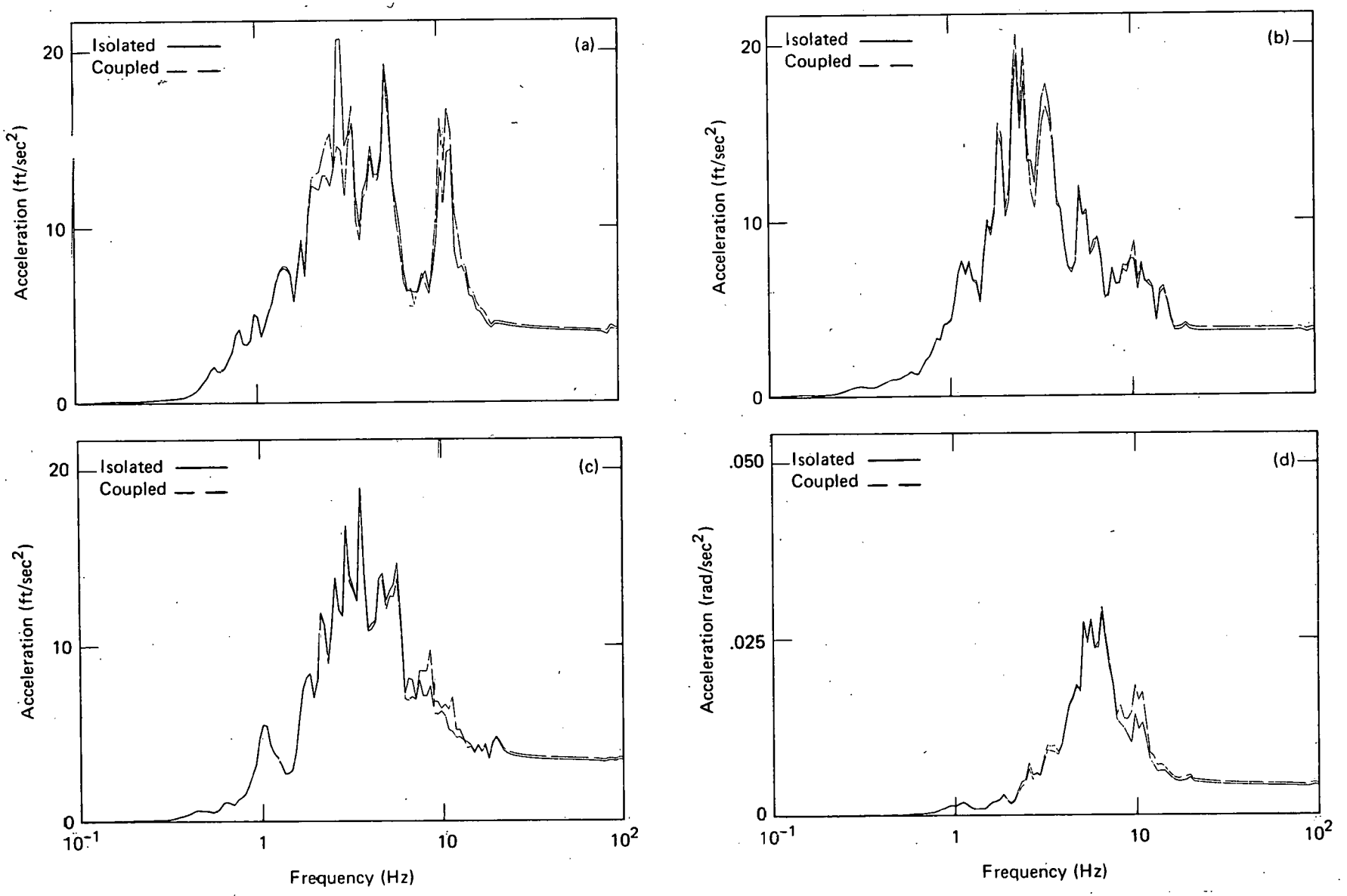

FIG. 5.21. Comparison of isolated and coupled foundation response on the AFT complex foundation, using synthetic earthquake data. Shown are (a) E-W translation, (b) N-S translation, (c) vertical translation, (d) N-S rocking.

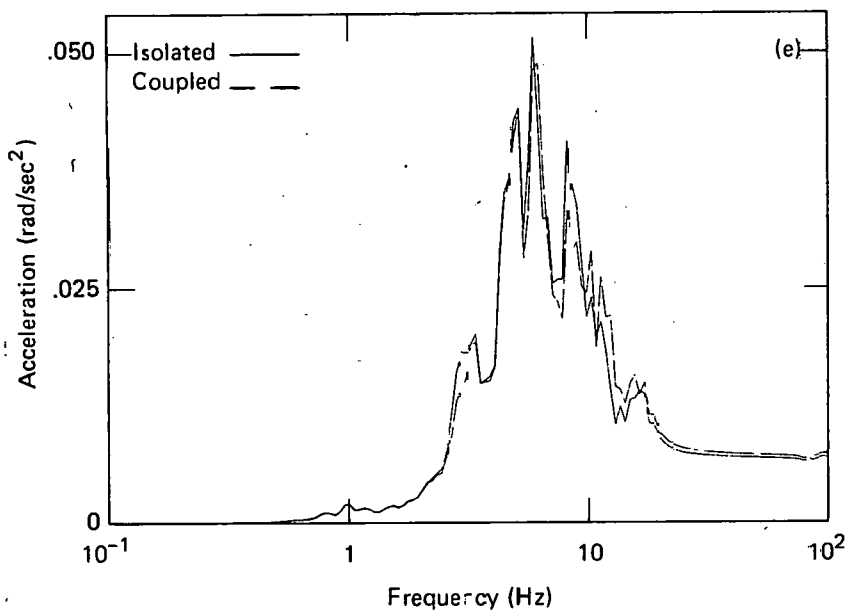

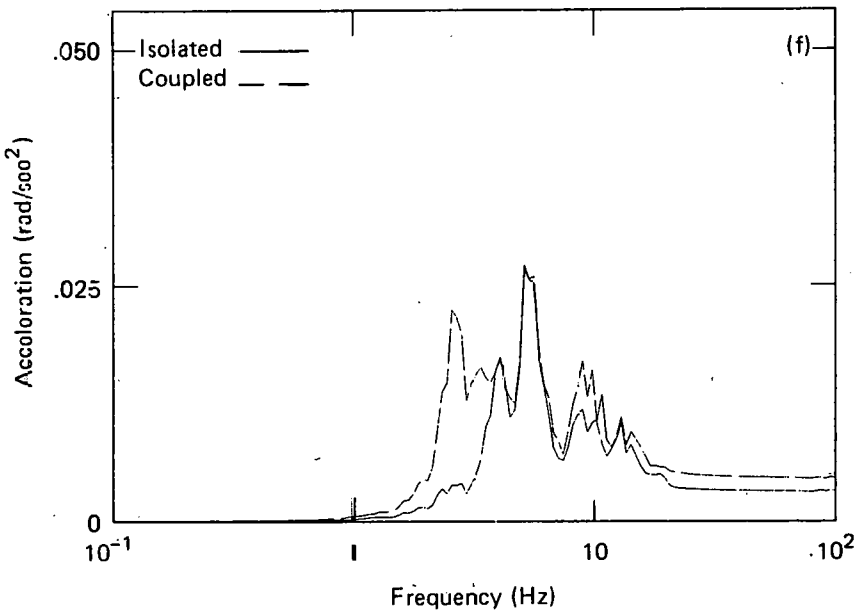

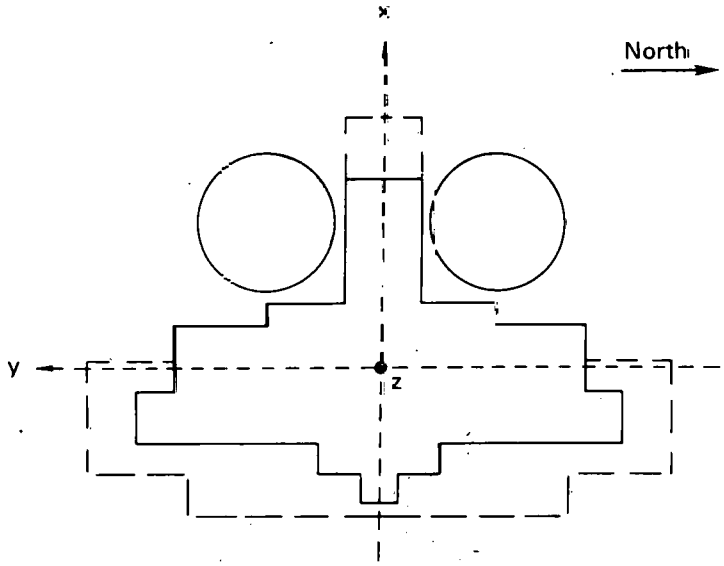

FIG. 5.21. (Continued). (e) E-W rocking, and (f) torsion.

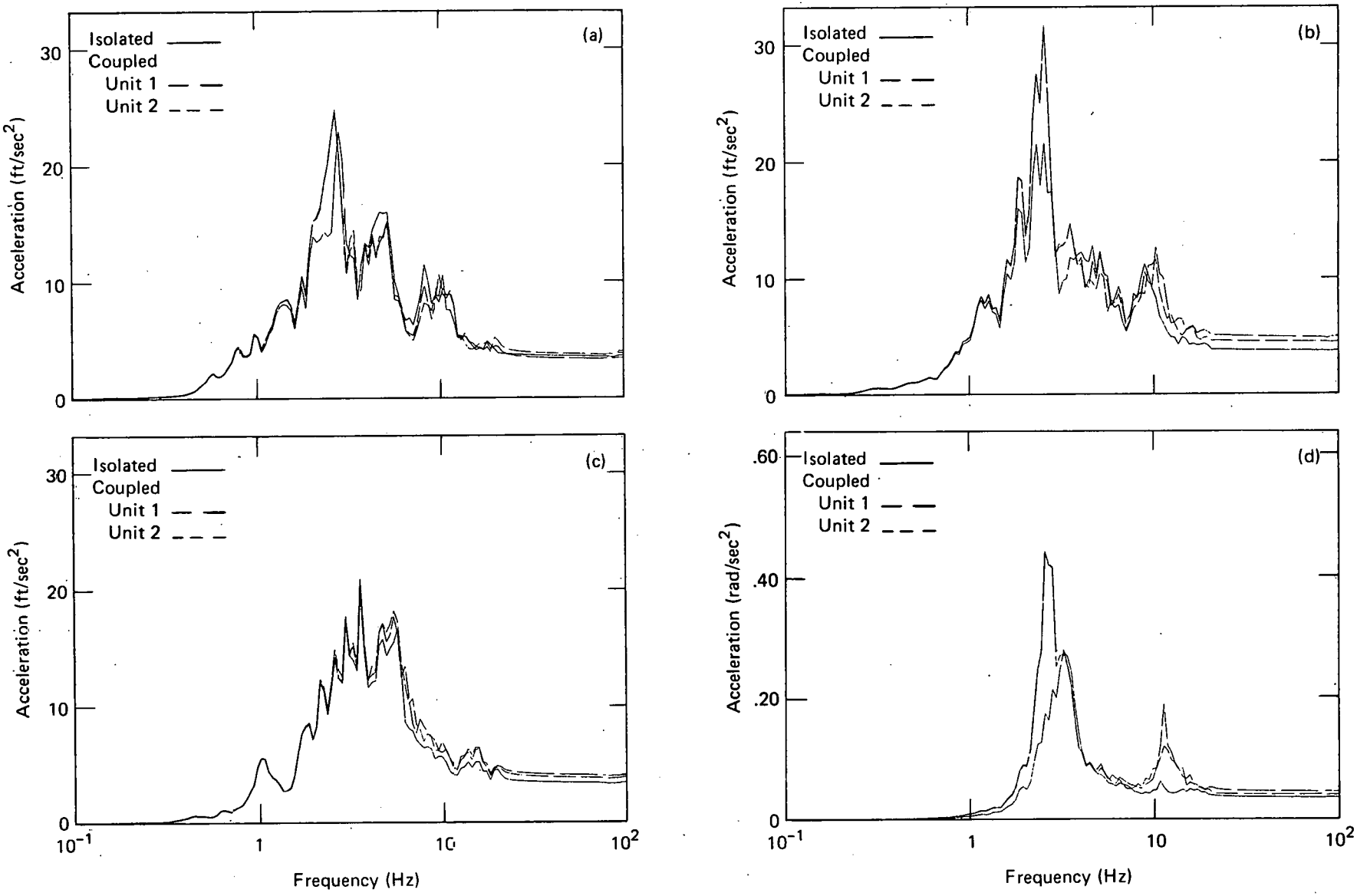

FIG. 5.22. Comparison of isolated and coupled response on the reactor building foundation, using synthetic earthquake data. Shown are (a) E-W translation, (b) N-S translation, (c) vertical translation, (d) N-S rocking.

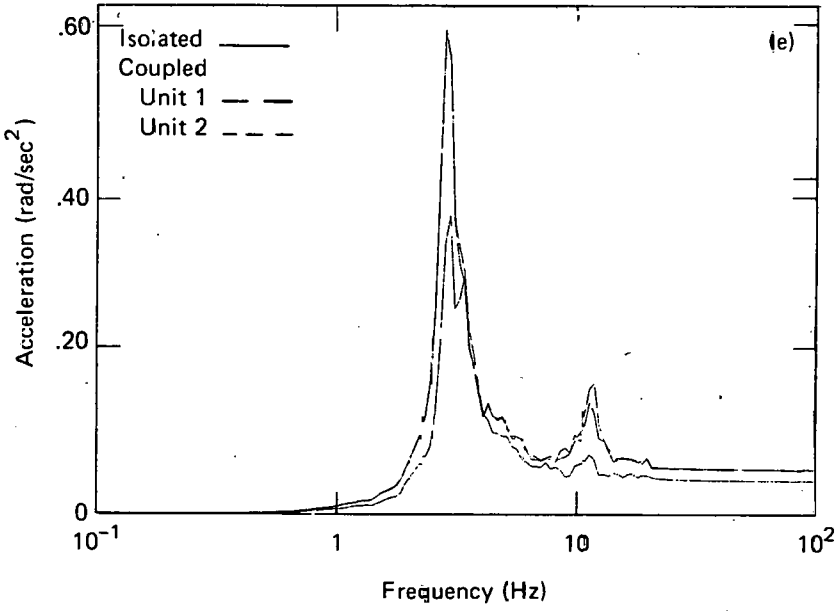

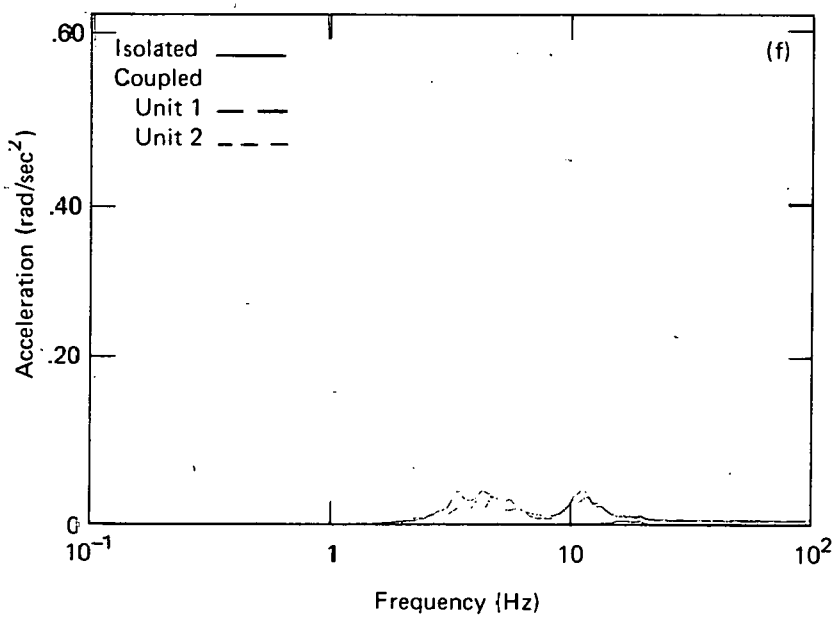

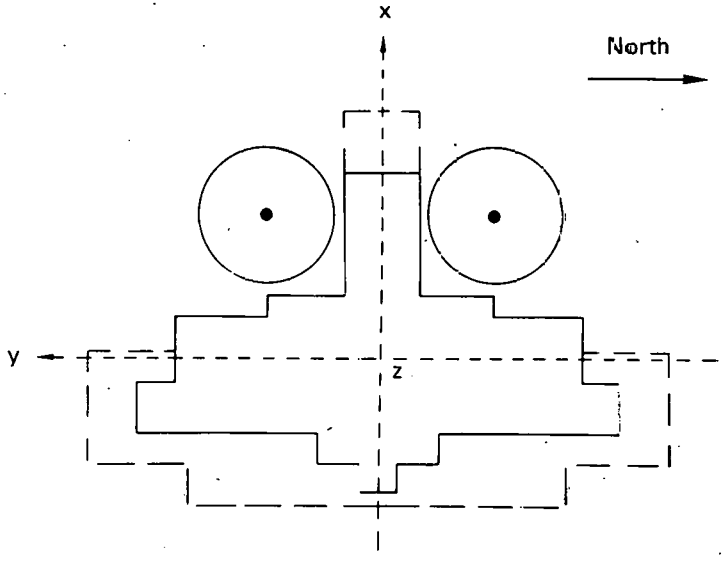

FIG. 5.22. (Continued). (e) E-W rocking, and (f) torsion.

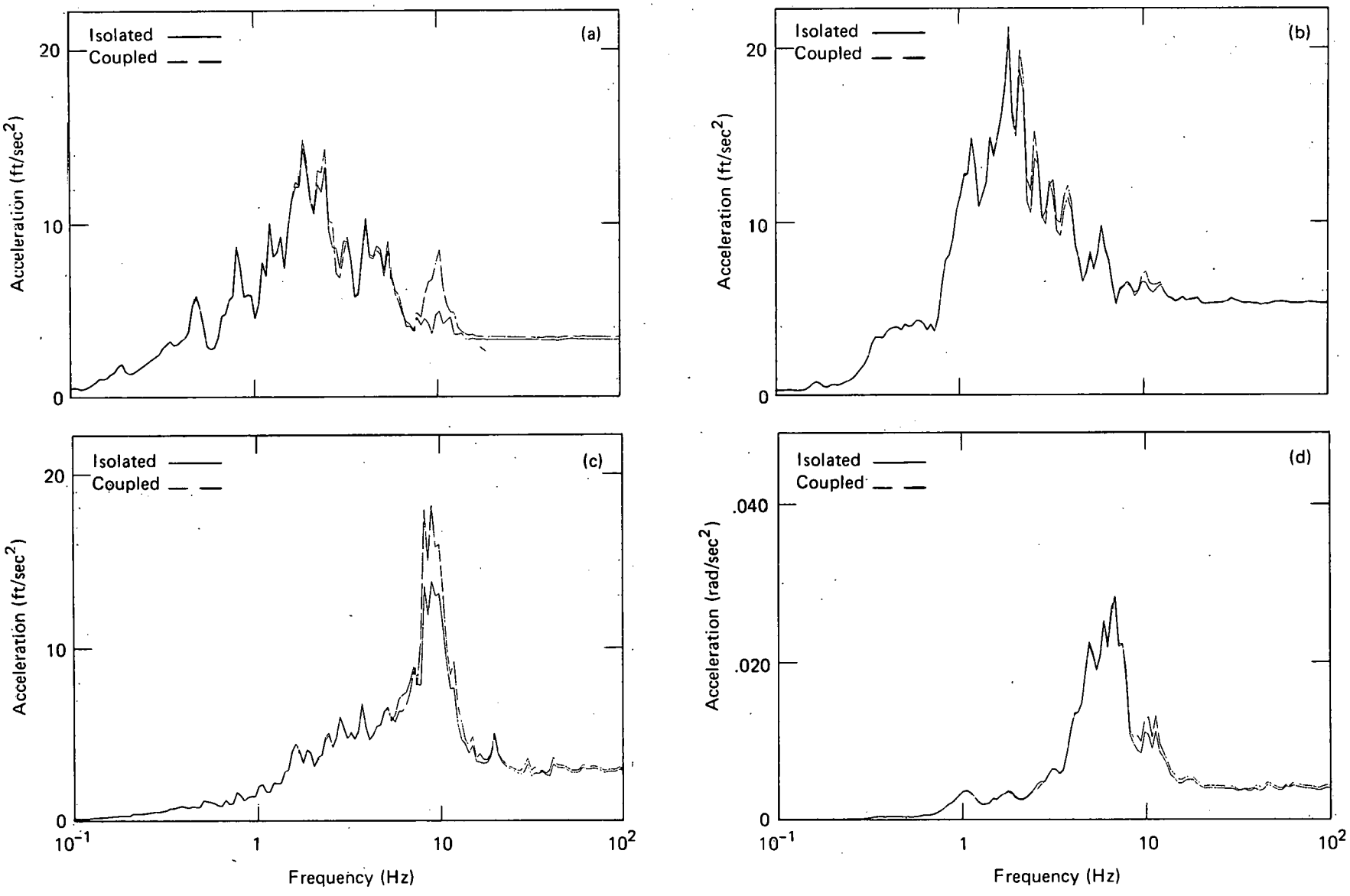

FIG. 5.23. Comparison of isolated and coupled response on the foundation of the AFT complex, using El Centro earthquake data. Shown are (a) E-W translation, (b) N-S translation, (c) vertical translation, (d) N-S rocking.

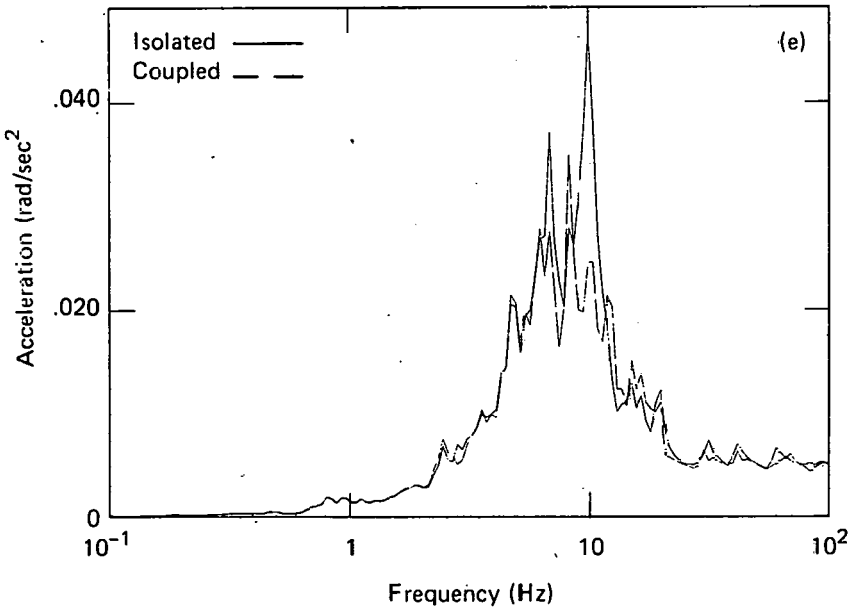

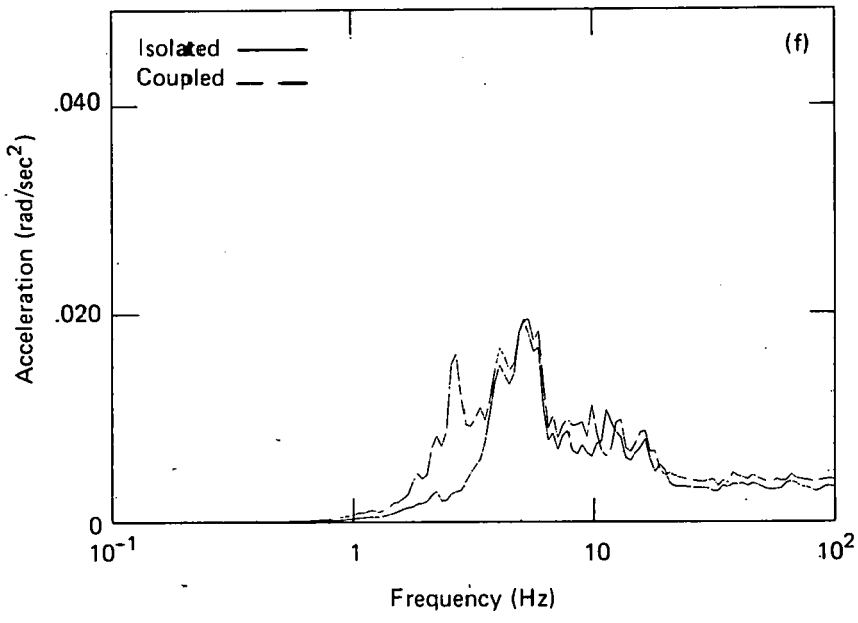

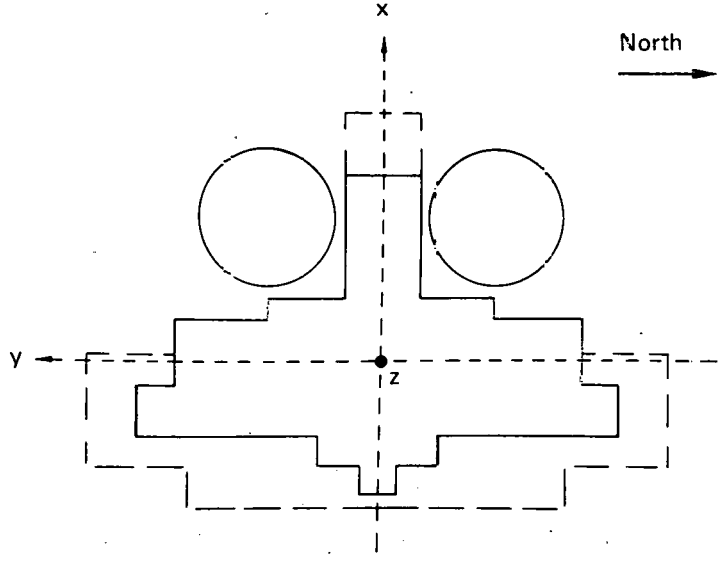

FIG. 5.23. (Continued). (e) E-W rocking, and (f) torsion.

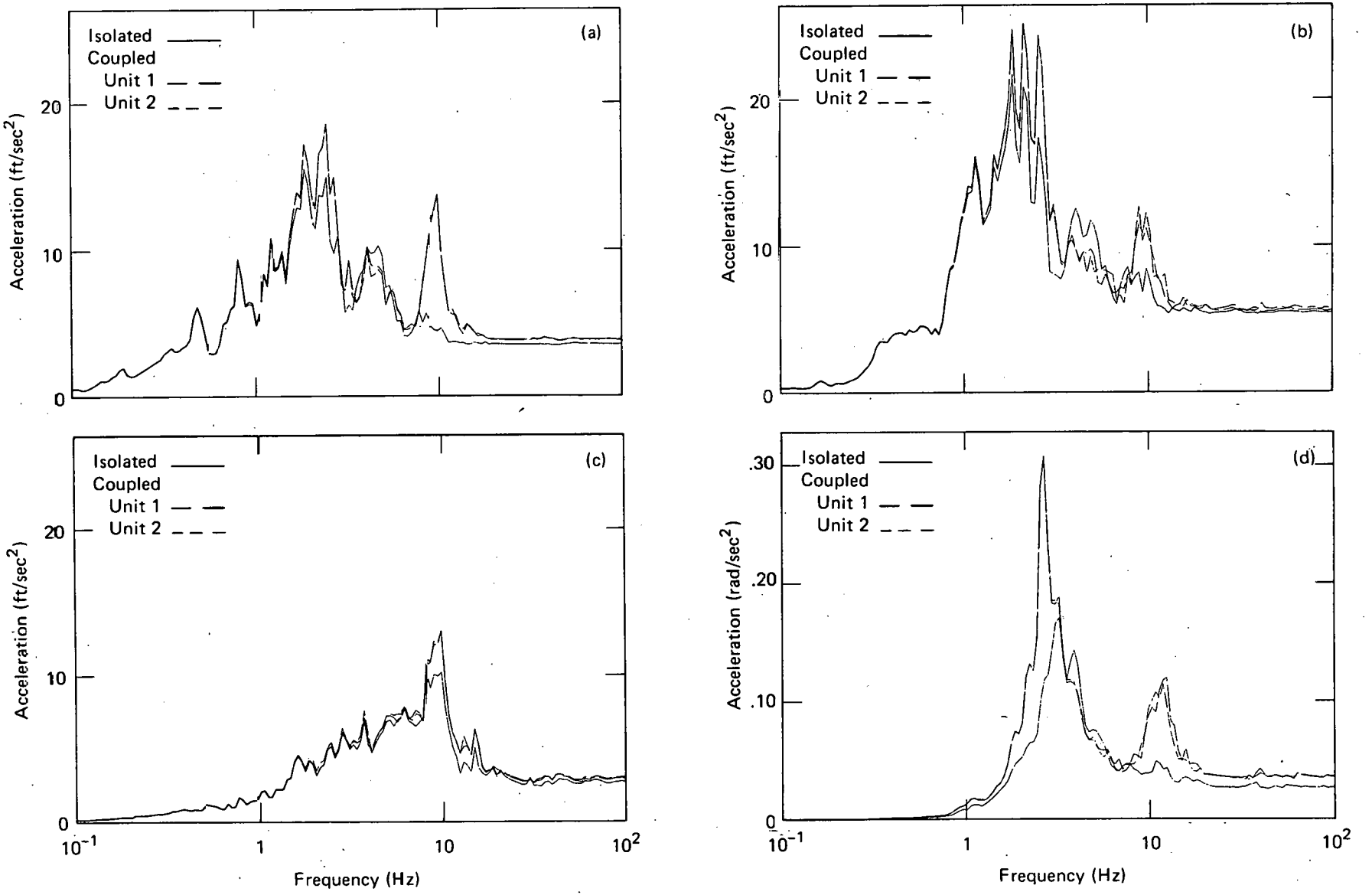

FIG. 5.24. Comparison of isolated and coupled response on the reactor building foundation, using El Centro earthquake data. Shown are (a) E-W translation, (b) N-S translation, (c) vertical translaton, (d) N-S rocking.

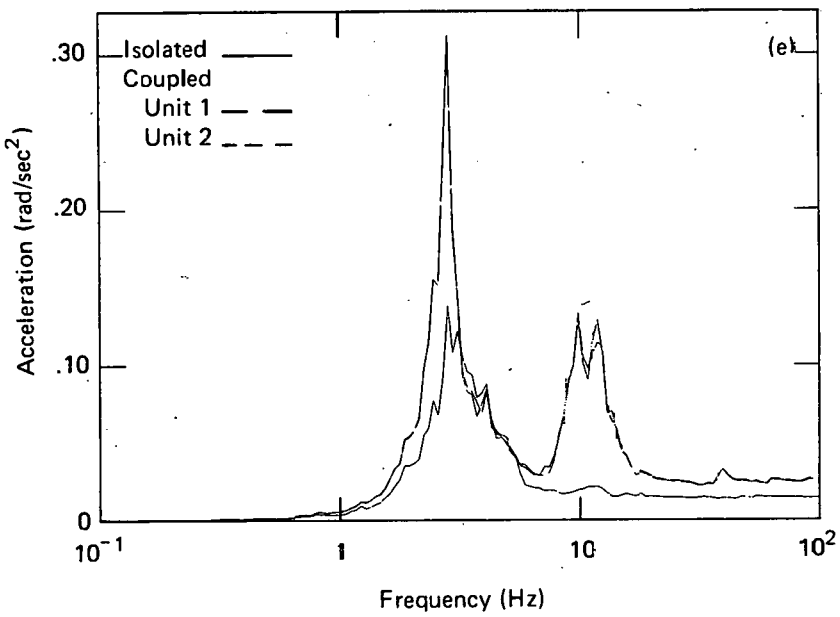

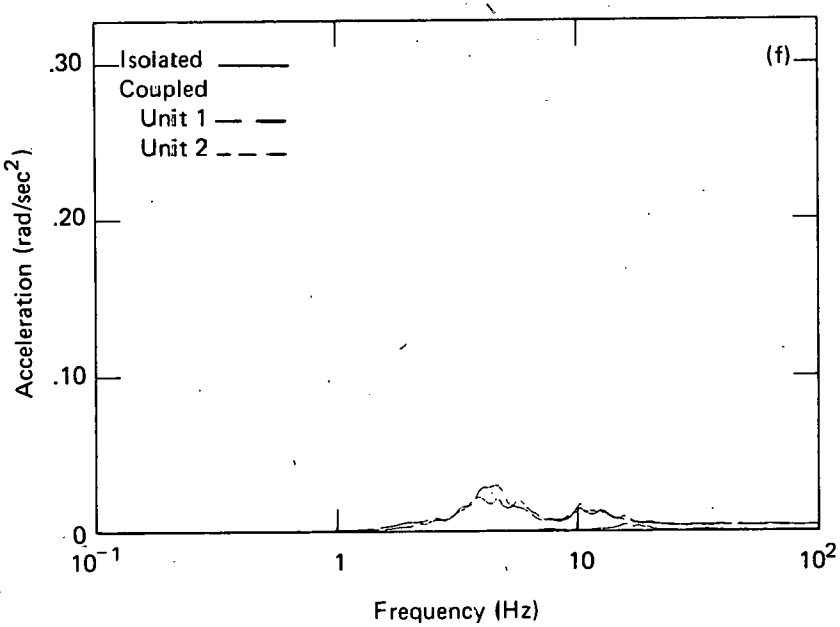

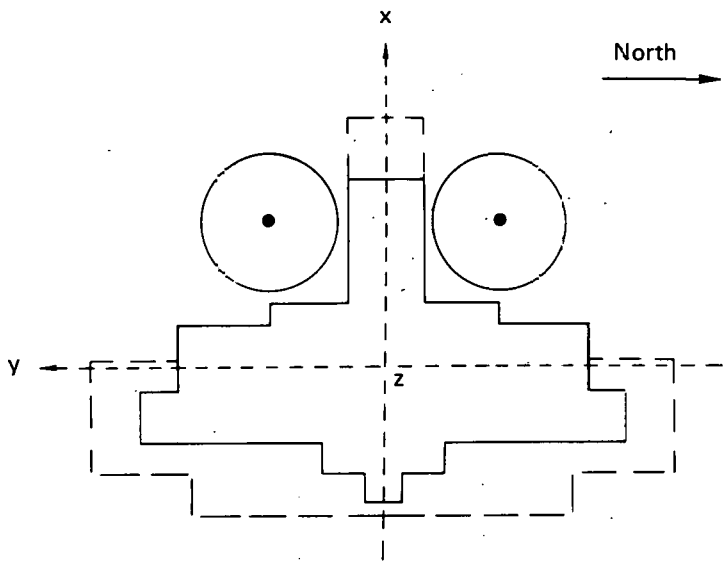

FIG. 5.24. (Continued). (e) E-W rocking, and (f) torsion.

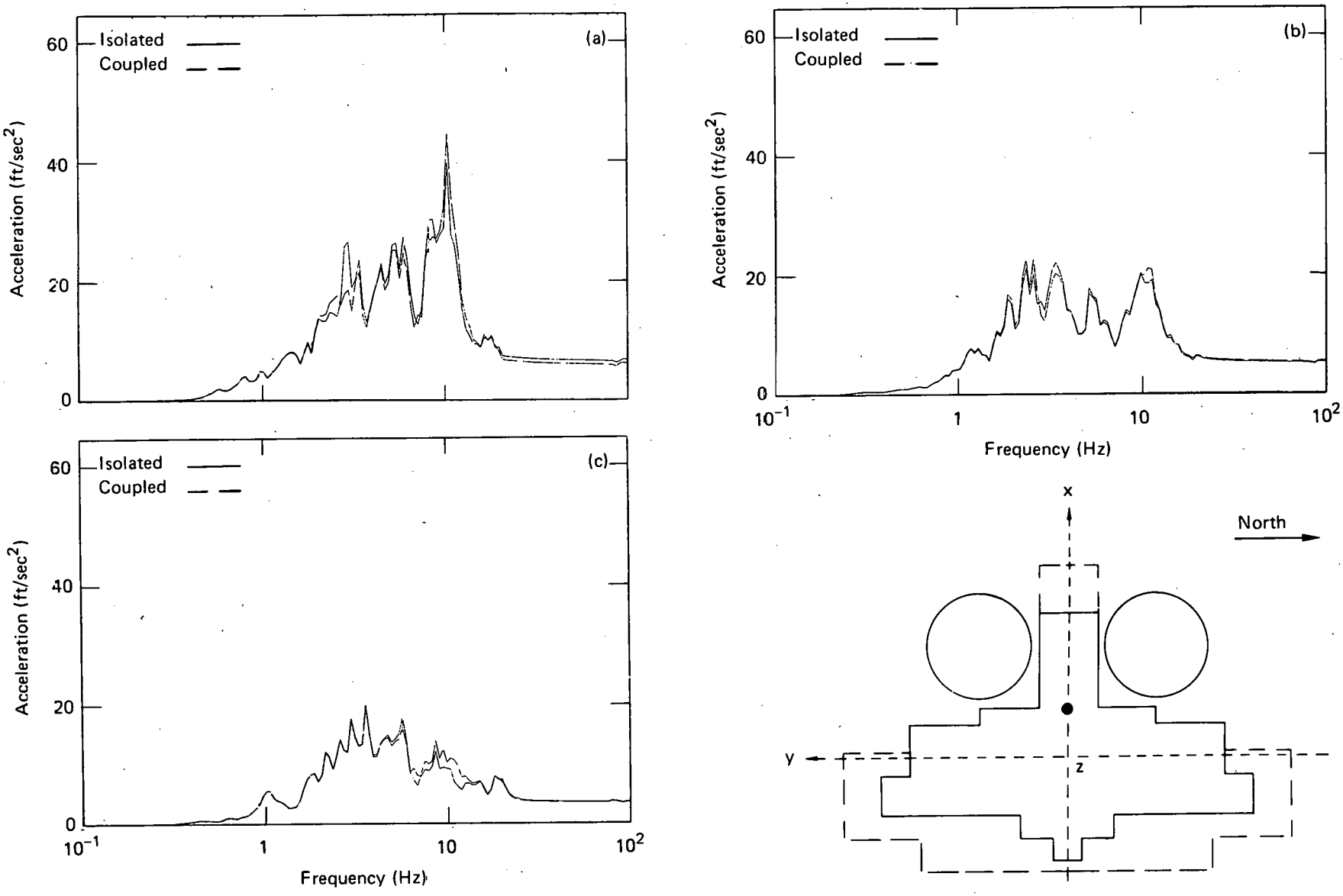

FIG. 5.25. Comparison of isolated and coupled response in the control room of the AFT complex. Shown are (a) E-W translation, (b) N-S translation, and (c) vertical translation.

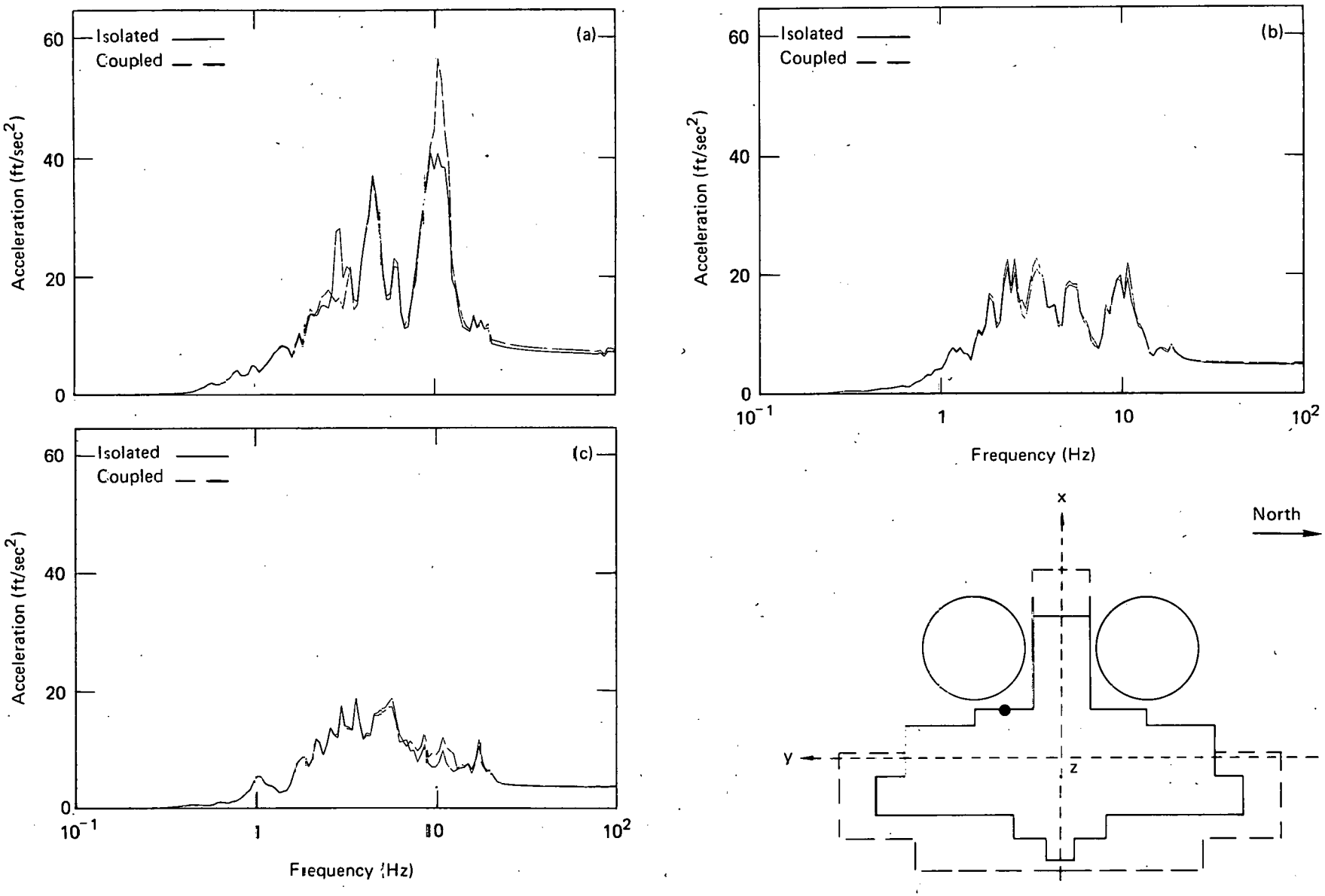

FIG. 5.26. Comparison of isolated and coupled response near the south end of the auxiliary building roof. Shown are (a) E-W translation, (b) N-S translation, and (c) vertical translation.

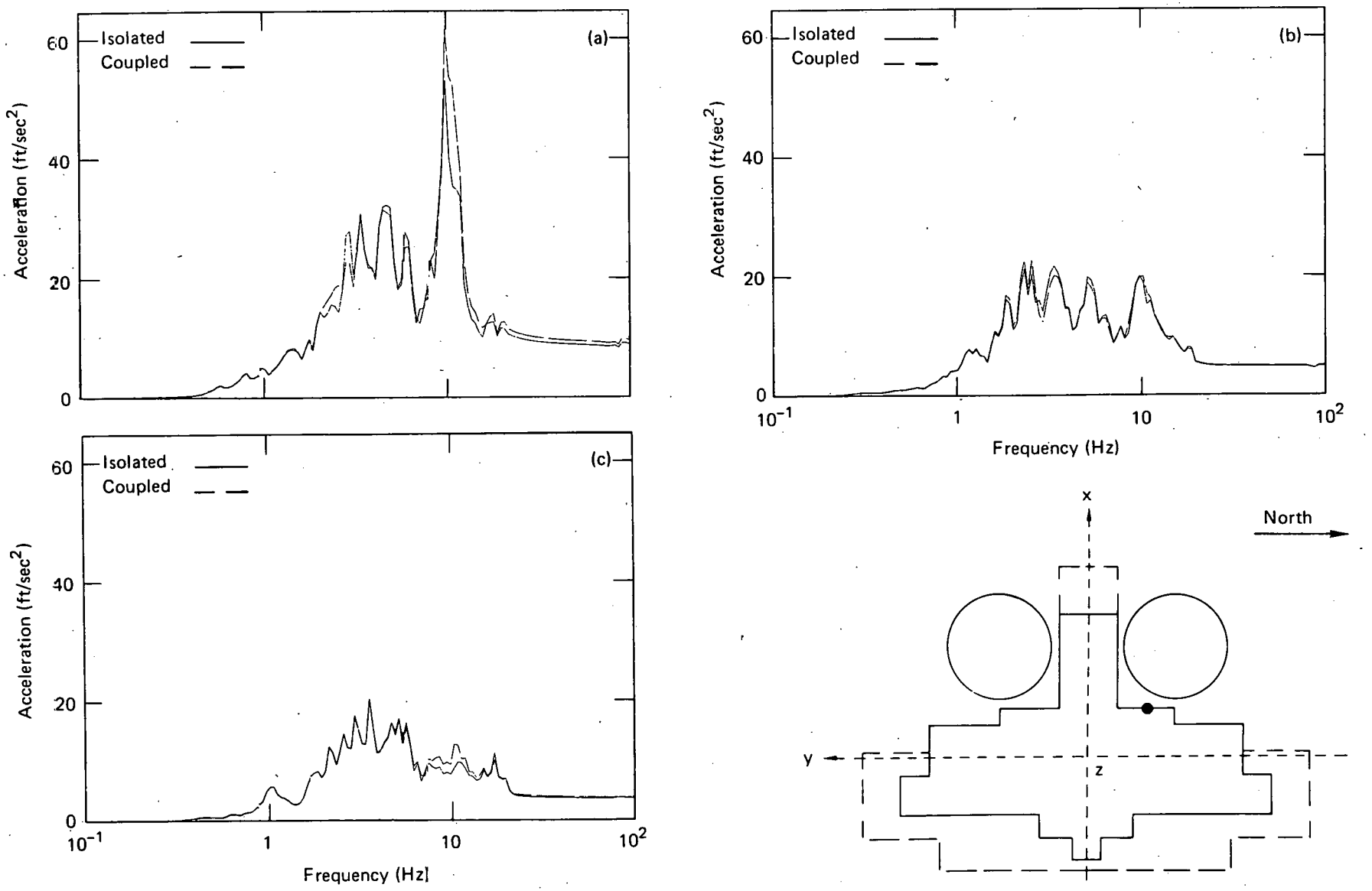

FIG. 5.27. Comparison of isolated and coupled response near the north end of the auxiliary building roof. Shown are (a) E-W translation, (b) N-S translation, and (c) vertical translation.

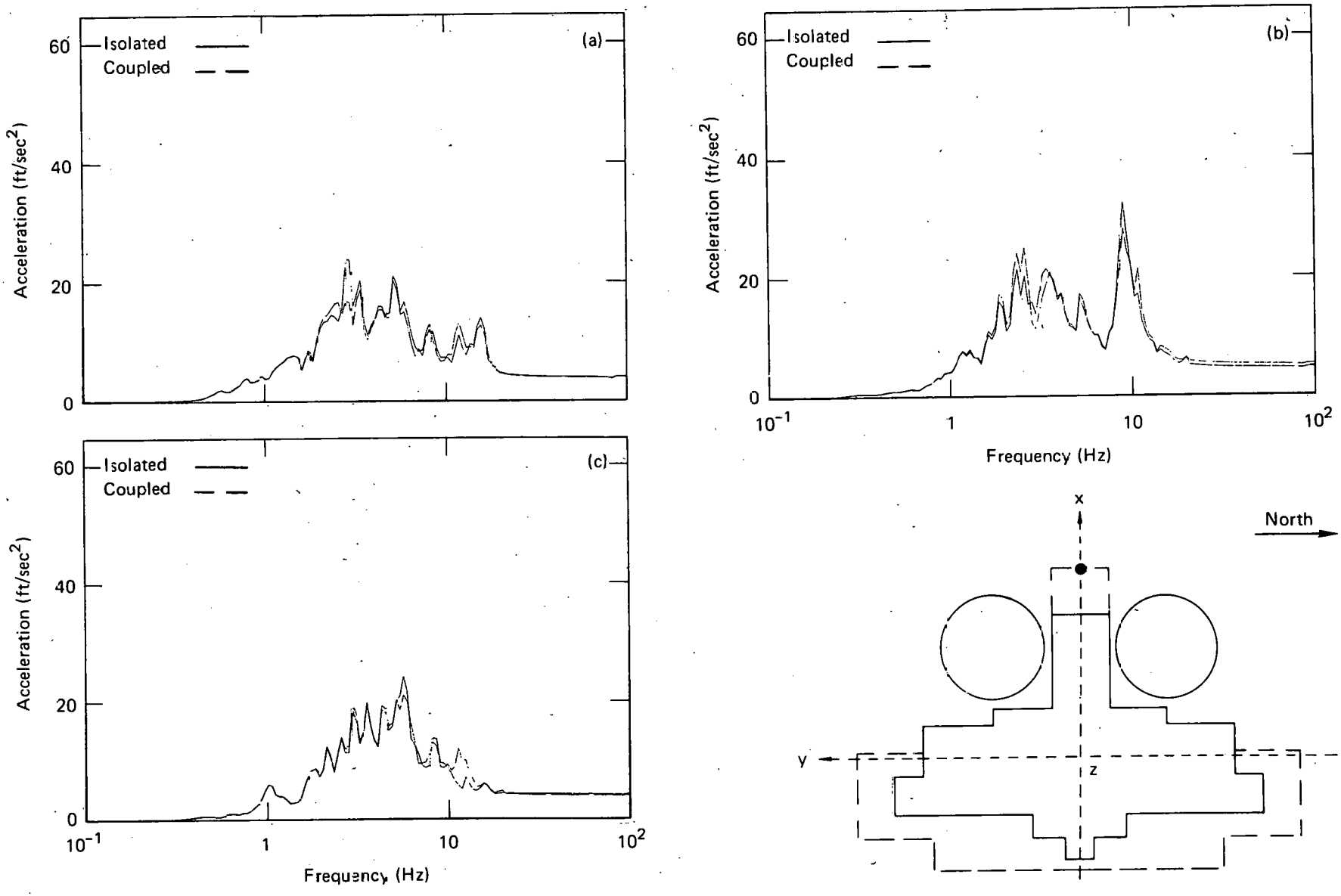

FIG. 5.28. Comparison of isolated and coupled response at the west wall of the AFT complex. Shown are (a) E-W translation, (b) N-S translation, and (c) vertical translation.

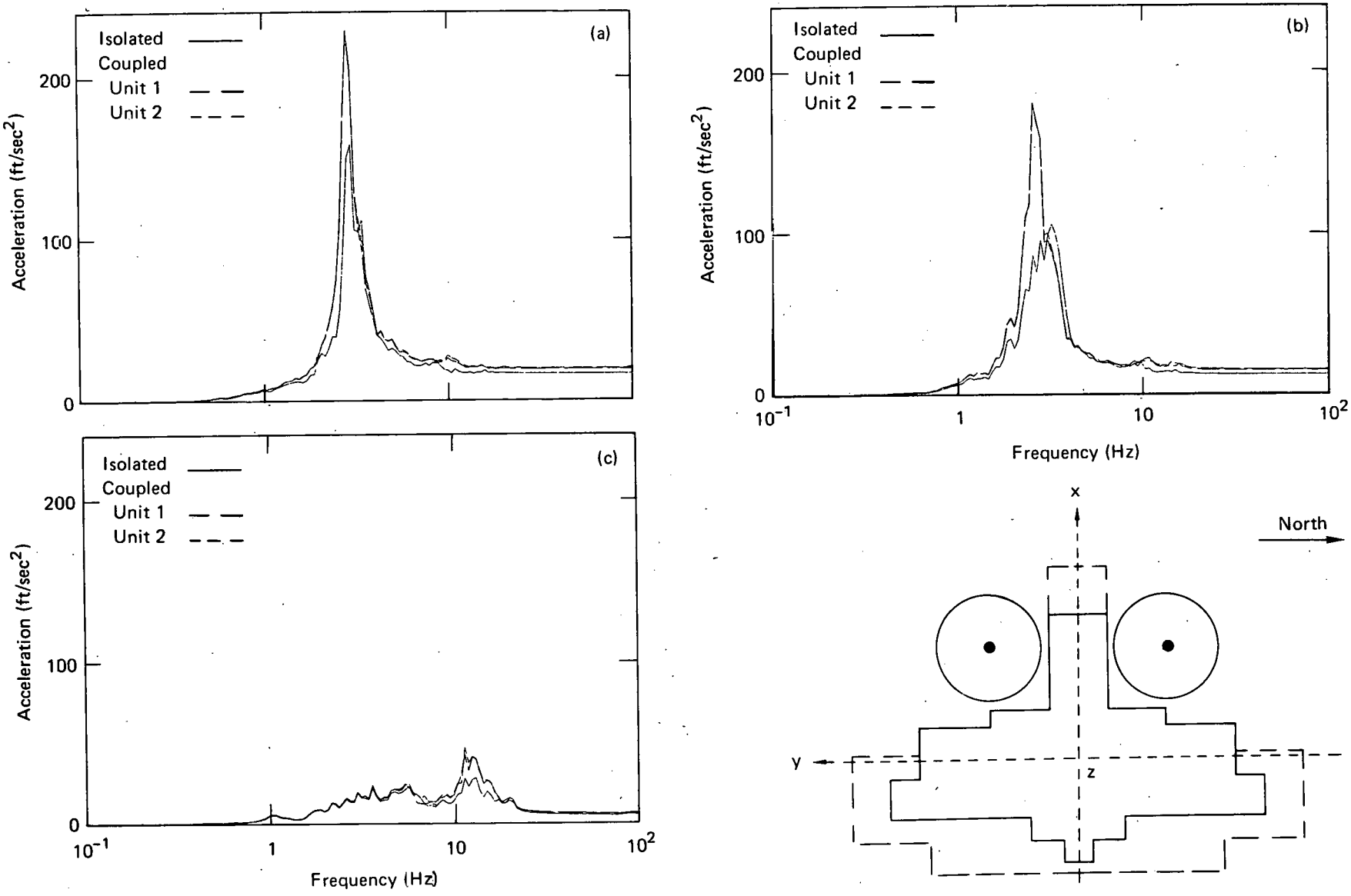

FIG. 5.29. Comparison of isolated and coupled response at the top of the reactor building containment shell. Shown are (a) E-W translation, (b) N-S translation, and (c) vertical translation.

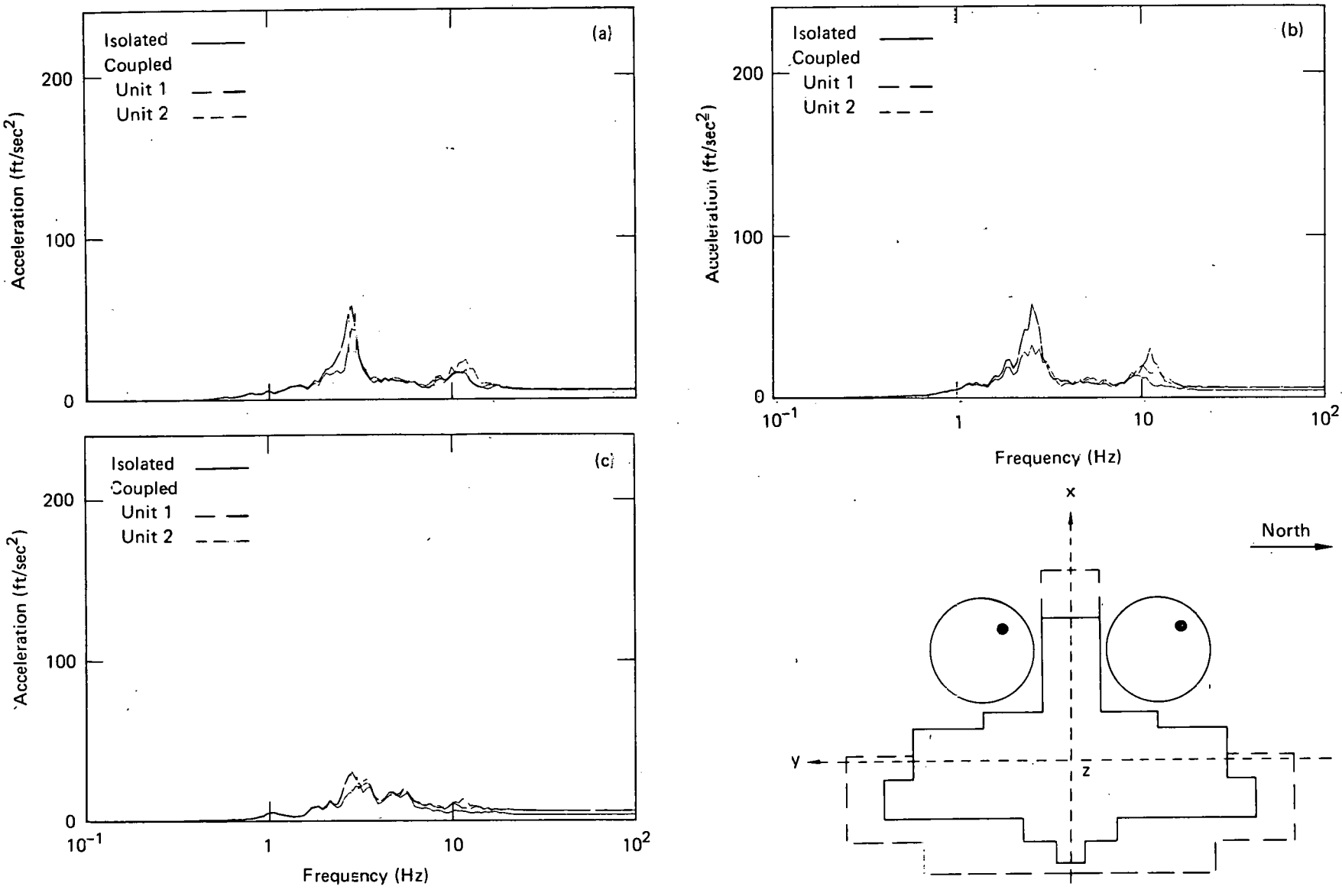

FIG. 5.30. Comparison of isolated and coupled response on the reactor building operating floor. Shown are (a) E-W translation, (b) N-S translation, and (c) vertical translation.

foundation case differed from those for the isolated foundation case generally by less than 5%. For the synthetic earthquake, the only component significantly affected was torsion, for which the peak acceleration increased by about 50% and an additional spectral peak occurred at about 2.5 Hz (Fig. 5.21f). Slight increases (15-35%) in spectral amplification are seen at about 10 Hz for the E-W and vertical translations, N-S rocking, and torsion. Spectral peaks for the E-W translation have decreased by 40% at 3 Hz and increased by 20% at 2.5 Hz. For the El Centro earthquake, differences in peak spectral accelerations on the AFT foundation are somewhat larger (see Fig. 5.23). The most significant changes occur in the 10 Hz spectral peaks for the E-W and vertical translations and E-W rocking, which vary by as much as a factor of 2. As with the synthetic earthquake, a new spectral peak occurs at 2.5 Hz for torsion.

The response on the reactor building foundations, however, was substantially affected by the presence of the AFT complex. For the synthetic earthquake, peak accelerations increased by up to 30%. Response spectra for E-W and N-S translations increased at about 2.5 Hz by as much as 50%. This is no doubt a result of interaction with the torsional motion of the AFT foundation. Rocking was also amplified significantly at about 2.5 and 12 Hz, and torsional motion was induced. These effects are similar for the El Centro earthquake except that the spectral amplifications at 10 to 12 Hz are much more evident. Note that the response of the two reactor buildings is not identical, and hence both results are shown in the figures.

We can conclude from these results that, assuming rigid foundations, the AFT complex is driving the reactor buildings to a significant extent, and that the effects of the reactor buildings on the AFT complex are minimal. This is as we might expect, for the mass of the AFT complex is about five times that of either reactor building.

In-Structure Response. The effects of structure-to-structure interaction on in-structure response are shown in Figs. 5.25 through 5.30 for the synthetic earthquake. Table 5.11 shows peak accelerations for both earthquakes. Here, the consequences of the differences in foundation motion become evident. Differences in response in the AFT complex are minimal, the only significant changes occurring in the 10 Hz spectral peaks in the E-W motions on the roof near the north and south ends of the auxiliary building. These are probably a result of the difference in foundation torsional response at that frequency.

The same is generally true for the El Centro earthquake except that vertical response is also somewhat amplified. In general peak accelerations changed by about 5% for both earthquakes.

In the reactor buildings, the effect of doubling the amplification of the foundation rocking motions at about 3 Hz is evident both at the top of the containment shell (Fig. 5.29) and on the operating floor (Fig. 5.30), where horizontal translations increase by up to 90% at that frequency. Similar increases are also seen on the operating floor at about 12 Hz but are not as evident at the top of the containment shell because of the predominance of its first mode.

6.0 SUMMARY AND CONCLUSIONS

To perform a comprehensive systems analysis, as we did in the SSMRP, it is necessary to obtain quantitative estimates of the realistic, or best estimate, seismic response and its uncertainty. Our inability to define and precisely represent each aspect of the seismic methodology chain (seismic input, SSI, structure response, and subsystem response) introduces uncertainty in the result. In the SSI area, there are many sources of uncertainty. One such source is the analysis procedure used to predict response, which is the subject of our present study.

Some general comments concerning the scope of our study and the application of the results are in order. The responses compared here represent two point estimates of structural response. These point estimates were calculated assuming that all parameters in the analysis were known, e.g., soil parameters, structure characteristics, foundation models, etc. It should be apparent that many additional factors such as these introduce uncertainty into our prediction of structural response. The present study was, therefore, limited to analysis procedures themselves and our implementation of them.

Neither analysis procedure we used can be deemed exact in that a large degree of engineering judgment was necessary for their implementation. However, each technique represents particular aspects of the problem better than its counterpart. For example, the CLASSI method models the three-dimensional character of the problem, while the FLUSH method models the details of the foundation embedment and the soil. Finally, this comparison does not reflect directly on design results because the design procedure entails selecting parameter values and variations to ensure conservative results.

Our basis of comparison in this study was in-structure response spectra, which we now place in a systems analysis context. Consider components supported within the structure, identified as important to accident mitigation, and whose seismic response may be related to spectral acceleration at its fundamental frequency and estimated damping. Variations in in-structure response spectra at specific frequencies are interpreted as

variations in subsystems or component response. In general, these variations result from all elements of the seismic methodology chain, a portion of which may be attributed to SSI analysis procedures. In the following discussion, three aspects of the response spectra will be addressed: peak acceleration or ZPA; portions of the amplified acceleration frequency range <33 Hz, but not necessarily the resonant frequency; and the resonant frequency of the coupled soil-structure system. In general, variability increased from the ZPA to accelerations at the resonant frequencies.

Our analysis of the reactor building as an isolated structure represented a benchmark comparison between FLUSH and CLASSI. The physical situation was relatively simple but representative of a real structure and foundation. Response at three points was compared: at the foundation, at the top of the containment shell, and on the operating floor. Results of this comparison showed excellent agreement between FLUSH and CLASSI for horizontal response--there was less than 10% difference over the entire response spectra, except at narrow frequency ranges near the resonant frequencies of the coupled soil-structure system, where differences approached 35%. This basic comparison was for iterated soil properties in FLUSH. When free-field soil properties were used, responses compared better.

Vertical response did not compare as well as horizontal. Variations in peak acceleration ranged up to about 25%, with the least variability at the top of the containment shell. Variations in the amplified frequency range (<33 Hz) went as high as 50%, depending on structural location and the control motion. Subsequent investigations of the elements of each analysis, such as a comparison of scattering matrices, revealed basic differences that require further study.

Before proceeding to a discussion of the multiple structure analysis, let us consider the AFT complex as an isolated structure. Whereas the reactor building was straightforward to model, the AFT complex required simplification. In the CLASSI analysis, the structure model was very detailed, but the foundation was idealized. First, the embedment configuration was simplified. Second, the foundation was assumed rigid. The embedment simplifications most likely have a smoothing effect on the impedances and scattering matrices. The rigid foundation assumption similarly

has a smoothing effect, and also over-predicts rocking and vertical stiffness. In terms of structure-to-structure interaction, the rigid AFT foundation mobilizes the entire AFT complex mass, which may overestimate its influence on the reactor building. In the FLUSH analysis, two-dimensional models of the structure and foundation were required. In general, two-dimensional models cannot model all aspects of three-dimensional soil-foundation-structure behavior. Modal equivalent models of the structure were its best representation; however, assumptions concerning mass distributions were still necessary. Finally, simulating a rigid foundation within FLUSH as our initial assumption was difficult and was only partially successful.

Response at five points in the AFT complex was considered--three points on the plane of symmetry (foundation, control room in the auxiliary building, and the west wall of the fuel-handling building) and two points on the roof of the auxiliary building symmetrical about this plane. Peak horizontal accelerations varied by less than 25% (about 10% on the average). Spectral accelerations in the amplified frequency range varied somewhat more. The largest variation occurred in the control room in the frequency range of 8 to 9 Hz; here the amplification of the FLUSH foundation motions was much more pronounced than those from CLASSI. In general, spectral accelerations fell within about 25% of each other. Variations in the vertical direction were less than for the horizontal, typically less than 20%. Differences of about 30% occurred between 6 and 10 Hz in the vertical foundation spectra. This was due in part to the location of our reference point and the difference in foundation shapes assumed for the FLUSH and CLASSI analysis (the FLUSH foundation necessarily being rectangular). The favorable comparison of vertical motion was due, at least in part, to higher resonant frequencies in the vertical direction.

The agreement between the FLUSH and CLASSI results for the isolated AFT complex was surprisingly good, considering the differences in the assumptions for the two methods. This may be explained by the fact that, because of the large horizontal area of the foundation, there was relatively little rocking; the rigid-body translation on the roof due to foundation rocking in either the

N-S or E-W direction is about one-tenth of their maximum accelerations. If foundation rocking had been more important, we would expect to see greater differences in the structural response.

Two aspects of the multi-structure analyses were to be considered: the effect of structure-to-structure interaction on structure response and the variability in structure response as predicted by CLASSI and FLUSH, including structure-to-structure interaction. The effect of structure-to-structure interaction on the response of the Zion reactor buildings and the AFT complex was assessed by comparing the results of the CLASSI analyses with and without interaction between the structures. The results show that the reactor buildings have a very small effect on the AFT complex. This is not unexpected, due to the large difference--a factor of 5--between mass of the AFT complex and each reactor building. Also, the assumption of a rigid AFT foundation means its entire mass is mobilized during interaction. The effect of structure-to-structure interaction on the reactor buildings is substantial. In general, motions of the AFT complex induce motions in the reactor buildings--frequencies associated with the AFT complex response are amplified in the reactor buildings. Peak acceleration of the foundation increased up to 25 or 30%, and similar or greater increases in spectral accelerations were observed on the foundation and in the structure.

A comparison of the reactor building's response as predicted by CLASSI and FLUSH, including structure-to-structure interaction, shows substantial differences--200% or more in some cases. Poor correlation between the two could be expected, due to the modeling of the AFT complex in the FLUSH analysis. Only FLUSH cross section A-A contained the reactor buildings and AFT complex. Modeling the AFT complex in this cross section was difficult, as described in paragraphs 4.5.3 and 5.2. The resulting model represented the state of stress in the soil properly but underestimated the total mass and stiffness of the structure-foundation system. The reactor building mass in the FLUSH model was twice that of the AFT complex, and consequently, reactor building response was not significantly changed from the isolated case. AFT complex response changed significantly. Modeling three-dimensional configurations with equivalent two-dimensional models is an issue which requires careful consideration.

The present study demonstrated and quantified the variability in structure response due to two SSI analysis procedures. Some general conclusions may be drawn:

- A well defined benchmark problem permits a good comparison between two analysis techniques. Close matches in amplitude and frequencies for horizontal response was obtained. A close frequency match resulted from careful development of the two-dimensional structure and foundation model used in FLUSH.
- Our benchmark problem did not result in a close comparison for vertical response. Our investigation of intermediate results showed basic model differences which require further understanding.
- Variability in structural response due to SSI analysis procedures increases with increased complexity in the physical situation to be modeled.
- Variability of in-structure response is greatest near the resonant frequencies of the coupled soil-structure system, less in the remaining amplified frequency range, and least at the ZPA. Interpreting these results in a systems context, we find that equipment and components with frequency characteristics in the amplified frequency range (<33 Hz) have greater uncertainty in response than those subjected to the ZPA.

In addition to specific conclusions concerning SSI analysis techniques, the following apply:

- Reduced models, in terms of two dimensions vs three dimensions or fewer degrees of freedom, must be developed carefully, reproducing three-dimensional detailed model characteristics. In our study, areas where reduced models were necessary included foundation simplifications for FLUSH and CLASSI, structure model simplifications for FLUSH, second-stage vs first-stage structure models, and cross sectional properties for FLUSH.
- When performing a second-stage analysis, it is essential to recognize that both translations and rotations must be used in exciting the system. In addition, horizontal translation and rocking have a unique phase relationship which should be maintained. Analyses which treat them separately and combine their effects post facto must account for this phase relationship.

- Our limited consideration of secondary soil nonlinearities showed them to have a minimal effect on response. However, the excitation level considered here did not induce a significant increment in soil nonlinear behavior due to structure vibrations.
- The effect of structure-to-structure interaction was found to have a significant effect on the amplitude and frequency content of the response of the least massive of the two structures. The magnitude of this effect is as great as the differences due to SSI analysis procedures.

REFERENCES

1. P. D. Smith, F. J. Tokarz, D. L. Bernreuter, G. E. Cummings, C. K. Chou, V. N. Vagliente, J. J. Johnson, and R. G. Dong, Seismic Safety Margins Research Program--Program Plan, Revision II, Lawrence Livermore National Laboratory, Livermore, CA, UCID-17824 Rev. II (1978).
2. H. L. Wong and J. E. Luco, Identification of Sensitive Parameters for Soil-Structure Interaction, to be published by Lawrence Livermore National Laboratory, Livermore, CA.
3. J. Lysmer, T. Udaka, C. F. Tsai, and H. B. Seed, FLUSH--A Computer Program For Approximate 3-D Analysis of Soil-Structure Interaction Problems, Earthquake Engineering Research Center, University of California, Berkeley, CA, Report No. EERC 75-30 (1975).
4. H. L. Wong and J. E. Luco, Soil Structure Interaction: A Linear Continuum Mechanics Approach (CLASSI), Department of Civil Engineering, University of Southern California, Los Angeles, CA, CE 79-03 (1980).
5. Strong-Motion Earthquake Accelerograms Digitized and Plotted Data, California Institute of Technology Earthquake Engineering Research Laboratory, Pasadena, CA, EERL 71-50, Vol. II, Part A (September 1971).
6. B. J. Benda, J. J. Johnson, and T. Y. Lo, Seismic Safety Margins Research Program Phase I Final Report--Major Structure Response (Project IV), Lawrence Livermore National Laboratory, Livermore, CA, UCRL-53021, Vol. 5, NUREG/CR-2015, Vol. 5 (1981).
7. J. E. Luco, Linear Soil-Structure Interaction, Lawrence Livermore National Laboratory, Livermore, CA, UCRL-15272 (1980).
8. E. Kausel, "Two-Step Approach in Soil-Structure Interaction: How Good Is It?", in Second ASCE Conference on Civil Engineering and Nuclear Power, 1980 (University of Tennessee, Knoxville, TN, 1980), pp. 10-2-1 to 10-2-10.

CDJ/km